

HOLOCENE CLIMATE OF THE SOUTHWEST YUKON TERRITORY, CANADA,
INFERRED FROM LAKE-LEVEL AND ISOTOPE ANALYSES OF SMALL
CARBONATE LAKES

A Dissertation Presented

by

LESLEIGH ANDERSON

Submitted to the Graduate School of the
University of Massachusetts Amherst in partial fulfillment
Of the requirements for the degree of

DOCTOR OF PHILOSOPHY

May 2005

Department of Geosciences

UMI Number: 3179851

INFORMATION TO USERS

The quality of this reproduction is dependent upon the quality of the copy submitted. Broken or indistinct print, colored or poor quality illustrations and photographs, print bleed-through, substandard margins, and improper alignment can adversely affect reproduction.

In the unlikely event that the author did not send a complete manuscript and there are missing pages, these will be noted. Also, if unauthorized copyright material had to be removed, a note will indicate the deletion.

UMI[®]

UMI Microform 3179851

Copyright 2005 by ProQuest Information and Learning Company.

All rights reserved. This microform edition is protected against unauthorized copying under Title 17, United States Code.

ProQuest Information and Learning Company
300 North Zeeb Road
P.O. Box 1346
Ann Arbor, MI 48106-1346

© Copyright by Lesleigh Anderson 2005

All Rights Reserved

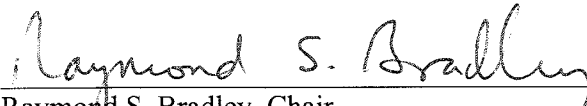
HOLOCENE CLIMATE OF THE SOUTHWEST YUKON TERRITORY, CANADA,
INFERRED FROM LAKE-LEVEL AND ISOTOPE ANALYSES OF SMALL
CARBONATE LAKES

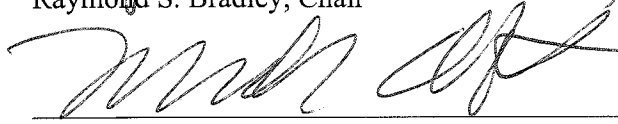
A Dissertation Presented

by

LESLEIGH ANDERSON


Approved as to style and content by:


Raymond S. Bradley, Chair


Mark B. Abbott, Member


Stephen J. Burns, Member


Elizabeth S. Chilton, Member


Michael L. Williams, Department Head
Department of Geosciences

DEDICATION

To the memory of Dr. Duwayne M. Anderson (1927-2002)

ACKNOWLEDGEMENTS

I wish to thank Mark Abbott for being my major advisor and friend and for making it possible for me to carry out this project. I also thank Bruce Finney, Mary Edwards, Steve Burns and Ray Bradley for their guidance, knowledge and humor. I would like to acknowledge Brandon Beierle because it was he who first suggested lakes near Carcross to me. His suggestion, as it turned out, was a good and generous one. My friends in the geosciences department provided a lot of laughter and have my special thanks: Mike Apflebaum, Carsten Braun, Lyn Gualtieri, Jesse Gunnard, Trent Hayden, Brett Longworth, Zach Lundeen, Adam McConnell, Whit Patridge, Bianca Perren, Pratigya Polissar, Joe Rodgers, and Heather Savage. I am grateful to Laurie Brown and Julie Brigham-Grette for their friendship and mentoring. It is for my mother, Shirley Ray, that I have special gratitude. Her strength and faith made the difference.

This research was supported by grants from the National Science Foundation to Mark B. Abbott, Bruce P. Finney and Mary E. Edwards at the University of Massachusetts Amherst (ATM-0296157) and the University of Alaska Fairbanks (ATM-0097127). The Department of Geosciences at the University of Massachusetts Amherst provided further assistance in the form of awards and a University of Massachusetts Amherst University Fellowship. The following individuals and institutes provided analytical services: Celeste Asikainen and the Amherst College Geochemistry Laboratory; Jason Curtis at the Stable Isotope Laboratory at the University of Florida in Gainesville, Frank Keimig at the Climate System Research Center at the University of Massachusetts Amherst; Andrea Krumhardt and the Stable Isotope Facility in the Institute of Marine Sciences at the University of Alaska Fairbanks; Richard Yuretich at the University of Massachusetts Amherst Department of Geosciences Aqueous Geochemistry Laboratory; Paul Wilkinson at the Freshwater Institute at the University of Manitoba. Maria Tsukernik and Trent Hayden provided assistance with sediment core analyses. Jon Sweetman, Andy Breckenridge, Joe Rodgers, Karin Morin, Brit Haugen, Nathan Stansell and Dan Nelson assisted in the field. This

research was assisted greatly by the efforts of these individuals and institutions and I thank them all.

ABSTRACT

HOLOCENE CLIMATE OF THE SOUTHWEST YUKON TERRITORY, CANADA INFERRED FROM LAKE-LEVEL AND ISOTOPE ANALYSES OF SMALL CARBONATE LAKES

MAY 2005

LESLEIGH ANDERSON, B.S., UNIVERSITY OF UTAH

M.S. UNIVERSITY OF MASSACHUSETTS AMHERST

Ph.D. UNIVERSITY OF MASSACHUSETTS AMHERST

Directed by: Professor Raymond S. Bradley

Analyses of sediment cores from two small lakes in the southwest Yukon, Jellybean Lake (60.35°N, 134.80°W, 730-m a.s.l.) and Marcella Lake (60.074°N, 133.808°W, 697-m a.s.l.) provide records of Holocene changes in atmospheric circulation, hydrology and humidity from millennial time-scales up to 5- 20-year resolution. An Aleutian Low mechanism for Holocene climate variability in the North Pacific sub-Arctic region is developed from the results of oxygen isotope records from these new sites. The climatic reconstruction and proposed mechanism lays the framework for evaluation of the paleoenvironmental and human response to climate changes in the region.

Jellybean Lake water reflects the isotope composition of mean annual precipitation and Holocene variations are inferred from the analyses of sedimentary carbonate oxygen isotopes. Recent variations correspond with changes in the North Pacific Index, a measure of the intensity and position of the Aleutian Low, the semi-permanent low-pressure system located over the Gulf of Alaska. This suggests that the Jellybean oxygen isotope record reflects changes in Aleutian Low intensity and position since ~7500 cal BP. Late Holocene changes correspond with changes in North Pacific salmon abundance and shifts in atmospheric circulation over the Beaufort Sea.

Marcella Lake is a small, hydrologically-closed, evaporation sensitive lake. Former water levels were driven by changes in regional effective moisture and reconstructed by multi-

proxy analyses of sediment cores from a shallow-to-deep water transect. Marcella Lake water oxygen isotopes are strongly affected by evaporation allowing past humidity changes to be reconstructed from sedimentary calcite oxygen isotope ratios. The record from Jellybean Lake accounts for variations related to atmospheric circulation and ambient temperature changes allowing an estimation of changes in ambient humidity driven by evaporation. Results suggest that late Holocene increases in aridity in the interior regions of the southwest Yukon are the result of long-term and sustained Aleutian Low intensifications and/or eastward shifts ~1200 and 400 cal BP.

The following climatic patterns are emerging. The early Holocene was warm and dry. Between 9000 and 10,000 cal BP there was a rapid increase in lake level suggesting a shift in the precipitation regime. The early aridity may have prevented the establishment of spruce forest. Between 7500 and 4000 cal BP, lake levels were relatively stable 5-m below modern levels and Aleutian Low intensity was predominantly weaker and/or westward than present. Between ~4500 and 3000 cal BP the Aleutian Low intensified and/or shifted eastward before weakening and/or shifting westward further between 3000 and 2000 cal BP. During this interval lake level and humidity were higher than modern and late Holocene glacial advances began. Rapid Aleutian Low intensifications and/or eastward shifts ~1200 and 400 cal BP correspond with aridity increases in the interior, Little Ice Age glacial advances and increases in North Pacific salmon abundance. Abrupt changes in the Aleutian Low intensity/position and humidity were more frequent during the last ~2000 years than the preceding period.

TABLE OF CONTENTS

	Page
ACKNOWLEDGEMENTS.....	v
ABSTRACT.....	vii
LIST OF TABLES.....	xii
LIST OF FIGURES.....	xiii
 CHAPTER	
1. INTRODUCTION AND BACKGROUND.....	1
Purpose and Objectives.....	1
Paleoclimatic Application of Lake Sediment.....	2
Lake Levels.....	2
Lacustrine Authigenic Calcium Carbonate Isotopes.....	3
Previous Research on the Holocene Paleoclimate of the Southwest Yukon Territory.....	3
Organization of the Dissertation.....	4
Additional Comments.....	5
 2. PALEOHYDROLOGY OF THE SOUTHWEST YUKON TERRITORY, CANADA, BASED ON MULTI-PROXY ANALYSES OF LAKE SEDIMENT CORES FROM A DEPTH TRANSECT.....	 7
Abstract.....	7
Introduction.....	8
Field Area.....	9
Limnology and Sedimentation.....	10
Methods.....	12
Results.....	13
Core A/B (960-cm BML).....	14
Core F (697-cm BML).....	16
Core C/E (430-cm BML).....	16
Core D (195-cm BML).....	17
Discussion.....	18
Lake-level Reconstruction.....	20
Holocene Paleoclimate.....	21
Early Holocene (11,000 to 7500 cal BP).....	21
Middle Holocene (7500 to 4000 cal BP).....	22

Late Holocene (4000 cal BP to present)	23
Conclusions.....	24
3. REGIONAL ATMOSPHERIC CIRCULATION CHANGE IN THE NORTH PACIFIC DURING THE HOLOCENE INFERRED FROM LACUSTRINE CARBONATE OXYGEN ISOTOPES, YUKON TERRITORY, CANADA	36
Abstract.....	36
Introduction.....	37
Paleoclimatic Application of Jellybean Lake Oxygen Isotopes	39
Field Area	40
Methods	41
Results.....	43
Limnology and Isotope Hydrology of Jellybean Lake	43
Core Sedimentology	45
Oxygen and Carbon Isotopes.....	47
Discussion.....	47
Carbon Isotopes	47
Oxygen Isotopes.....	48
Oxygen Isotopes, Precipitation and Atmospheric Circulation	49
Holocene Paleoclimate	52
4. LATE HOLOCENE HUMIDITY IN THE SOUTHWEST YUKON TERRITORY, CANADA, INFERRED FROM LACUSTRINE CARBONATE STABLE ISOTOPES	67
Abstract.....	67
Introduction.....	68
Marcella Lake Oxygen Isotopes	69
Field Area	70
Methods	71
Results.....	73
Limnology and Hydrology of Marcella Lake	73
Oxygen and Carbon Isotopes.....	74
Discussion.....	75
Carbon Isotopes	75
Oxygen Isotopes.....	76
Isotopic Enrichment and Ambient Humidity Estimates	77
Holocene Paleoclimate	78
5. SUMMARY AND CONCLUSIONS	
Introduction.....	89

Holocene Paleoclimate Inferred from Jellybean and Marcella Lake.....	89
Holocene Vegetation, Landscape and Humans	91
Vegetation	91
Landscape.....	92
Humans.....	93
Climate Change and Humans.....	94
10,000 to 8500 cal BP.....	94
8500 to 4500 cal BP.....	95
4500 to 1500 cal BP.....	95
1500 cal BP to Present.....	96
Recommendations for Future Research.....	96

APPENDICES

A. TABLE OF SEDIMENT CORES RETREIVED.....	100
B. SEVEN MILE LAKE DATA	105
C. WADDINGTON POND DATA.....	115
D. JELLYBEAN LAKE DATA	123
E. MARCELLA LAKE DATA.....	134
F. SURFACE WATER DATA	144
G. LEAD AND CESIUM RADIOGENIC DATA.....	153
H. PRINCIPLE COMPONENT DATA	158
REFERENCES CITED.....	160

LIST OF TABLES

Table		Page
2.1	AMS Radiocarbon data from Marcella Lake	25
2.2	Sediment description and lake-level interpretation with estimated ages.....	26
2.3	Summary of bulk sediment properties and inferred water depth.....	27
3.1	Oxygen and hydrogen isotope values for precipitation in the southern Yukon	55
3.2	General characteristics of surface water and surficial sediments in the southern Yukon region	56
3.3	Geochronological data for Jellybean Lake	57
3.4	Relationships between Aleutian Low, $\delta^{18}\text{O}$, Gulf of Alaska, and Alaskan salmon	58
4.1	Marcella Lake surface water and sediment data.....	81
4.2	Marcella Lake core C/E chronostratigraphic data	82
5.1	Summary of Holocene climate, vegetation, landscape, fauna and human history of the southwestern Yukon Territory	98

LIST OF FIGURES

Figure	Page
2.1	Location of the Yukon Territory, Marcella Lake and Birch Lake (modified from the Atlas of Canada, Natural Resources Canada) indicating core locations for this study and that of Cwynar (1988). (Photograph A22408, copyright 1949 by Her Majesty the Queen in Right of Canada, reproduced from the collection of the National Air Photo Library, with permission of Natural Resources Canada)..... 28
2.2	Surface sediment %LOI (unpublished data, courtesy of L.C. Cwynar) and water column measurements of Marcella Lake in July 2000..... 29
2.3	Core A/B pollen percentages of key taxa with depth for: (a) the whole section without adjustment and (b) after adjustment by removing suspect material between 429 and 260-cm depth 30
2.4	Core A/B, 960 cm water depth, showing stratigraphy, organic carbon (elemental analyzer method), calcium carbonate, C/N, $\delta^{13}\text{C}$, $\delta^{15}\text{N}$ and median calibrated radiocarbon ages by depth..... 31
2.5	Core C/E, 430 cm water depth, showing stratigraphy, magnetic susceptibility, dry bulk density, organic matter (%LOI method), calcium carbonate and median calibrated radiocarbon ages by depth..... 32
2.6	Core D, 195 cm water depth, showing stratigraphy, magnetic susceptibility, dry bulk density, organic matter (%LOI method), calcium carbonate and median radiocarbon calibrated ages by depth 33
2.7	Lake level reconstruction with A/B, C/E and D stratigraphies below modern level (BML) on a calibrated radiocarbon age scale. Lines between calibrated ages (black circles) indicate continuous sedimentation (solid line) and discontinuous sedimentation (dash). Gray shading represents lake-level estimates..... 34
2.8	Correlation on a calibrated radiocarbon time scale of Marcella Lake water levels with glacier activity in the St. Elias Mountains (Denton and Karlén, 1977), July insolation at 60 °N (Berger and Loutre, 1991) and water levels at Birch Lake, Alaska (Abbott et al., 2000). High stands occurred when summer insolation was high in early Holocene and when it was relatively low in the late Holocene..... 35
3.1	(a) Location map showing the Yukon Territory and sites referred to in the text. The general atmospheric circulation around the Aleutian Low in the Gulf of Alaska is indicated by the arrow, (b) bathymetry of Jellybean Lake where arrows indicate the locations of artesian springs and open circles the coring sites 59

3.2	Monthly mean temperature (black line) and total precipitation (gray bars) at Whitehorse, Yukon Territory, between 1944 and 1990 AD (Environment Canada, 2003) shown with monthly averages of oxygen isotope ratios of precipitation between 1962 and 1964 AD (filled circle; IAEA/WMO, 2001).....	60
3.3	Jellybean Lake surface-sediment ^{210}Pb ages from a constant rate of supply (CRS) age model shown with ^{137}Cs activity levels indicating that the site where core C was recovered has a constant sedimentation rate and that surface sediments are undisturbed.....	61
3.4	Jellybean Lake core properties including (a) magnetic susceptibility, (b) dry bulk density, (c) %LOI at 550°C, (d) weight percent calcium carbonate and (e) median calibrated ages plotted against depth.....	62
3.5	Oxygen and hydrogen isotope ratios of 71 surface water and precipitation samples from the southern Yukon Territory including Jellybean Lake (JBL): (a) precipitation from Mayo and Whitehorse (crosses) (IAEA/WMO, 2001), and rivers, groundwater or springs (open diamonds). GMWL is the Global Meteoric Water Line (Rozanski et al., 1992). LMWL is the Local Meteoric Water Line, a linear regression of Mayo and Whitehorse data; (b) hydrologically-open lakes (open circles), (c) hydrologically-closed lakes (open triangles). The LEL is the Local Evaporation Line, a linear regression of the lake data; (d) all data.....	63
3.6	Jellybean Lake $\delta^{18}\text{O}_{\text{Ca}}$ and $\delta^{13}\text{C}_{\text{Ca}}$ plotted on a (a) depth scale (cm) and (b) calibrated age scale (cal yr B.P.). Black bars indicate depths of radiocarbon ages. The horizontal line at 64-cm depth is the stratigraphic position of the White River tephra (Clague et al., 1995)	64
3.7	Normalized Jellybean Lake $\delta^{18}\text{O}_{\text{Ca}}$ data (black line) is shown with the NP index since 1900 AD (gray shade is annual data, dashed line is 5-year running average; Trenberth and Hurrell, 1994). Negative NP anomalies represent an strong/eastward Aleutian Low. Error bars on $\delta^{18}\text{O}_{\text{Ca}}$ data represent \pm 5-yr age uncertainty based on the ^{210}Pb and ^{137}Cs measurements (Figure 3.3).....	65
3.8	Normalized Jellybean Lake $\delta^{18}\text{O}_{\text{Ca}}$ is shown with sedimentary- $\delta^{15}\text{N}$ from Karluk Lake, Alaska since 2200 cal yr B.P. (Finney et al., 2002). $\delta^{15}\text{N}$ is a proxy for sockeye salmon abundance where enriched $\delta^{15}\text{N}$ records periods of higher salmon abundance (Finney et al., 2000). Note that changes during the 20 th century also reflect the influence of commercial fishing in addition to that of climate. Timing of glacier advances in the St. Elias Mountains are indicated by vertical bars (Denton and Karlén, 1977). Vertical line on $\delta^{18}\text{O}_{\text{Ca}}$ scale labeled ‘modern’ is an average of the last 30 years of data. WRA indicates the stratigraphic position of the White River tephra.	66
4.1	Location map that indicates the Yukon Territory, general atmospheric circulation around the Aleutian Low in the Gulf of Alaska, the St. Elias Mountains and the study area including Marcella and Jellybean Lakes, Whitehorse and Teslin.....	83

4.2	Mean-monthly temperature, precipitation, afternoon (1500 hr) relative humidity at Whitehorse (filled diamonds) and Teslin (open), over the period 1944-1990 (Environment Canada, 2003) and mean-monthly oxygen isotope ratios of precipitation (filled circles) at Whitehorse between 1962 and 1964 (IAEA/GNIP, 2002). The instrumental humidity data indicates a May through September humidity range (morning and afternoon) between 45 and 50% while the annual humidity range is between 60 and 63%.	84
4.3	PCA bi-plots of (a) limnochemical, and (b) physiolimnological variables of water sampled from eight lakes, including Jellybean Lake (JBL) and Marcella Lake (ML), and three springs located in the southwest and central Yukon Territory (Appendix F).	85
4.4	Marcella Lake core C/E <i>Chara</i> calcite oxygen and carbon isotope ratios ($\delta^{18}\text{O}_{\text{Ca}}$ and $\delta^{13}\text{C}_{\text{Ca}}$) plotted (a) on a depth scale (cm) and (b) with chronostratigraphic data including the surface (2002 AD), the ^{210}Pb dating horizon, the radiocarbon age of the White River tephra (2-sigma range; Clague et al. 1995) and three AMS radiocarbon ages of terrestrial macrofossils (one-sigma range; Table 4.1).	86
4.5	Oxygen isotope ratios for (a) Marcella Lake and, (b) Jellybean Lake on a calibrated age scale shown after 200-yr, 100-yr and 50-yr smoothing. The difference between (a) and (b) is (c) $\Delta\delta$, isotopic enrichment due to evaporation and summer ambient humidity, h, also shown as 200-yr, 100-yr and 50-yr smoothed results (Gat, 1995). Arrows indicate the change in trends from (a) to (c) between 3000 and 1200 cal BP. Dashed lines indicate high and low humidity and $\Delta\delta$ values for the record: ~8‰ and 70% between 3000 and 1200 cal BP and ~11.4‰ and 58%, the average for the last 100 years of data.....	87
4.6	Marcella Lake $\Delta\delta$ anomalies (50-yr smooth, difference from the mean for the record) and 50-yr smoothed Jellybean Lake $\delta^{18}\text{O}_{\text{Ca}}$, a record of Aleutian Low intensity and/or position on a calibrated age scale since 5000 cal BP shown with late Holocene glacial activity in the St. Elias Mountains (Denton and Karlén, 1977)..	88

CHAPTER 1

INTRODUCTION AND BACKGROUND

Purpose and Objectives

The purpose of this research is to examine lake-sediment sequences from the southwest Yukon and investigate Holocene paleoclimatic variations and forcing mechanisms. Previous paleoclimatic studies in North Pacific sub-arctic regions have identified long-term millennial-scale climatic fluctuations since the late Pleistocene, but few studies have documented long-term high-resolution climatic variability beyond the last millennia. Little is known about the relative importance of temperature and effective moisture or about quantitative changes in effective moisture. This dissertation presents new evidence for variations in lake-level, atmospheric circulation and humidity for the southwest Yukon Territory. The sampling resolution, geochemical sensitivity and sediment core chronologies presented here range from millennial to decadal time-scale resolution.

Paleoclimatic Application of Lake Sediment

Lakes are an attractive source of paleoenvironmental information because they are sensitive to climatic change, contain records of continuous sedimentation and can be precisely dated. Lake-sediment is used to document climate change at all time scales. Temporal resolution depends on accumulation rates and sedimentary structure preservation. In the rare occasion that sedimentary rhythmites are preserved and represent annual deposition (varves), annual sampling resolution is possible. More commonly, however, ages of Holocene lake sediments are

determined by AMS radiocarbon, lead and cesium radiometric methods with error estimates ranging from decades to centuries. Sedimentary analyses and sampling strategies typically integrate periods of time ranging from decades to centuries. In this study, relatively rapid sedimentation, high sampling resolution and high-precision radiometric dating allow decade to century scale climatic reconstructions.

Geochemical proxies of paleoclimatic and paleohydrologic change are used in this study. Stable isotope methods for oxygen, carbon, hydrogen and nitrogen were developed during marine sediment core and polar ice sheet drilling projects and eventually applied to materials in lake-sediment. Lakes are numerous, diverse and isotope ratios preserved in lakes sediments have been shown to be sensitive proxies for climatic and hydrologic changes within their watersheds. They provide the opportunity to produce high-resolution geochemical paleoclimatic data from previously undocumented continental regions.

Lake Levels

An objective of this study is to document changes in effective moisture, or precipitation-evaporation, in the southwest Yukon. Lake-level records of terminal closed-basin lake systems, where outflow is restricted by evaporation, provide a means to determine changes in regional precipitation-evaporation balance (Harrison and Digerfeldt, 1993; Ritchie and Harrison, 1993; Street-Perrott and Harrison, 1985). Former water levels are reconstructed from historical and instrumental data and shoreline features if they are available. Where that data are not available, changes in sedimentary sequences can be used. Basin wide sedimentary evidence is difficult to identify from the small cross section of one sediment core. A shoreline-to-center transect of cores method was developed by Digerfeldt (1986) and Abbott, et al. (2000) used stratigraphic changes from a shoreline-to-center transect of cores verified by seismic profiles of sub-bottom sediments.

The lake-level reconstruction presented here is based on multi-proxy analyses of sediment cores from a shoreline-to-center depth transect.

Lacustrine Authigenic Calcium Carbonate Isotopes

This study uses oxygen and carbon isotope ratios from calcium carbonate precipitated in lake water that accumulates in bottom sediments. The ratios of oxygen and carbon isotopes are derived from lake water. Isotope ratios of carbon in lake water are affected by numerous processes that in some cases are indirectly or directly related to climate. In contrast, oxygen isotope ratios of lake water are directly related to climate and hydrology. In hydrologically-closed lakes where outflow is restricted to evaporation, lake-water oxygen isotope ratios are closely related to relative humidity. In hydrologically-open lakes where inflow and outflow rates are rapid, lake-water oxygen isotope ratios are typically evaporation-insensitive. In this case, oxygen isotope ratios may be primarily controlled by input water and/or atmospheric and lake-water temperature changes. Here I present and explore carbon isotope ratios but focus on oxygen isotope data for climatic interpretations.

Previous Research on the Holocene Paleoclimate of the Southwest Yukon Territory

The primary objective of this research is to improve the detail and resolution of the regional climatic history in the southwest Yukon interior region which is presently understood in broad terms. Previous research was pollen-based paleoecological studies of lake-sediment and/or peat and investigations of glacial moraine evidence. Between 14,000 and 11,000 years ago the northwest portions of the Laurentide and the Cordilleran ice sheets began to recede and new plant species arrived (Dyke et al., 2002). Evidence from pollen studies of lake-sediments and thaw unconformities indicate that the early Holocene (10,000 to 9,000 years ago) was warm. This has

been attributed to high summer solar insolation at 60°N (Burn 1997; Burn et al., 1986; Mackay, 1992; Ritchie et al., 1983). In the interior of Alaska, lakes were either seasonally dry or dessicated prior to 13,000 years ago and filled between 13,000 and 8000 years ago (Abbott et al., 2000; Barber and Finney, 2000). Spruce forests developed region-wide between 9000 and 8500 years ago (Wang and Geurts, 1991). By 4000 years ago peatland and permafrost development indicate cooler and wetter climate (Mackay, 1992; Vardy et al., 1997). Glacier expansion on the northern flank of the St. Elias Mountains and coastal Alaska began ~3400 BP indicating cooler or wetter climate (Denton and Karlen, 1977). A century-scale paleolimnological study of a small hyper-saline pond indicates increasing aridity since ~2000 years ago (Pienitz et al., 2000). Coastal and interior glaciers fluctuated during the late Holocene but maximum advances occurred during the Little Ice Age between 1500 AD and the early 20th century (Denton and Karlén, 1977; Wiles et al., 1999).

Organization of the Dissertation

This dissertation is comprised of three main chapters that have each been written as individual manuscripts for peer-reviewed journals. Here, they are presented in a sequential order where results and conclusions are used to develop successive hypotheses.

Chapter Two, entitled "Paleohydrology of the southwest Yukon Territory, Canada, based on multi-proxy analyses of lake sediment cores from a depth transect," is currently in press for the November 2005 issue of *The Holocene*. Co-authors are Mark B. Abbott, Bruce P. Finney and Stephen J. Burns.

Chapter three, entitled "Regional atmospheric circulation change in the North Pacific during the Holocene inferred from lacustrine carbonate oxygen isotopes, Yukon Territory, Canada" is in press for the July 2005 issue of *Quaternary Research*. Co-authors are Mark B. Abbott, Bruce P. Finney and Stephen J. Burns.

Chapter four, entitled "Late Holocene humidity in the southwest Yukon Territory, Canada, inferred from lacustrine carbonate stable isotopes" has been submitted to *Quaternary Science Reviews*. Co-authors are Mark B. Abbott, Bruce P. Finney and Stephen J. Burns.

Chapter five is a summary of results and a comparison with previous evidence for changes in Holocene vegetation, landscape and humans. Appendices include data from Jellybean and Marcella Lakes and the surface water. Furthermore, the appendices include the data from Waddington Pond and Seven Mile Lake, two additional lakes initially investigated for this study. For the research objectives of this study, these two sites require further investigation. Here, I focus on Jellybean Lake and Marcella Lake for climatic interpretations.

Additional Comments

This research takes advantage of two important aspects of the geology, topography and climate of the southwest Yukon. First, the thick tills and outwash deposits in the region are calcium rich. Two, the region is located in the rain shadow of the St. Elias Mountains ~250 km to the northeast of the Gulf of Alaska. The primary source region for airflow in the southwest Yukon is the Gulf of Alaska (Wahl et al., 1987). The brief summers are warm and dry. These conditions are favorable for summer productivity in calcium-rich lakes that causes rapid carbonate sedimentation, 0.3 to 0.5 mm/year, creating the opportunity for analyses at 5- to 20-year resolution. The effect of the rain shadow on oxygen isotope ratios in precipitation creates large depletions caused by rain out and transport across the average ~3000-m high topographic barrier. The intensity and position of the Aleutian Low, the semi-permanent low-pressure system located over the Gulf of Alaska, has emerged as an important control on North Pacific Holocene climate. The study sites presented here are ideally located for documenting Holocene changes in Aleutian Low intensity and/or position and the climatic effects in interior regions.

The two lakes of this study have contrasting hydrology: Jellybean Lake is evaporation-insensitive and hydrologically-open while Marcella Lake is evaporation-sensitive and hydrologically-closed. Used together, the oxygen isotope ratios provide new climatic reconstructions related to variations in Aleutian Low intensity and/or position. These results link North Pacific salmon abundance, changes in the position and intensity of the Beaufort Gyre and humidity changes in the interior regions of the northwest sub-Arctic. The Aleutian-Low based climatic reconstruction and mechanism provided here is a new hypothesis to be tested by future paleoclimatic investigations.

CHAPTER 2

PALEOHYDROLOGY OF THE SOUTHWEST YUKON TERRITORY, CANADA, BASED ON MULTI-PROXY ANALYSES OF LAKE SEDIMENT CORES FROM A DEPTH TRANSECT

Abstract

Lake-level variations at Marcella Lake, a small, hydrologically closed lake in the southwestern Yukon Territory, document changes in effective moisture since the early Holocene. Former water levels, driven by regional paleohydrology, were reconstructed by multiproxy analyses of sediment cores from four sites spanning shallow to deep water. Marcella Lake today is thermally stratified, being protected from wind by its position in a depression. It is alkaline and undergoes bio-induced calcification. Relative accumulations of calcium carbonate and organic matter at the sediment-water interface depend on the location of the depositional site relative to the thermocline. We relate lake level fluctuations to down-core stratigraphic variations in composition, geochemistry, sedimentary structures and to the occurrence of unconformities in four cores based on observations of modern limnology and sedimentation processes. Twenty-four AMS radiocarbon dates on macrofossils and pollen provide the lake-level chronology. Prior to 10 000 cal BP water levels were low, but then they rose to 3- to 4-m below modern levels. Between 7500 and 5000 cal BP water levels were 5- to 6-m below modern but rose by 4000 cal BP. Between 4000 and 2000 cal BP they were higher than modern. During the last 2000 years, water levels were either near or 1- to 2-m below modern levels. Marcella Lake water-level fluctuations correspond with previously documented paleoenvironmental and paleoclimatic changes and provide new, independent effective moisture information. The improved

geochronology and quantitative water-level estimates are a framework for more detailed studies in the southwest Yukon.

Introduction

Previous paleoecological studies in the semi-arid regions of central Alaska and southwest Yukon have identified long-term millennial-scale climatic fluctuations since the late Pleistocene (Cwynar, 1988; Stuart et al., 1989; Cwynar and Spear, 1991; Wang and Geurts, 1991; Anderson and Brubaker, 1994; Edwards and Barker, 1994; Lacourse and Gajewski, 2000). Little is known, however, about the relative importance of temperature and effective moisture during the Holocene, or about quantitative changes in effective moisture (Ritchie and Harrison, 1993; Abbott et al., 2000; Barber and Finney, 2000). Lake-level records provide a direct means to determine regional effective moisture because they reflect the water table, which is controlled by effective moisture. In central Alaska, lake level records from Birch Lake (Figure 2.1) provide evidence for effective moisture during the late Pleistocene and early Holocene (Abbott, et al., 2000; Barber and Finney, 2000; Finney, et al., 2000). Birch Lake was either seasonally dry or desiccated prior to 14 000 cal BP. It subsequently filled, but levels fluctuated between 13 000 and 9000 cal BP. Soon after 5500 cal BP it overflowed, which is broadly coincident with oxygen isotope evidence for a transition to cooler and wetter climatic conditions in the central Brooks Range of northern Alaska (Anderson, et al., 2001). However, once overflowing, the lake was no longer sensitive to further increases in effective moisture and the late Holocene record is largely unknown. Less information is known about post-glacial effective moisture variability in the southwest Yukon (Ritchie and Harrison, 1993). Previous studies have documented early Holocene warmth in the northern Yukon (Ritchie et al., 1983; Burn 1997), and a middle-Holocene wet phase in the central Yukon (Pienitz et al., 2000). Late-Holocene glacial advances

occurred in the southwest Yukon, interpreted as evidence for cooler temperatures (Denton and Karlén, 1977; Calkin et al., 2001)

This paper presents new evidence for lake level variations in the southwest Yukon. Modern limnology and surface sediment data from Marcella Lake were used to develop a sedimentary model for shallow, intermediate and deep-water sites. During summer the lake is thermally stratified and surface-sediment composition variations are controlled by thermocline depth. Assuming that lake level changes adjust thermocline depths, variations in surface sediment composition at different water depths record lake-level variations through time (e.g. Digerfeldt, 1986). Following this approach, we reconstructed a quantitative lake-level record from variations in sediment cores along a gently sloping bathymetric profile. The sampling resolution and sediment core chronologies are of sufficient quality to document the timing of effective moisture shifts at the millennial scale, or better.

Field Area

Marcella Lake (60.074 °N, 133.808 °W, 697 m asl) is located in a northwest to southeast trending depression on a terrace of unconsolidated till and outwash east of the Lubbock River in the southern Yukon Plateau physiographic region (Figure 2.1). The larger depression is interpreted as a former melt-water channel that presumably formed ~11 000 cal BP during recession of the northern edge of the Cordilleran Ice Sheet (Dyke et al., 2002). The lake is small (0.4 km²), shallow (9.7 m) and sits ~20 m below the terrace surface in a well-defined 0.8-km² watershed. Surface inflow is limited to the local basin and outflow appears to be restricted to evaporation. Bathymetry is simple with a gently dipping slope from the shallow southeast bay to the deepest area of the basin (Figure 2.1). The watershed is dominated by open stands of lodgepole pine (*Pinus contorta*), trembling aspen (*Populus tremuloides*) and white spruce (*Picea glauca*). Sage (mainly *Artemisia frigida*) and grasses (*Poaceae*) grow on treeless well-drained

south-facing slopes. Submerged charophyte vegetation dominates the southeast bay. Otherwise, littoral plant communities are diverse, but limited to shallow near-shore areas. Water levels today reflect water-table depth.

Marcella Lake is located ~200 km northeast of the Gulf of Alaska in a pronounced rain shadow of the St. Elias Mountains restricting mean annual precipitation in the interior to ~260 mm/yr (Wahl et al., 1987). The intensity and position of the Aleutian Low, centered over the Gulf of Alaska, influences the trajectory and intensity of storms entering the region. A precipitation maximum occurs between May and September (Mock et al, 1998; Wahl et al., 1987). Mean annual temperatures measured at nearby Teslin and Whitehorse are between -2 and 0 °C. January mean temperatures range between -15 and -20°C and July mean temperatures are between 10 to 15°C (Wahl et al., 1987; Environment Canada, 2003). Regional lake-ice break up occurs between April and May and freeze-up occurs between October and November. Cwynar (1988) produced a detailed late-Quaternary pollen record for this site; in his study the lake was called Kettlehole Pond.

Limnology and Sedimentation

Limnological measurements made in July 2000 provide a basis for understanding the controls on modern sedimentary facies and a means to interpret down-core sedimentary facies changes in terms of lake level. Autochthonous sedimentation of bioinduced calcium carbonate and organic matter are predominant throughout the lake. The wind-protected basin experiences a strong thermal stratification, which is shown by temperature and dissolved oxygen profiles of the water column (Figure 2.2). Surface-water was 16.3°C, a thermocline occurred between 5- and 8-m depth and bottom water temperatures were 5.5°C. Dissolved oxygen concentrations at the surface, 9.2 mg L⁻¹, decreased to <0.3 mg L⁻¹ in the hypolimnion. However, intact surface sediments from gravity cores taken in 9.6-m depth clearly showed the sediments to be

bioturbated. The lake probably overturns at least once, but more likely twice per year during the spring and/or fall.

Thermocline depth is controlled by lake volume and heat capacity, and is strongly influenced by lake level (*e.g.* Fee et al., 1996). In general, for lakes with simple bathymetry, an increase in lake volume will result in a decrease in thermocline depth and vice versa. Marcella Lake basin morphometry is simple and has been modified very little by Holocene sedimentary infilling. If past thermoclines formed at depths similar to today (~5 to 8 m), then contrasting sedimentation above and below the thermocline provides a means to reconstruct former lake levels from sediment cores from shallow-to-deep depths.

Marcella Lake water alkalinity, calcium and magnesium concentrations (339 mg CaCO₃/L, 25.4 mg/L Ca²⁺ and 70.8 mg/L Mg²⁺) sustain bio-induced carbonate precipitation within surface waters and by Charophytes (*Chara* sp.) in the shallow southeast bay (McConnaughey, 1991; McConnaughey et al., 1994). Randomly collected surface sediments (collected by L.C. Cwynar) demonstrate how relative proportions of calcium carbonate and organic matter are related to thermocline depth (Figure 2.2). In general, sediments accumulating above the thermocline (≤5 m) contain significantly more calcium carbonate (30 to 80%) than organic matter (20 to 50%). Sediments accumulating within the upper-thermocline (5 to 6 m) contain approximately equal proportions, and calcium carbonate is predominantly intact charophyte encrustations rather than fine-grained calcite. Sediments accumulating below the thermocline (≥7 m) contain significantly more organic matter (>60%) than calcium carbonate (<20%). This relationship appears to be related to acidity, temperature and dissolved oxygen in the water column (*e.g.*, Stabel, 1986; Dean and Megard, 1993; Dean 1999; Ramisch et al., 1999). At depositional locations below the thermocline, raining carbonate particles apparently dissolve, either during deposition or before burial. Raining carbonate particles accumulate at depositional sites located above the thermocline.

In our interpretation we assume the following sedimentation scenarios. If water depths were ≥ 5 m (within or below the thermocline) at a given depositional location, then organic matter accumulation would exceed that of calcium carbonate. This occurs because carbonate is dissolved either within the thermocline, in the hypolimnion or at the sediment water interface. In contrast, if water depths were ≤ 5 m (above the thermocline) then calcium carbonate accumulation would increase relative to organic matter. Furthermore, in littoral zones, lower water levels could create sedimentary unconformities by wave action, thereby decreasing shallow-water sedimentation rates. In contrast, deep-basin sedimentation rates would be uninterrupted and rapid due to sediment focusing. The possibility also exists that sediment re-working due to lower water levels could disrupt sedimentation, resulting in displaced material at depth.

Methods

Bathymetry was determined by fish-finder soundings. A Hydrolab Surveyor 4 and Datasonde 4 were used to collect water column temperature, pH, specific conductivity and dissolved oxygen. Sediment cores were retrieved from a platform with a modified square rod piston corer at 1.95-, 4.30-, 6.97- and 9.60-m below modern level (BML) (Figure 2.1). Sediments were visually logged for Munsell color, sedimentary structures, biogenic features and smear slide features. Magnetic susceptibility was measured on half cores at 5-mm intervals with a Bartington Susceptibility Meter. Smear-slide analyses showed that mineral rich sediments (lower organic and carbonate content) were higher in dry bulk density and higher in magnetic susceptibility. Organic matter (% organic matter) and calcium carbonate content were determined by the loss-on-ignition (%LOI) method (Bengtsson and Enell, 1986; Heiri et al., 2001). Weight %CaCO₃ was based on the following calculation of the mass lost after a 4-hour burn at 1000°C: [%LOI_{1000°C}*(100/44)]. Elemental carbon (% organic carbon) and nitrogen content and $\delta^{13}\text{C}$ and

$\delta^{15}\text{N}$ were analyzed on selected samples after acid pre-treatment using an elemental analyzer coupled with a Finnigan Delta-plus mass spectrometer. Isotope sample reproducibility is $\pm 0.2\%$. Carbon and nitrogen isotope ratios are reported in δ -notation, $\delta = [R_{\text{sample}}/R_{\text{standard}}] - 1 \times 1000$ where $R = {}^{13}\text{C}/{}^{12}\text{C}$ or ${}^{15}\text{N}/{}^{14}\text{N}$, and are expressed as per mil (‰) relative to the international standards: Vienna Pee Dee Belemnite (VPDB) for carbon and air (VAIR) for nitrogen.

The core chronologies are based on AMS radiocarbon dates from terrestrial macrofossils (Table 2.1) and the median calibrated (2-sigma) age of the White River tephra, 1150 cal BP (Clague et al., 1995). At stratigraphic levels where terrestrial macrofossils were not present in sufficient quantities, intact aquatic macrofossils and purified spruce pollen samples were used (Brown et al., 1989). Radiocarbon ages were calibrated using CALIB 4.0 following the methods of Stuiver et al., 1998. Both the measured radiocarbon and median calibrated ages are reported but, only calibrated ages are used for discussion. Rates of sedimentation were determined by linear interpolation between dated stratigraphic depths.

Results

The cores were taken on a transect from deep to shallow water (Figure 2.1). Core A and B were taken within 2 m of each other at 960-cm BML and have overlapping stratigraphic intervals. The cores were matched visually and with bulk sediment data to make composite core A/B (Figure 2.3 and 2.4). Core F was taken on the slope between A/B and C/E. It contained 340 cm of reworked lacustrine mud interspersed with shell lag deposits. With the exception of an AMS radiocarbon age of the basal sediments, no other sedimentary analyses were performed on core F. Core C and E were taken within 1 m of each other at 430-cm BML. They contain overlapping stratigraphic intervals and were matched in a similar manner as A and B (Figure 2.5). Core D (195 cm BML) contained 360 cm of stratigraphically intact sediment (Figure 2.6). Sedimentary facies descriptions and water depth interpretations are summarized in Table 2.2.

Core A/B (960-cm BML)

Bulk sedimentary data and the pollen record from core A/B contain features that indicate a sedimentary discontinuity, both when examined for internal consistency and compared with Cwynar's (1988) record. At 428.5-cm depth, bulk sedimentary values are abruptly interrupted and a visible centimeter-scale unconformable surface occurs. The overlying dark brown organic-rich sediments upwards to ~260-cm depth contain disturbed textures, and otherwise rare aquatic mosses, and produced suspiciously old radiocarbon ages (Table 2.1). Figure 2.3a shows percentages of key pollen taxa with depth for the whole section, prior to any adjustments. Upwards from near the base, the early spruce zone (~470-425 cm) shows increasing *Picea*, stable *Juniperus* and *Alnus*, and decreasing *Betula*, *Salix*, *Populus*, *Artemisia*, and *Cyperaceae*. Between the samples at 428.5 cm and 408.5 cm these patterns are abruptly interrupted and succeeded by a zone (labelled 'displaced material') in which taxa prominent prior to the spruce rise dominate, and *Picea* and *Juniperus* are largely absent. Towards the top of this zone (~340-300 cm), small quantities of *Picea* and *Juniperus* reappear, suggesting that there may have been some mixing of the sediments as the displaced material moved. From ~300-260 cm, the pollen curves are almost identical to those of the early spruce zone and this repeat is taken to mark the uppermost portion of the displaced material. Figure 2.3b shows that removal of the suspect material (thickness, according to the pollen stratigraphy, ≤ 170 cm) yields a pollen curve consistent with Cwynar's (1988). Statistically identical radiocarbon ages from depths immediately above (259 cm) and below (429 cm) provided further constraints on the thickness of the displaced material and the timing of the event (~7850 cal BP). Figure 2.4 shows core A/B stratigraphy and bulk sedimentary data after removing the suspect sediment (unit 3a) and adjusting the depths for samples below 260 cm.

Overlying basal gravel (unit 4), unit 3c (348-328 cm, corrected depth) is composed of gray silty, marl characterized by a relatively high magnetic susceptibility (>3 SI), high dry bulk density (>0.6 g/cm³), low organic carbon ($<30\%$; elemental analyzer method) and high calcium carbonate ($>40\%$) primarily in the form of bivalve shell fragments. $\delta^{13}\text{C}$ values are low (-31%) and C/N ratios are relatively low (12). A radiocarbon age reversal indicated on an aquatic macrophyte at 505 cm, $10\,650 \pm 50$ (OS-12130), indicates either a significant reservoir effect or sediment re-working.

The lower boundary of unit 3b (328-260 cm, corrected depth) is marked by a transition to strongly laminated organic marl. The shift is distinguished by decreased magnetic susceptibility (0 SI), decreasing dry bulk density (<0.2 g cm⁻¹), increased organic carbon (30 to 40%) and highly variable but lower carbonate content (20 to 40%). C/N ratios rise to ~ 14 and $\delta^{13}\text{C}$ values increase (-28%). Radiocarbon ages of 8605 ± 40 (CAMS-96834) and 8560 ± 60 (OS-12129), at 296 and 288 cm corrected-depths respectively, and 7060 ± 40 (CAMS-73154) at 259 cm corrected-depth, support the stratigraphic integrity of unit 3b.

Lowermost unit 2b (260-165 cm) is dark-brown organic mud, which becomes olive-brown faintly laminated organic mud up-core. Organic carbon, calcium carbonate and C/N ratios increase while $\delta^{13}\text{C}$ remains relatively unchanged. Unit 2a (165-90 cm) is marked by a transition to black, gelatinous organic mud containing micro-scale laminae. Smear-slide analyses indicated the laminae alternate between diatoms and fine-grained organic mud. Both organic carbon and calcium carbonate decrease, presumably due to an increased proportion of biogenic silica in the diatom laminae. $\delta^{13}\text{C}$ increases (-26%), C/N ratios decrease, and $\delta^{15}\text{N}$ decreases by 4‰.

The transition from unit 2a to unit 1 at 95 cm is a gradual change in color and texture. Unit 1 is faintly color banded, bioturbated, olive-brown, gelatinous, organic mud. The 1.0-cm thick White River tephra (Clague et al., 1995) occurs at 64 cm. Organic carbon is lower than in unit 2a (35 to 40%) and calcium carbonate content higher is higher (15 to 25%), $\delta^{13}\text{C}$ decreases

and C/N ratios are relatively unchanged. Radiocarbon ages are in stratigraphic order after adjusting for the displaced material (Table 2.1) except for a reversal between 241 and 249 cm. A linear age model (after adjustment) indicates faster sedimentation rates between 10 000 and 8000 cal BP and slower rates since 8000 cal BP (Figure 2.4).

Core F (697-cm BML)

With the exception of the lowermost portion of the section, core F is composed of chaotically structured dark-brown organic mud interspersed with shell lag deposits and bryophyte layers. The White River tephra was neither visible nor detected by magnetic susceptibility. However, overlying basal gravel is faintly laminated marl. Spruce pollen was extracted 3-cm above the base of the core within this laminated sediment. The resultant age 6595 ± 40 (CAMS-92157; 7,477 cal BP; Table 2.1) was used to identify the approximate onset of lacustrine sedimentation at this location.

Core C/E (430-cm BML)

Overlying basal gravel, unit 4 (200-185 cm) is gray-brown, silty, organic mud containing abundant mollusk shell fragments. Magnetic susceptibility and dry bulk density are low (0 SI, 0.2 to 0.3 g/cm³). Organic matter (%LOI method) is between 20 and 25% and calcium carbonate fluctuates between 60 and 70%. The transition to unit 3 is a gradual color and textural change.

Unit 3 (185-155 cm) is brown, bryophyte-rich, organic mud containing mollusk shell fragments and *Chara* encrustations. At the base of unit 3, macrophyte fragments interrupt bands of mollusk shells on an unconformable surface (177 cm). Magnetic susceptibility peaks, organic matter increases and calcium carbonate decreases. The upper portion of unit 3 is macrophyte-rich organic mud. Another unconformable surface marks the boundary between unit 3 and unit 2,

where there is a rise in magnetic susceptibility, increased organic matter and decreased calcium carbonate.

Unit 2 (155-130 cm) is olive-brown, strongly laminated, fine-grained, organic marl containing abundant and well-preserved *Chara* encrustations. Magnetic susceptibility and dry bulk density are low (0 SI, 0.3 to 0.4 g/cm³). Organic matter is between 20 and 30% while calcium carbonate is between 40 and 60%. The transition to unit 1 is a gradual shift towards lower organic matter content and higher calcium carbonate content. Unit 1 (130-0 cm) is light, olive-brown, fine-grained, strongly laminated marl containing abundant well-preserved *Chara* encrustations. The White River tephra is 1.0-cm thick at 64-cm depth. Radiocarbon ages and the White River tephra are in stratigraphic order (Table 2.1). A linear age model suggests slower sedimentation rates between ~5500 and 4000 cal BP and more rapid rates to present (Figure 2.5).

Core D (195 cm BML)

Core D was taken near the submerged *Chara* vegetation in the southeast bay (Figure 2.1). Living *Chara* varied in thickness between 30 to 50 cm and the coring site was chosen to avoid penetrating living vegetation. Overlying basal gravel, unit 3 (360-330 cm) is dark olive-brown, strongly laminated organic mud containing mollusk and gastropod shell fragments. Magnetic susceptibility and dry bulk density are low (0 SI, 0.2 to 0.4 g/cm³), organic matter (%LOI method) varies between 20 and 30% and calcium carbonate (%LOI method) varies between 60 and 80%.

Strongly laminated structures are disrupted at the boundary between unit 3 and unit 2 (330-245 cm). At the base of unit 2 there are bands of mollusk shell fragments overlain by disturbed, fine-grained, organic mud. Variability of organic matter and calcium carbonate content increases in unit 2. Four or possibly six unconformable surfaces were visually identified.

The transition from unit 2 to unit 1 (245-0 cm) is identified by a change to strongly laminated, light olive-brown, fine-grained, organic marl containing abundant *Chara* encrustations. Dry bulk density increases, organic matter decreases and calcium carbonate increases. Based on cores A/B and C/E, the depth of the White River tephra would be 58- to 66-cm depth, but the tephra was not visible or magnetically detected. Instead, a band of green, unusually well-preserved *Chara* vegetation occurs at 68 cm. Between 40 and 70 cm, increased dry density, decreased organic matter and increased calcium carbonate may indicate an unconformity or re-working. Radiocarbon ages in core D are in stratigraphic order (Table 2.1). Similar to core C/E, sedimentation rates prior to 4200 cal BP were slower. The radiocarbon age at 233 cm of 3830 ± 60 (CAMS-73150) could be too old due to hard water effects but if the age is accurate, then after 4200 cal BP core D rates are higher than core C/E. At the core D site, sediments appear to have accumulated on a flat shelf, while core C/E sediments dip 15° towards the deep basin, possibly leading to some down-slope sediment sloughing.

Discussion

If our lake-level-thermocline model is correct we can use sedimentary properties to infer past water depth. When water depths were ≤ 5 m in the deep basin, there was an unstratified water column and calcium carbonate accumulation exceeded that of organic matter. Following this model, down-core sedimentary properties interpreted as low-lake-level facies include: i) color banded or laminated fine-grained micrite containing plant macrophytes, ostracode tests and *Chara* crusts, ii) mollusk shell-lags and iii) abrupt sedimentary unconformities (see Table 2.3), a classification of magnetic susceptibility, dry density, organic matter or organic carbon, calcium carbonate, $\delta^{13}\text{C}$, C/N and $\delta^{15}\text{N}$ ratios). In contrast, water depths ≥ 8 -m deep are associated with a thermally stratified water column and permanent or temporary meromictic conditions. Sedimentary properties interpreted as deep-water facies include strongly laminated dark-brown or

black gelatinous organic mud with bulk sedimentary characteristic that are distinct from those of shallow water facies (Table 2.3). For example, in core A/B unit 2, when laminations indicate the lake was meromictic, organic matter $\delta^{13}\text{C}$ ratios were high, C/N ratios were relatively low and $\delta^{15}\text{N}$ ratios were very low (Figure 2.4). Meromictic conditions may be caused by a number of factors including higher lake level, shifts in biological productivity due to increased nutrient loading by watershed run-off, or longer ice cover duration causing diminished spring and fall overturn. Either of the first two possibilities supports an increase in the regional effective moisture and the third case, ice cover, is an unlikely explanation.

Mixing regime variations may be a significant factor for carbon and nitrogen isotope variations (*e.g.* Hodell et al., 1998). Organic matter $\delta^{13}\text{C}$ records the isotopic composition of lake-water dissolved inorganic carbon (DIC). DIC is in turn a reflection of organic carbon sequestration rates and carbon isotope ratios of CO_2 -sources from atmospheric dissolution, biological respiration and groundwater (Oana and Deevey, 1960; McKenzie, 1985; Dean and Stuiver, 1993). It has been observed that during thermal stratification, DIC pools within the epilimnion and hypolimnion evolve in isolation. In the epilimnion, sequestration of ^{12}C -enriched DIC into organic matter eventually leads to the accumulation of ^{13}C -enriched-DIC and progressively higher organic matter $\delta^{13}\text{C}$ values. In contrast, hypolimnion DIC becomes relatively ^{13}C -depleted because the primary DIC source is respired ^{12}C -enriched- CO_2 . Mixing epilimnion and hypolimnion DIC pools tends to decrease epilimnion-DIC- $\delta^{13}\text{C}$ values and hence organic-matter- $\delta^{13}\text{C}$ values (Hodell et al., 1998). Organic matter- $\delta^{15}\text{N}$ is possibly related to the degree of nitrogen recycling within the lake (Kendal, 1998).

Lake-level Reconstruction

Figure 2.7 shows the lake-level reconstruction; stratigraphic data are shown as depth below modern level (BML) on a calibrated age scale. Radiocarbon ages illustrate relative sedimentation rates at each site and sedimentary interpretations provide maximum and minimum water depth estimates indicated by the gray shading (Table 2.1). The thickness of the gray shading indicates the range of water depth estimates.

The lowermost sediment in A/B and D suggest lake level initially rose 9 m (4- to 5-m BML) soon after deglaciation. Intact sediment from the southeastern slope appears to have been displaced into the deep basin ~8000 cal BP (unit 3a core A/B). This resulted in an apparent delay in the onset of sedimentation at F (7500 cal BP) and slow, disturbed sedimentation at D (unit 2). Such slope failures are due to instability that could be caused by a variety of events including seismic activity, sediment de-gassing or lower lake levels that expose shelf sediments to wave-action. If the slope failure was due to a lower lake stand, water levels could have lowered 3-m (7- to 8-m BML). After 7500 cal BP, deep-water sedimentation at A/B (unit 2b) and shallow sedimentation at C/E (unit 3) suggest lake level was 4-m BML. It likely remained stable until 5000 cal BP, when several lines of evidence suggest an additional lake-level lowering by 1.5 to 2 m. These include an unconformity at 600-cm BML at C/E (unit 2), multiple unconformities between 550 and 460-cm BML at D (unit 2) and water depths between 5 and 7-m BML at A/B (unit 2b). The lake was meromictic probably due to a higher lake level between 4000 and 2000 cal BP. In addition to the diatom laminae at A/B (unit 2a), rising water levels are indicated at C/E (unit 2 and 1) and by water depths from 2.5 to 5-m at D (unit 1). Indications of raised shorelines are circumstantial evidence in support of this hypothesis, but require further investigation (L.C Cwynar, personal communication, 2005). A possible unconformity between 258 and 266-cm BML in D (unit 1), and increasing calcium carbonate in A/B (unit 1) support subsequently lower lake levels since 2000 cal BP.

Holocene Paleoclimate

The lake-level reconstruction indicates that, after correcting for sediment infilling, water levels were 3-m lower than modern between 10 000 and 5000 cal BP, higher than modern between 4000 and 2000 cal BP, and slightly below or near modern after 2000 cal BP (Figure 2.8). This lake-level history corresponds with the climatic history inferred from pollen by Cwynar's (1988) core retrieved at 760-cm BML (Figure 2.1) and reflected in the pollen record (Figure 2.3b). Cwynar (1988) used an age-model derived from 15 conventional radiocarbon dates of bulk sediment. Although there is some difference in timing (probably related to the different properties of bulk sediment dates) the two records are broadly consistent. The abundance of *Populus* (poplar) and *Artemisia* (sage) prior to 10 000 cal BP is interpreted as evidence of a warm, dry climate. Rising water levels after 10 000 cal BP correspond with the appearance of *Picea glauca* (white spruce), suggesting increasing effective moisture. By 6000 ¹⁴C BP (6800 cal BP), the *Picea glauca* (white spruce) woodland changed to a mixed spruce forest dominated by *Picea mariana* (black spruce), possibly indicating an increase in effective moisture (Cwynar, 1988; see also Cwynar and Spear, 1995). Rising lake levels also indicate increasing effective moisture, but only after 4000 cal BP. An overall decline in spruce and the disappearance of *Picea mariana* by 2000 ¹⁴C BP (2000 cal BP) corresponds with the establishment of lodgepole pine (*Pinus contorta*). It is unclear if this shift was driven by climate. Its timing at Marcella Lake coincides with decreasing lake levels. A comparison of these results with other regional proxies for early, middle and late Holocene paleoclimate follows.

Early Holocene (11 000 to 7500 cal BP)

During glacial times, lower sea level in addition to cooler North Pacific sea surface temperatures reduced moisture advection to interior regions (Mann and Hamilton 1995). Pollen

studies in Alaska and terrestrial evidence in the Yukon reflect late glacial aridity (Bigelow and Edwards 2001; Lauriol et al, 2001; 2002; Wang and Geurts, 1991). Rising sea level correlates with initial lake-level rises in Birch Lake (Abbott et al., 2000). The climatic response in the southwest Yukon to rising late-Pleistocene sea levels was delayed, perhaps by local climatic effects caused by the Cordilleran ice sheet. The first wet phase in Marcella Lake occurred later, between 10 000 and 9000 cal BP, which appears to correlate with the third wet phase at Birch Lake.

Several environmental changes in the northern Yukon indicate climate was warmer during this period when solar insolation was at a maximum. Spruce micro- and macrofossils found on the north coast suggest a northward position of boreal forest tree line (Ritchie et al., 1983). Additionally, a prevalent thaw unconformity dating ~9000 cal BP formed at the base of an active layer 2.5 times thicker than present (Burn, 1997). In the central Yukon, a thaw unconformity dates ~9500 cal BP (Burn 1986). Northern Yukon thaw lake formation was at a maximum ~9000 to 8000 cal BP (Mackay, 1992). In the southern Yukon, the early part of this period was arid, compared with the present day or the middle Holocene. These data are evidence for a warm and dry early Holocene. At 9000-10 000 cal BP there was a rapid increase in lake level, suggesting a shift in the precipitation regime. The early aridity may have prevented the regional establishment of spruce forest.

Middle Holocene (7500 to 4000 cal BP)

Between 7500 and 5000 cal BP lake levels were relatively stable 5-m BML, indicating conditions considerably drier than present and the immediately preceding period. This is consistent with reduced snow accumulation in the alpine zone of the southwest Yukon between 6700 and 4700 ¹⁴C-yr BP (Farnell et al., 2004), but conflicts with a high-resolution diatom-inferred salinity profile in the central Yukon that indicates a wet middle Holocene (Pienitz et al.,

2000). In terms of temperature, fossil spruce deposits on the eastern slopes of the St. Elias Mountains were found up to 70 m higher than modern tree line suggesting warmer conditions at 6500 cal BP (Denton and Karlén, 1977). Later, temperatures in the northern Yukon decreased. Peat-land permafrost development by 4700 cal BP suggests decreasing temperatures (Vardy et al., 1997) and ice-wedge growth, which was uncommon in the early Holocene, was underway by 4500 cal BP (Mackay 1992).

Late Holocene (4000 cal BP to present)

Regional cooling occurred during a period of higher than modern water levels between 4000 and 2000 cal BP and is contemporaneous with valley glacier advances in the St. Elias Mountains (Denton and Karlén, 1977). Three intervals of glacier expansion were documented (3400-2400, ~1200 and 400-90 cal BP) (Figure 2.8). Thus, as in central and northern Alaska, late Holocene glacial advances in the southwest Yukon appear to coincide with increasingly wet climatic conditions in addition to a millennial-scale decrease in summer insolation (Anderson et al., 2001; Lamoreaux and Cockburn, in press). Fossil spruce found above modern tree line dated between 4000-3000 and 2000-1000 cal BP, suggest favorable growing conditions occurred at times during a generally cooler and moister late Holocene. Marcella Lake levels dropped to near or slightly below modern by 2000 cal BP. This shift corresponds with increases in the paleosalinity documented by Pienitz et al. (2000) that also suggest increasing aridity. The resolution of the lake-level estimates is limited, but continuous sedimentation at shallow depths indicates water levels have remained near modern, with no major lowering since 1200 cal BP. Recent glacial advances since 400 cal BP represent, in most cases, maximum advances since deglaciation (Calkin et al., 2001) and probably reflect significant cooling during the Little Ice Age. Thus, the late Holocene has trended away from a moisture maximum and conditions during the last millennium have likely been drier than any since the middle Holocene.

Conclusions

Holocene sedimentation at Marcella Lake can be interpreted in terms of lake-level variation, providing a quantitative record of effective moisture variability. An early Holocene lake-level rise may have been significant for the regional establishment of spruce forest, but the region remained drier than present until 4000 cal BP. Early Holocene high stands in Marcella Lake coincide with higher than modern summer insolation. Wetter than modern conditions probably occurred between 4000 and 2000 cal BP, and coincide with the onset of late Holocene glacial activity and decreasing summer insolation. Nevertheless, after 2000 cal BP lake levels dropped and Little Ice Age glacial advances occurred under drier conditions than preceding millennia.

This long-term moisture record, together with modern climatological observations, allows us to propose a hypothesis for circulation adjustments that have controlled Holocene moisture changes. Moisture delivery in the region is strongly influenced by the strength and position of the Aleutian Low centered over the Gulf of Alaska. A weakened Aleutian Low favors more zonal atmospheric flow that could allow more moisture to reach interior areas. Such a scenario could be invoked for the period between 4000 and 2000 cal BP when lake levels were higher than today. In contrast, when effective moisture trends reversed 2000 cal BP, the Aleutian Low may have intensified, enhancing meridional on-shore airflow that intensifies the rain shadow effect and restricts moisture flow to the interior. Indeed, an increasing body of evidence suggests just such a mechanism (Spooner et al., 2004; Anderson et al., in press) and forthcoming research will evaluate this hypothesis in further detail (e.g. Fisher et al., 2004). This lake-level reconstruction serves to constrain the timing and direction of large-scale changes in effective moisture and thereby provide a framework for further, more detailed studies.

Table 2.1 AMS Radiocarbon data from Marcella Lake

Core Name	Core Depth	Depth BML	Material	Lab #	Measured Age	Median Calibrated	1 Sigma Range
Marcella Core A	31	991	Charcoal	CAMS-96830	1085 ± 35	970	952-1051
Marcella Core A	101	1061	Wood	CAMS-96832	2365 ± 40	2350	2345-2358
Marcella Core B	181	1141	Wood	CAMS-73153	4520 ± 40	5140	5050-5301
Marcella Core A	198	1158	Wood	CAMS-73144	5330 ± 40	6070	5995-6181
Marcella Core A	241	1201	Wood	CAMS-73145	7370 ± 110	8180	8031-8333
Marcella Core B	259	1219	Wood	CAMS-73148	7000 ± 40	7800	7757-7922
Marcella Core A	328.5	1288.5	Seed + wood	CAMS-98814	8955 ± 55	10170	9923-10210
Marcella Core A	361	1321	Macros + seeds	CAMS-96833	9260 ± 40	10445	10289-10500
Marcella Core A	378.5	1338.5	Aquatic macro ¹	CAMS-73146	11110 ± 50	13135	12990-13171
Marcella Core B	405	1365	Wood	CAMS-73147	9200 ± 50	10330	10241-10474
Marcella Core A	429 (259)	1389	Wood	CAMS-73154	7060 ± 40	7900	7793-7938
Marcella Core B	458 (288)	1418	Wood	OS-12129	8560 ± 60	9530	9499-9550
Marcella Core A	466 (296)	1426	Wood	CAMS-96834	8605 ± 40	9550	9533-9553
Marcella Core B	478 (308)	1438	Aquatic macro ¹	OS-12130	10650 ± 50	12715 ¹	12631-12894
Marcella Core A	520 (350)	1480	Wood	OS-12131	9090 ± 55	10220	10213-10242
Marcella Core E	41	471	Wood	OS-38713	930 ± 25	830	791-915
Marcella Core C	44	474	Plant stem	CAMS-96826	980 ± 60	925	793-951
Marcella Core E	133	573	Plant stem	OS-38714	4080 ± 35	4545	4451-4781
Marcella Core C	154	584	Wood	CAMS-96827	3880 ± 90	4330	4152-4420
Marcella Core C	161	591	Aquatic macro ¹	CAMS-73149	4410 ± 50	5020 ¹	4870-5047
Marcella Core C	174	604	Wood	CAMS-96828	4980 ± 40	5665	5655-5743
Marcella Core D	233	428	Aquatic macro ¹	CAMS-73150	3830 ± 60	4200 ¹	4098-4350
Marcella Core D	327.5	522.5	Wood	CAMS-96829	7770 ± 110	8580	8413-8638
Marcella Core D	353	548	Seed	CAMS-73151	8530 ± 130	9530	9433-9595
Marcella Core D	359	554	Seed	CAMS-73152	8840 ± 120	10100	9634-10177
Marcella Core F	337	1037	Pollen ²	CAMS-92157	6595 ± 40	7475 ²	7430-7561

¹ Aquatic material is suspect because of possible hard water effects ² Brown *et al.* (1989) Shaded ages are within the displaced material removed from the adjusted stratigraphy (Figure 2.4)

Depths in parenthesis are corrected for displaced material removed from

Table 2.2 Sediment description and lake-level interpretation with estimated ages

Core	Unit	Description	Interpretation	Est. Age (cal BP)
A/B	1	Olive-brown gelatinous organic mud. Irregular, faint laminations.	Modern depth, ~9.7m.	2-0
	2a	Black gelatinous organic mud. Millimeter-scale diatom laminations.	>10 m water depth. Meromixis.	4.5-2
	2b	Dark-olive-brown organic mud. Faint color banded structure.	6 to 8 m water depth.	7.5-4.5
	3a	Dark-brown organic mud. Unconformity at base of unit.	Displaced sediment. Possible low-stand.	8.0-7.5
	3b	Strongly-laminated brown organic marl. Shells. Unconformity at base.	9 to 10 m water depth.	9.5-8.0
	3c	Dark-gray silty marl.	Re-worked shoreline sediment. Rising lake-levels.	10-9.5
	4	Gravel and sand.	Subaerial exposure.	>10
C/E	1	Light-olive brown strongly-laminated organic marl. Well-preserved <i>Chara</i> .	4 to 6 m water depth.	4.5-0
	2	Olive-brown, strongly-laminated organic marl. Poorly-preserved <i>Chara</i> . Unconformity at base.	> 6 m water depth.	5-4.5
	3	Dark-brown macrophyte-rich organic mud. Strongly laminated. Poorly preserved <i>Chara</i> . Bivalve shells.	1 to 3 m water depth.	6-5
	4	Gray-brown shelly silt.	Reworked shoreline sediment.	7.5-6
D	1	Light olive-brown strongly-laminated organic marl. Well-preserved <i>Chara</i> .	3 to 5 m water depth.	4.5-0
	2	Olive-brown organic marl. Shells. Multiple unconformities.	Reworked shoreline sediment.	8.5-4.5
	3	Dark-olive-brown strongly-laminated organic mud. Bivalve shells.	1 to 2 m water depth.	10-8.5
		Gravel	Sub-aerial exposure.	>10

Table 2.3 Summary of bulk sediment properties and inferred water depth

Measurement	>8 m deep	5 to 8 m deep	<5 m deep
Magnetic Susceptibility	0 (SI)	0 (SI)	0 to 10 (SI)
Bulk density	0.1 to 0.2 (gcm ⁻¹)	0.1 to 0.2 (gcm ⁻¹)	0.3 to 0.5 (gcm ⁻¹)
% LOI (550°C)	60 to 80% ¹	30 to 40%	10 to 20%
% CaCO ₃	0 to 20%	30 to 40%	70 to 80%
δ ¹³ C	-26 to -27.5‰	-28.5 to -29.5‰	-30.5 to -31.5‰
δ ¹⁵ N	0 to -1‰	2 to 3 ‰	2 to 3‰
C/N ratio	14 to 16.5	11 to 13	12 to 13

¹ %LOI (550°C) values are ~2.8x larger than %organic carbon for comparison with core A/B values in Figure 2. 4.

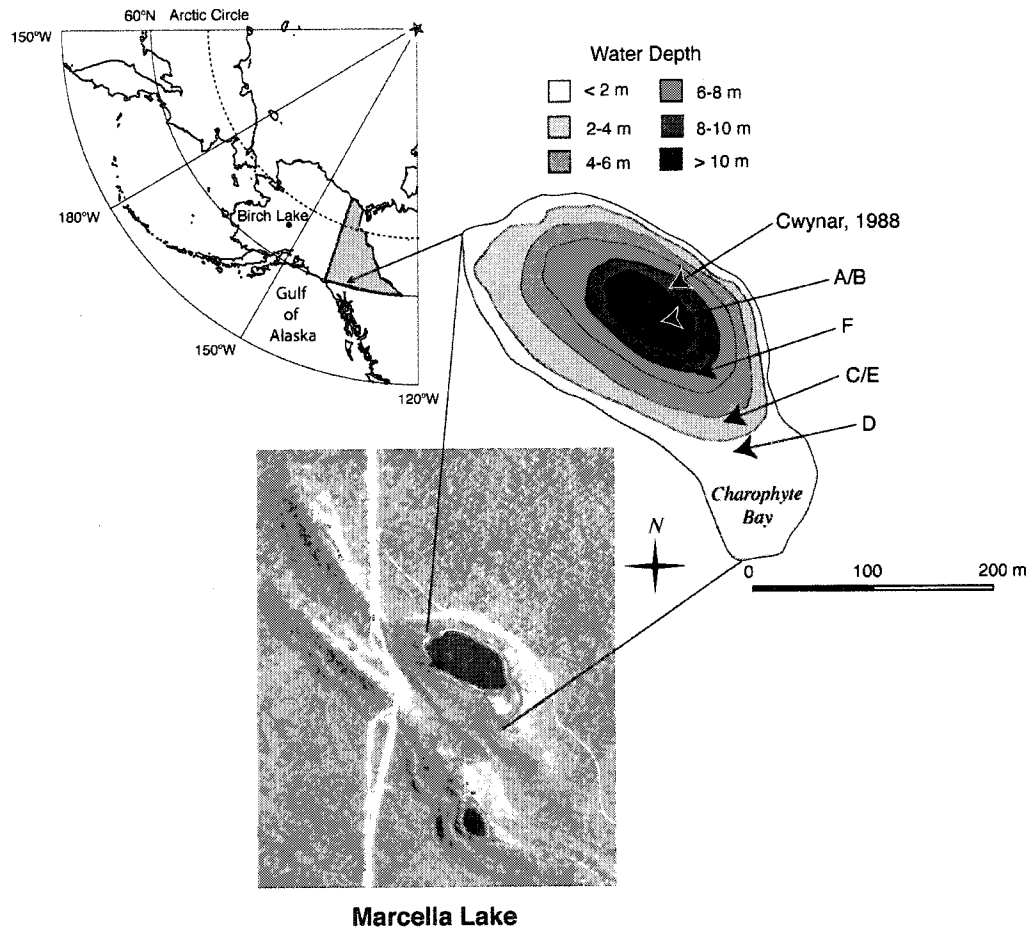


Figure 2.1. Location of the Yukon Territory, Marcella Lake and Birch Lake (modified from the Atlas of Canada, Natural Resources Canada) indicating core locations for this study and that of Cwynar (1988). (Photograph A22408, copyright 1949 by Her Majesty the Queen in Right of Canada, reproduced from the collection of the National Air Photo Library, with permission of Natural Resources Canada).

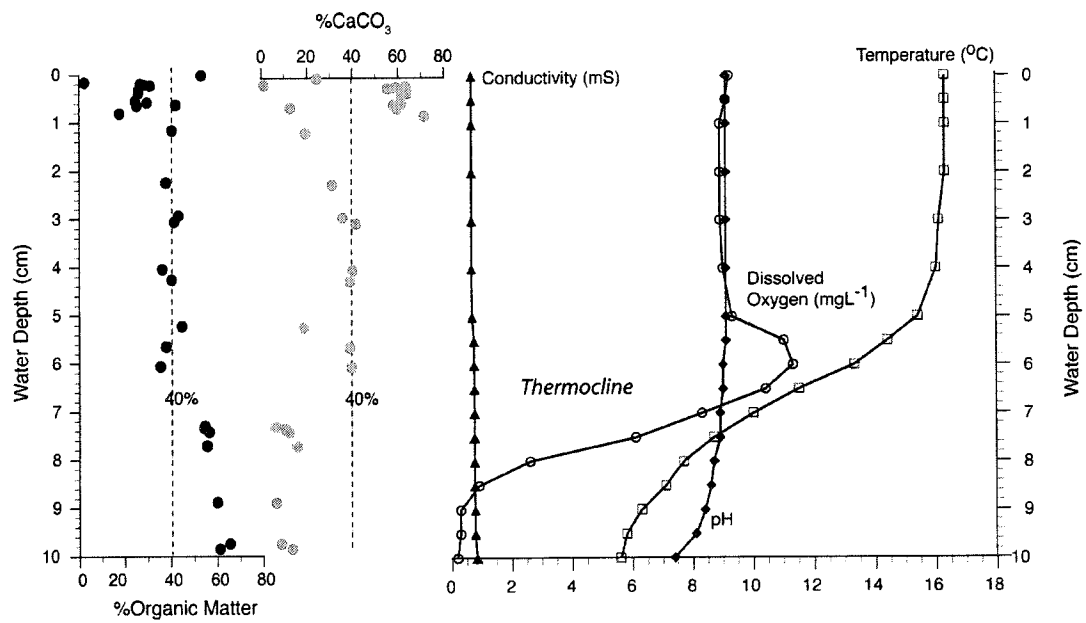


Figure 2.2. Surface sediment %LOI (unpublished data, courtesy of L.C. Cwynar) and water column measurements of Marcella Lake in July 2000.

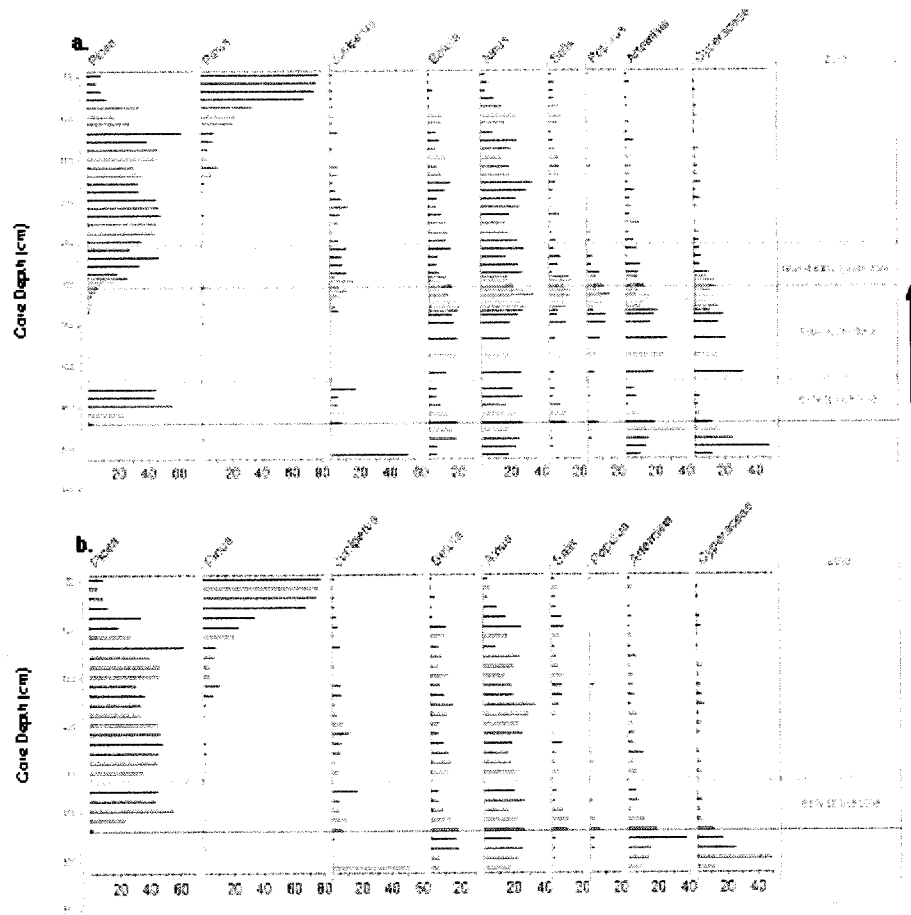


Figure 2.3. Core A/B pollen percentages of key taxa with depth for: (a) the whole section without adjustment and (b) after adjustment by removing suspect material between 429 and 260-cm depth.

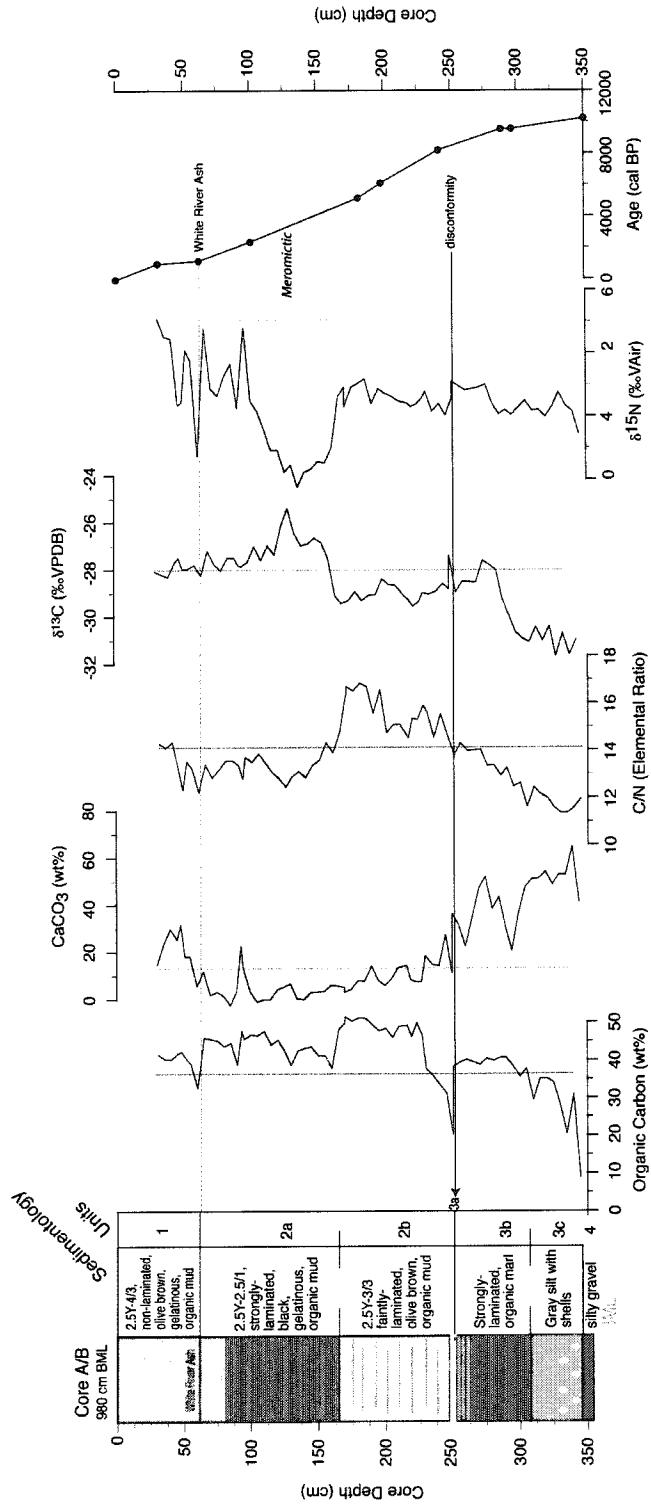


Figure 2.4. Core A/B, 960 cm water depth, showing stratigraphy, organic carbon (elemental analyzer method), calcium carbonate, C/N, δ¹³C, δ¹⁵N and median calibrated radiocarbon ages by depth

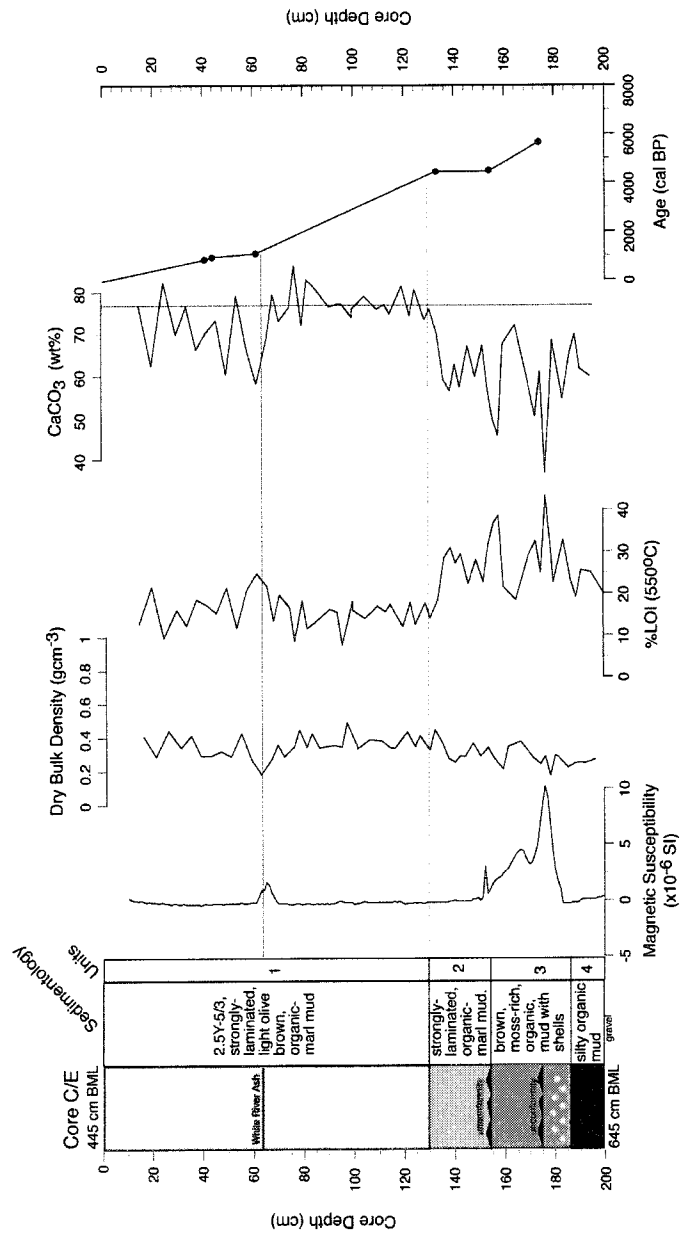


Figure 2.5. Core C/E, 430 cm water depth, showing stratigraphy, magnetic susceptibility, dry bulk density, organic matter (%LOI method), calcium carbonate and median calibrated radiocarbon ages by depth

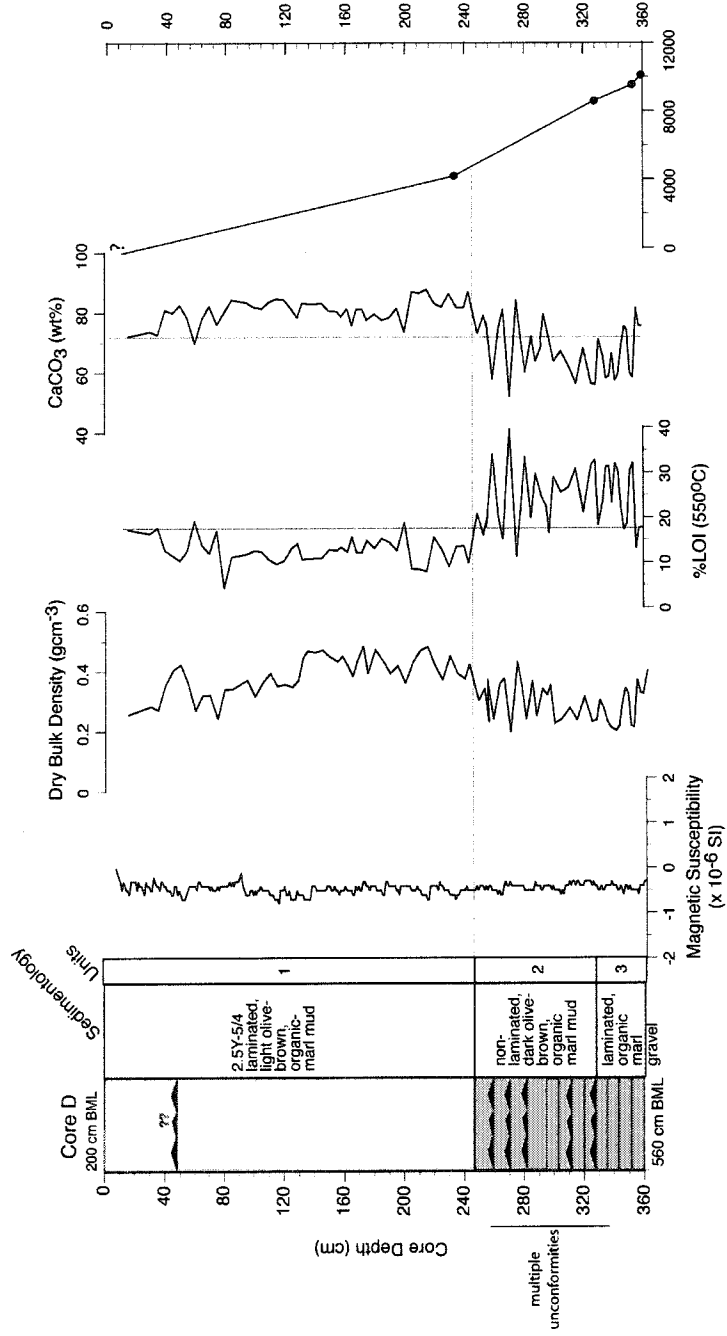


Figure 2.6. Core D, 195 cm water depth, showing stratigraphy, magnetic susceptibility, dry bulk density, organic matter (%LOI method), calcium carbonate and median radiocarbon calibrated ages by depth

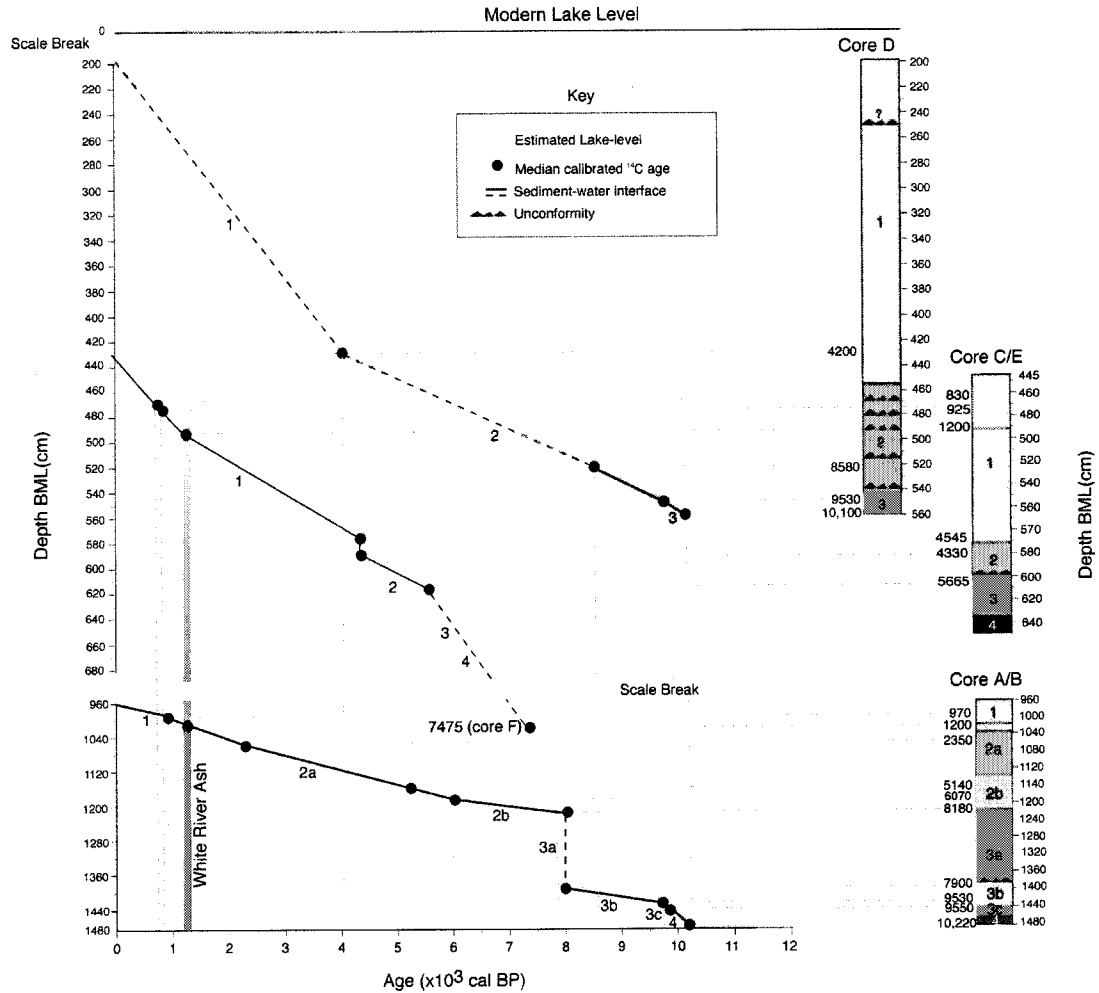


Figure 2.7. Lake level reconstruction with A/B, C/E and D stratigraphies below modern level (BML) on a calibrated radiocarbon age scale. Lines between calibrated ages (black circles) indicate continuous sedimentation (solid line) and discontinuous sedimentation (dash). Gray shading represents lake-level estimates.

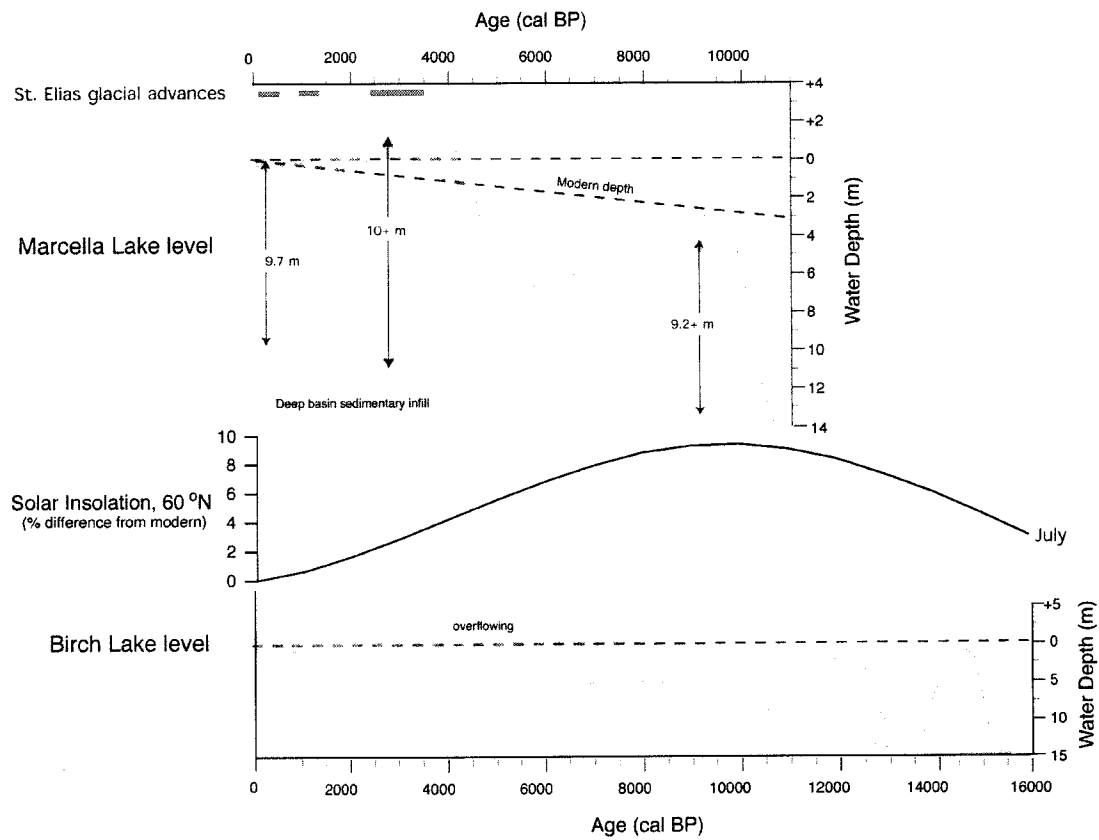


Figure 2.8. Correlation on a calibrated radiocarbon time scale of Marcella Lake water levels with glacier activity in the St. Elias Mountains (Denton and Karlén, 1977), July insolation at 60 °N (Berger and Loutre, 1991) and water levels at Birch Lake, Alaska (Abbott et al., 2000). High stands occurred when summer insolation was high in early Holocene and when it was relatively low in the late Holocene.

CHAPTER 3

REGIONAL ATMOSPHERIC CIRCULATION CHANGE IN THE NORTH PACIFIC DURING THE HOLOCENE INFERRED FROM LACUSTRINE CARBONATE OXYGEN ISOTOPES, YUKON TERRITORY, CANADA

Abstract

Analyses of sediment cores from Jellybean Lake, a small, evaporation-insensitive groundwater-fed lake, provide a record of changes in North Pacific atmospheric circulation for the last ~7500 years at five- to thirty-year resolution. Isotope hydrology data from the southern Yukon indicates that the oxygen isotope composition of water from Jellybean Lake reflects the composition of mean-annual precipitation, $\delta^{18}\text{O}_p$. Recent changes in the $\delta^{18}\text{O}$ of Jellybean sedimentary calcite ($\delta^{18}\text{O}_{ca}$) correspond to changes in the North Pacific Index (NP), a measure of the intensity and position of the Aleutian Low pressure system (AL). This suggests that $\delta^{18}\text{O}_p$ variability was related to the degree of fractionation during moisture transport from the Gulf of Alaska across the St Elias Mountains and that Holocene shifts were controlled by the intensity and position of the AL. Following this model, between ~7500 and 4500 cal BP, long-term trends suggest a predominantly weaker and/or westward AL. Between ~4500 and 3000 cal yr B.P. the AL shifted eastward and/or intensified before shifting westward and/or weakening between ~3000 and 2000 cal yr B.P. Rapid shifts eastward and/or intensification occurred ~1200 and 300 cal yr B.P. Holocene changes in North Pacific atmospheric circulation inferred from Jellybean Lake oxygen isotopes correspond with late Holocene glacial advances in the St Elias Mountains, changes in North Pacific salmon abundance and shifts in atmospheric circulation over the Beaufort Sea.

Introduction

The intensity and position of the Aleutian Low (AL), the semi-permanent low pressure located over the Gulf of Alaska, has emerged as an important control on Northwest Pacific Holocene climate (e.g. Heusser et al., 1985; Latif and Barnett, 1994; Mann et al., 1998; Edwards et al., 2001). Decadal-scale variability of the AL was recognized by analyses of instrumental data and described by indexes, such as the North Pacific index (NP) (Trenberth and Hurrell, 1994) and the Pacific Decadal Oscillation (PDO) (Mantua et al., 1997). These indices were correlated with tree-ring and salmon abundance data (e.g., Biondi et al., 2001; Mantua et al., 1997) and snow accumulation, a proxy for moisture delivery (Bitz and Battisti 1999; Moore et al., 2002a, 2002b). The AL is the main synoptic climate feature related to moisture delivery to the St Elias Mountains of Alaska and the interior of the southern Yukon (Mock et al., 1998; Wahl et al. 1987). The St Elias Mountains have a dramatic effect on the oxygen-isotope values of precipitation on both the coastal and interior sides of the mountains. Relatively ^{18}O -enriched precipitation falls on the coastal side compared to strongly ^{18}O -depleted precipitation just 200-km inland. This large fractionation between coastal and interior precipitation suggests that changes in air mass trajectories and moisture transport history from the Gulf of Alaska either over or around the St. Elias Mountains are a principle influence on precipitation- $\delta^{18}\text{O}$ at Jellybean Lake, located ~250 km inland in the southwest interior Yukon (Figure 3.1).

Few studies have documented long-term high-resolution climatic variability beyond the last millennia from high latitudes in northwestern North America (e.g., Heusser et al., 1985; Pienitz et al., 2000; Anderson et al., 2001; Hu et al., 2001). Although recent climatic and environmental changes around the Gulf of Alaska have been documented by tree-ring and ice core studies (Holdsworth et al., 1992; Mann, et al., 1998; Wiles et al., 1998, 1999; D'Arrigo et al., 1999; Wake et al., 2002; Davi et al., 2003), these records generally extend from <100 to a

maximum of ~1000 years B.P. Comparatively little is known about high-resolution climatic variability during the Holocene in the nearby interior regions of the Yukon Territory (Pienitz et al., 2000). Holocene climate changes at century to millennial time-scales in the interior Yukon Territory were inferred by geomorphological evidence of late Holocene glacial advances (Denton and Karlen, 1977; Calkin et al., 2001), pollen records (Heusser et al., 1985; Cwynar, 1988; Wang and Guerts, 1991; Keenan and Cwynar, 1992; Cwynar and Spear, 1995; Spear and Cwynar, 1997; Lacourse and Gajewski, 2000) and multiproxy paleolimnological investigations (Pienitz et al. 2000).

There is considerable spatial climatological variability in the southern Yukon Territory and adjacent Alaska due to complex topography and the influence of airmasses originating in the Arctic, Gulf of Alaska and Bering Sea (Streten 1974; Wahl et al., 1987). Such regional climatic heterogeneity and absence of long-term high-resolution paleoclimatic data make it difficult to adequately describe sub-century scale regional paleoclimate and investigate forcing mechanisms that caused Holocene climatic change. Recent studies have explored the possibility of cyclic variations in solar output (Hu et al., 2003; Wiles et al., 2004) and North Pacific ocean-atmosphere circulation changes (Heusser et al., 1985; Moore et al., 2002a, b; Spooner et al., 2003).

We analyzed oxygen isotopes in sediment cores from Jellybean Lake (Figure 3.1), located in the southern Yukon interior, to improve the detail and resolution of the regional climatic history and investigate mechanisms for Holocene climatic change. Jellybean Lake is a small, hydrologically-open lake located in the rain shadow of the St. Elias Mountains. Precipitation of calcium carbonate occurs within the water column, thereby allowing us to measure sedimentary carbonate oxygen isotope ratios to produce a record of paleoenvironmental change. The sampling resolution, sensitivity of the geochemical data and chronology are of sufficient detail at this new site to document Holocene climatic variability at ~5 to 30-year resolution back to ~7500 cal yr B.P.

Paleoclimatic Application of Jellybean Lake Oxygen Isotopes

Oxygen isotope ratios of authigenic lake sediment carbonate ($\delta^{18}\text{O}_{\text{Ca}}$) are related to climate because $\delta^{18}\text{O}_{\text{Ca}}$ is a function of: 1) lake-water temperature and 2) lake-water $\delta^{18}\text{O}$. The latter is, in turn, controlled by lake hydrology and regional climate (e.g., Talbot, 1990; Edwards et al., 1996; von Grafenstein et al., 1996). Lake-water $\delta^{18}\text{O}$ in hydrologically-closed lakes with a small catchment to surface area ratio may be strongly influenced by the effects of evaporation. Increased evaporation leads to lake-water ^{18}O -enrichment. In contrast, hydrologically-open lakes that have large catchment to surface area ratio, or short residence times, are typically less affected by evaporation. In such lakes the $\delta^{18}\text{O}$ is mainly controlled by the $\delta^{18}\text{O}$ of inflow water. The oxygen isotope composition of inflow water, is influenced by several processes within the climate system including the source of the moisture, its transport path and rainout history, as well as seasonality and the air temperature during precipitation events (Ingraham, 1998). There is a strong correlation between air temperature and the $\delta^{18}\text{O}$ of precipitation in northern latitudes (Dansgaard, 1964; Rozanski et al., 1992). Derivations of past atmospheric temperature from lacustrine-sediment $\delta^{18}\text{O}$ usually assume that other factors such as changes in moisture source area, transport, and air mass history are relatively insignificant (e.g., Shemesh et al., 2001; Hu and Shemesh, 2003), which will not always be the case. One way to assess these factors is through studying modern isotopic, hydrologic, and limnologic conditions of the individual lakes within a study area (e.g., Leng and Anderson 2003; Hammerlund et al., 2003; Rosqvist et al., 2004). Comparing modern lake water $\delta^{18}\text{O}$ with environmental factors such as hydrology and elevation allows more reliable climatic interpretations of paleo-lake water $\delta^{18}\text{O}$ results.

Field Area

Jellybean Lake (informal name, 60.35 °N, 134.80 °W, 730-m a.s.l.) is a small (0.4 km²), relatively deep (11.6 m), elongate lake located 40 km south of Whitehorse in the southern Yukon Territory, Canada (Figure 3.1). The lake is situated in a large esker complex characterized by numerous narrow ridges 15 to 50-m high composed of well-sorted gravel and sand. The esker complex presumably formed in subglacial and englacial tunnels during deglaciation of the southern Yukon ~11,000 years ago (Dyke et al., 2002). The 50-m high esker ridges along the north, east and west sides of the lake define the lake basin. The watershed is dominated by open stands of trembling aspen (*Populus tremuloides*) and white spruce (*Picea glauca*). Sage (*artemesia*) and grasses (*poaceae*) grow on the well-drained south facing slopes. The surrounding esker ridges define a small local watershed around the lake and there is no surface inflow or outflow. A broad north-south trending ridge, 1640-m a.s.l., defining the eastern side of the Robinson Valley, is located ~12 km east of Jellybean Lake and likely provides the source area for the local groundwater.

Jellybean Lake is located ~250 km northeast of the Gulf of Alaska (Figure 3.1). Coastal climate stations report over 3000 mm/yr of annual precipitation, but a strong rain shadow effect limits annual precipitation in the southern interior regions to ~250 mm/yr (Wahl et al., 1987). Approximately 60% of annual precipitation occurs during ice-free months between May and September, when daylight is at a maximum (Figure 3.2). The Gulf of Alaska is the primary source region for airflow in the Yukon (Wahl et al., 1987). Mean annual temperatures at Whitehorse are between -2 and 0°C. July mean temperatures are between 10 and 15°C (Environment Canada, 2003; Figure 2.2). Monthly $\delta^{18}\text{O}$ measurements between 1962 and 1964 AD show a seasonal $\delta^{18}\text{O}$ cycle ranging from -24.6 to -16.8‰ (IAEA/WMO, 2001; Figure 3.2). More ¹⁸O-enriched precipitation occurs during the summer months. The average $\delta^{18}\text{O}$ and $\delta^2\text{H}$

from May through September between 1961 and 1965 AD was -18.3 and -142.8‰, respectively (Table 3.1). Mean annual $\delta^{18}\text{O}$ and $\delta^2\text{H}$ values were -20.4 and -160.1‰ from 1962 to 1964 AD.

Methods

Water samples were collected from Jellybean Lake, 7 nearby lakes, 3 local springs, and 61 other lakes throughout the southern Yukon in July 2000 and 2002 to document the local and regional isotope hydrology (Anderson, 2005). Samples were taken from near-shore areas or the middle of each lake in a 30-ml HDLP Nalgene bottle. Bottles were rinsed with lake water before sample collection and sealed to avoid air bubbles. Precipitation was collected from a sustained rain event on August 6, 2000 (Table 3.1). Water samples were analyzed for oxygen and hydrogen isotopic composition by automated constant temperature equilibration with CO_2 and automated H/D preparation systems, respectively, for isotope ratio mass spectrometry. Results are expressed as δ -values, representing deviations in per mil (‰) from Standard Mean Ocean Water (VSMOW) such that $\delta_{\text{sample}} = [(R_{\text{sample}}/R_{\text{standard}})-1]*1000\text{‰}$, where R is the $^{18}\text{O}/^{16}\text{O}$ and $^2\text{H}/^1\text{H}$ ratios in sample and standard, respectively. Analytical uncertainties are within $\pm 0.5\text{‰}$ and $\pm 0.05\text{‰}$ for hydrogen and oxygen, respectively.

Water column temperature, pH, conductivity and dissolved oxygen were measured in July of 2000 with a Hydrolab Surveyor 4 and Datasonde 4 device. Dissolved carbon dioxide in surface lake water ($p\text{CO}_2$) was determined by applying Henry's Law to samples of ambient air and samples of CO_2 gas collected from a head space of known volume from a container of agitated lake water (Plummer and Busenberg, 1982). Surface water samples for cation and anion chemistry were collected in 30-ml HDLP Nalgene bottles and stored in the dark at cool temperatures. Alkalinity was determined by titration in the laboratory. Cation and anion

concentrations were determined by a Dionex DX500 ion chromatograph and reported in mgL^{-1} (Table 3.2).

Lake bathymetry was determined by sonar soundings (Figure 3.1). A 78-cm and 3.6-m long sediment core were retrieved from the deepest parts of Jellybean Lake from a floating platform in July 2000 and 2002 using a modified Livingstone square rod coring device that allowed preservation and extrusion of the uppermost sediments in 0.5 cm increments. Multiple sedimentary properties were used to describe the general sedimentology of the cores. Sediments were visually logged to identify Munsell color, sedimentary structures, and biogenic features. Magnetic susceptibility was used as a proxy for changes in mineral content and measured on half cores at a 0.5 cm interval with a Bartington susceptibility meter (Thompson, 1986). Wet and dry bulk density and water content were determined. Weight percent organic matter and calcium carbonate were determined by the loss-on-ignition (%LOI) method (Bengtsson and Enell, 1986; Heiri et al., 2001). Weight percent CaCO_3 was estimated based on the proportion of CO_2 in CaCO_3 using the following calculation: $[\% \text{LOI} - 1000^\circ\text{C} * (100/44)]$.

The sediment core chronology is based on ^{210}Pb , ^{137}Cs , AMS ^{14}C measurements on identifiable macrofossils, and the White River tephra (Claugue et al., 1995; Table 3.3). Terrestrial macrofossils were not present in sufficient quantities for radiocarbon measurements at some stratigraphic levels. Therefore, purified spruce pollen samples were used (Brown et al., 1989). Both measured and calibrated ages are reported, but only calibrated ages are used for discussion. Radiocarbon ages were calibrated using CALIB 4.1 following Stuiver et al. (1998). ^{210}Pb and ^{137}Cs activities for Jellybean Lake were measured on 0.5-cm slices extruded in the field from a polycarbonate-barrel piston interface core. A constant rate of supply model (CRS) was used to determine ^{210}Pb ages (Appleby, 2001; Figure 3.3). A prominent ^{137}Cs peak is within 0.5 cm of the slice estimated to correspond to 1963 AD based on the ^{210}Pb age model, leading to an estimate of ± 5 -yr precision for the last 100 years. An age model for Jellybean Lake was constructed using the ^{210}Pb and ^{137}Cs data, 7 ^{14}C measurements, and the White River tephra

(Figure 3.4f). A linear interpolation between dated depths was used to determine ages of sediment samples. The chronology indicates a fairly uniform sedimentation rate, ~0.05 to 0.075 mm/year. Based on sedimentation rates and sample thickness, the oxygen and carbon isotope samples integrate 3 to 6 years in the uppermost 16.5-cm, and 10 to 30 years for the remainder of the core.

The core was continuously sampled at high resolution for oxygen and carbon isotopes. Sub-samples of bulk sediment were taken at a 0.5-cm increment for the uppermost 30 field-extruded samples and every 1-cm for the remainder of the core for a total of 351 samples. The samples were freeze dried, examined for purity, and powdered before sub-sampling and CO₂ extraction by a Kiel automated device for isotope ratio mass spectrometry on a Finnigan Delta XL mass ratio spectrometer. Oxygen and carbon isotope results are expressed as δ -values, representing deviations in per mil (‰) from the Vienna Peedee Belemnite standard (VPDB) such that $\delta_{\text{sample}} = [(R_{\text{sample}}/R_{\text{standard}})-1]*1000\text{‰}$, where R is the ¹⁸O/¹⁶O and ¹³C/¹²C ratios in sample and standard, respectively. Analytical uncertainties are within $\pm 0.1\text{‰}$ and $\pm 0.05\text{‰}$ for oxygen and carbon, respectively. $\delta^{18}\text{O}_{\text{Ca}}$ and $\delta^{13}\text{C}_{\text{Ca}}$ values were duplicated within the range of analytical error.

Results

Limnology and Isotope Hydrology of Jellybean Lake

Jellybean Lake is currently thermally unstratified and chemically mixed. The water column measurements indicate only minor changes in temperature, pH, specific conductivity, and dissolved oxygen with water depth (Anderson, 2005). Sub-surface artesian springs feed the lake at several depths, presumably maintaining the mixed state during the ice-free season. Water level appears to vary inter-annually, as the lake level in July 2002 was 1-m higher than July 2000.

Interannual lake-level variability is probably related to seasonal and annual changes in hydraulic pressure in the recharge area. Jellybean Lake water has a pH of 8.2 and is supersaturated in CO₂, rich in dissolved calcium and cooler (14.8 °C) than a nearby thermally stratified, hydrologically-closed lake of similar size (16.3 °C; Table 3.2). Jellybean Lake specific conductivity and major ion concentrations are lower than the hydrologically-closed lake, reflecting the effects of short residence times. The δ¹⁸O of Jellybean Lake water (average -20.4‰) was identical to mean annual precipitation (-20.4‰) and almost identical to local spring water sampled within a few km of Jellybean Lake (-21.5‰; Table 3.2). Since groundwater dynamics tend to smooth the effects of individual rainstorms and seasonal variations, groundwater-δ¹⁸O tends to reflect mean annual isotope composition of precipitation (Ingraham, 1998; Gonfiantini et al., 1998; Table 3.1 and 3.2).

We conducted a survey of the oxygen and hydrogen isotope ratios of water throughout the southern Yukon to compare Jellybean Lake water with precipitation, springs, rivers and other lakes in the region (Figure 3.5; Table 3.2). Hydrologically-closed lakes in this region are strongly influenced by evaporation as indicated by relatively δ¹⁸O-enriched isotope values. The precipitation data from Whitehorse and Mayo was used to define the Local Meteoric Water Line (LMWL) and has a slope of ~6. The LMWL has a slightly lower slope than the Global Meteoric Water Line (GMWL) which has a slope of ~8. Surface water from lakes in the Yukon defines a local evaporation line (LEL) with a slope of ~4. The LEL has a lower slope than the LMWL and GMWL because diffusion controlled isotopic fractionation that occurs during evaporation causes greater ¹⁸O-¹⁶O separations than ²H-¹H. Most evaporation-sensitive lakes have δ¹⁸O values ranging between -14‰ and -7.7‰. In contrast, most evaporation-insensitive lakes such as Jellybean Lake have more depleted δ¹⁸O values ranging between -22‰ and -17‰. The intersection point of the LEL and LMWL defines the average isotope values for unmodified mean annual precipitation, and corresponds with our data for groundwater and Jellybean Lake.

Taken together, the strong similarities between Jellybean Lake $\delta^{18}\text{O}$ and regional groundwater, precipitation and other hydrologically-open lakes, suggests that despite its small catchment and lack of surface inflow or outflow, Jellybean Lake acts as an evaporation-insensitive lake. Subsurface inflow and outflow must be rapid enough to prevent significant evaporative enrichment above the regional average of precipitation and groundwater $\delta^{18}\text{O}$ values. Jellybean Lake water $\delta^{18}\text{O}$ is therefore a good representative of regional precipitation. Surface sediment carbonate in Jellybean Lake is in isotopic equilibrium with lake-water $\delta^{18}\text{O}$ as indicated by the temperature equation of Epstein et al. (1953). The predicted surface water value for $\delta^{18}\text{O}_{\text{Ca}}$ at 14.8°C of -20.3‰ (VPDB) is very similar to the measured $\delta^{18}\text{O}_{\text{Ca}}$ value of -19.9‰ (VPDB; Table 3.3).

Core Sedimentology

A suite of multi-proxy sedimentary analyses was performed on cores from Jellybean Lake to document changes in paleolimnology and evaluate controls on the isotope data. The 340-cm sediment stratigraphy is primarily composed of olive to light gray laminated marl with minor mineral matter, reflected by low magnetic susceptibility and dry bulk density (Figure 3.4). The White River tephra at 64 cm (1150 cal BP, Clague et al., 1995), is easily identified both visually and by a sharp increase in magnetic susceptibility (~60 SI). The calcium carbonate content varies between 80 and 85%. Sedimentary laminations are typically between 0.25 to 1.0-cm thickness. Smear slide analyses indicate that the color variations between laminae are caused by changes in the relative proportion of organic carbon and calcium carbonate content. The lake water is clear (Secchi disk depths >8m) and calcite crystals form within the water column when photosynthetic activity alters the bicarbonate equilibrium during intense periods of productivity. Smear slide studies of the sediments show that they are nearly pure authigenic micrite. Other carbonate

components such as ostracode tests, charophyte encrustations, mollusks and gastropod shells were not observed in the nearly pure fine-grained calcium carbonate muds with the exception of some gastropods in the lowermost 15-cm.

Sedimentary color, texture and composition variations are generally consistent throughout the core. The only exception is where ~30-cm of sediment overlying the White River tephra at 64-cm depth are darker and more faintly laminated. Calcium carbonate weight percentages decrease to less than 5% and organic carbon increases by ~30%. Magnetic susceptibility values are slightly higher, reflecting a higher proportion of mineral material that was also evident in smear slide observations. Nevertheless, by ~34 cm-depth, calcium carbonate concentrations recover to >30% and range from ~40 to 60% to the core top. The uniform character of the sediments throughout the majority of the core suggests that physical and chemical characteristics similar to the modern lake have been stable for the last ~7500 years.

In addition to the evidence for interannual water-level variations observed at Jellybean Lake today, there is sedimentary evidence for lake-level changes in the past. There are two visible changes in the sediments to pelletized marl between 150-160 cm and 240-250 cm (Figure 3.4). Such pelletized marls were noted on sub-aerial shoreline surfaces around the lake today. There are minor changes in the bulk density within these intervals, but organic carbon and calcium carbonate content are not significantly altered. If these layers were formed during lower lake-levels, with possible sub-aerial exposure, neither the oxygen isotope values nor the sediment accumulation rates appear to have been affected (Figure 3.6). The events were either sufficiently brief and/or the open-hydrological status of the lake remained unaffected because these periods were not registered in the $\delta^{18}\text{O}_{\text{ca}}$ record.

Oxygen and Carbon Isotopes

Oxygen isotope values of sedimentary carbonate vary between -18.5 and -20.5‰ (Figures 3.6 and 3.2; Table 3.1). Carbon isotopes have a larger range of variability (~4.5‰) and are relatively ^{13}C -depleted (-3.5 to -7.5‰). The oxygen and carbon isotopes are poorly correlated ($r=0.24$), a general characteristic of carbonates formed in open lake systems (Talbot, 1990). However, both the $\delta^{18}\text{O}_{\text{Ca}}$ and $\delta^{13}\text{C}_{\text{Ca}}$ rapidly decrease near the White River tephra at 64 cm. Close examination of the data indicates that $\delta^{18}\text{O}_{\text{Ca}}$ began to deplete before deposition of the tephra, while the $\delta^{13}\text{C}_{\text{Ca}}$ depletion occurred after the tephra was deposited. Thereafter, $\delta^{13}\text{C}_{\text{Ca}}$ values increased more slowly than $\delta^{18}\text{O}_{\text{Ca}}$ values.

Discussion

Carbon Isotopes

Carbon isotopes of lacustrine carbonate ($\delta^{13}\text{C}_{\text{Ca}}$) reflect the isotopic composition of dissolved inorganic carbon (DIC). DIC is in turn a reflection of the balance between sources in groundwater and precipitation, atmospheric exchange, and $p\text{CO}_2$ derived from respiration of isotopically depleted organic matter within the lake and its water sources (Oana and Deevey, 1960; McKenzie, 1985; Siegenthaler and Eicher, 1986; Herczeg and Fairbanks, 1987; Dean and Stuiver, 1993). Changes in $\delta^{13}\text{C}_{\text{Ca}}$ may reflect changes in rates of biological productivity, atmospheric CO_2 exchange within the lake, stratification, hydrology or some combination of all of these factors, which may be directly or indirectly related to climatic change. Jellybean $\delta^{13}\text{C}_{\text{Ca}}$ values (-3 to -7.5‰) are typical of productive lakes. Groundwater generally has relatively depleted values between -10 and -15‰, while exchange with atmospheric CO_2 via mixing and photosynthesis leads to DIC ^{13}C -enrichment. The relatively depleted carbon isotope values of

Jellybean Lake DIC probably represent the signature of ^{13}C -depleted groundwater that is subsequently modified by biological productivity and atmospheric exchange.

The decrease in $\delta^{13}\text{C}_{\text{Ca}}$ values above the White River tephra suggests a shift in biological activity and watershed run-off. The tephra could have lowered lake-pH and increased turbidity. These changes might have lead to decreased photosynthesis, decreased carbonate production and/or increased carbonate dissolution (Figures 3.4 and 3.6) and explain why $\delta^{13}\text{C}_{\text{Ca}}$ -recovery is notably longer than $\delta^{18}\text{O}_{\text{Ca}}$. Increased clastic sedimentation during this interval suggests that vegetation around the watershed was diminished and more clastic sediment was mobilized during precipitation events and/or spring run-off. The carbon isotope response to the White River tephra illustrates the complications associated with a direct climatic interpretation of $\delta^{13}\text{C}_{\text{Ca}}$ in Jellybean Lake. Therefore, we chose to use the oxygen isotope data for climatic interpretations.

Oxygen Isotopes

Our results from water samples collected from a range of hydrological settings across the region suggest that variations in the oxygen isotope composition of precipitation ($\delta^{18}\text{O}_p$) are responsible for driving the observed changes in Jellybean Lake $\delta^{18}\text{O}$ and of the calcite formed in that lake water ($\delta^{18}\text{O}_{\text{Ca}}$). What then controls temporal variation in the $\delta^{18}\text{O}_p$ in the region? Holdsworth et al. (1992) explored the relationship between $\delta^{18}\text{O}_p$ and temperature in the Northwest Pacific. They found that the Mt. Logan Summit ice core $\delta^{18}\text{O}$ (5340-m a.s.l.) was not significantly correlated with instrumental temperature records or paleotemperatures inferred from dendrochronologies. The $\delta^{18}\text{O}$ data from the Eclipse ice core on Mount Logan (3017-m a.s.l.) has a weak correlation with temperature, explaining only 10-15% of the variance (Wake et al., 2002).

The average relation for middle and high latitudes between $\delta^{18}\text{O}_p$ and mean annual surface temperature is $\sim 0.6\text{‰}$ per $^{\circ}\text{C}$ (Dansgaard, 1964; Rozanski et al, 1992). Combining this

factor with the fractionation coefficient for calcite formation and lake-water temperature, -0.25‰ per $^{\circ}\text{C}$ (Friedman and O'Niell, 1977), leads to an estimated change in $\delta^{18}\text{O}_{\text{Ca}}$ of $\sim -0.35\text{‰}$ per $^{\circ}\text{C}$ of atmospheric temperature change for Jellybean Lake (e.g. Yu et al., 1997; Anderson et al., 2001). The observed range of $\delta^{18}\text{O}_{\text{Ca}}$ in Jellybean Lake is $\sim 2.0\text{‰}$ (Figure 3.6), corresponding to a temperature range of $\sim 5.7^{\circ}\text{C}$ which we consider to be too large for this period based on comparison with other regional paleorecords (Heusser et al., 1985; Hu et al., 2001). In addition, the abrupt $\delta^{18}\text{O}_{\text{Ca}}$ shifts during the last 1500 years are up to 1.5‰ , which would correspond to a change of $\sim 4.3^{\circ}\text{C}$. These large inferred temperature changes, combined with the poor correlation between Jellybean Lake $\delta^{18}\text{O}_{\text{Ca}}$ and a 300-year dendrochronology record from the Mackenzie River delta, interpreted to reflect growing season temperatures for the region (Szeicz and MacDonald 1995, 1996), suggest that temperature is not the primary control. Furthermore, isotope-modeling studies by Bowen and Wilkinson (2002) identify northwestern Canada as an area where $\delta^{18}\text{O}_{\text{p}}$ has high magnitude deviations from typical temperature controlled relationships. Based on these observations, we conclude that multi-annual $\delta^{18}\text{O}_{\text{p}}$ variation in this region is not driven by temperature changes alone. We suggest that temporal changes in atmospheric circulation across the St Elias Mountains are the major control on the oxygen isotope composition of precipitation in the interior of the southern Yukon and hence, hydrologically-open lakes such as Jellybean.

Oxygen Isotopes, Precipitation and Atmospheric Circulation

Numerous oxygen isotope studies of sediment from evaporation-insensitive lakes have inferred past changes in atmospheric circulation (e.g., Edwards et al., 1996; Yu et al., 1997; Hammerlund et al., 2002; Wolfe et al., 2003; Jones et al., 2004; Rosqvist et al., 2004). Precipitation data shows that maritime airmasses reaching the coast of southwest Alaska are relatively ^{18}O -enriched (Adak, -8 to -11‰) compared to precipitation falling from these same

airmasses in the interior of the Yukon (Whitehorse, -18 to -21‰; IAEA/WMO 2001). Such large depletions occur because of the effects of Rayleigh distillation during airmass uplift, rainout and transport across the average ~3000-m-high topographic barrier of the St Elias Mountains (Rozanski et al., 1993). We hypothesize that changes in airmass trajectory and the intensity of moisture transport through time across the St Elias Mountains control the mean annual isotopic value of precipitation falling in the interior of the Yukon. A likely mechanism is multi-decadal fluctuations in the location and strength of the AL that directs maritime airmasses into the interior with varying effects on fractionation during transport.

The NP index represents changes in AL position and strength (Trenberth and Hurrell, 1994). Figure 3.7 shows the normalized Jellybean Lake $\delta^{18}\text{O}_{\text{Ca}}$ -record for the last 100 years compared with the NP index. Although the NP index is calculated for each year, the Jellybean data are integrations of 3 to 6 years during the 20th century that are not regularly spaced in time. We used the 5-year running average of the NP index to identify anomaly values for the 23 years that corresponded with the ^{210}Pb -determined ages for the sediment samples. Correlation of the 23 pairs of data is significant at the 0.05 confidence level ($r=0.48$) and accounts for a relatively small fraction of explained variance ($r^2=0.23$). However, a relatively low correlation might be expected given the uncertainties in our age model and the nature of the signals being recorded. The NP-index is a seasonal signal because the AL is strongest in the winter and diminishes during the summer. The Jellybean Lake- $\delta^{18}\text{O}_{\text{Ca}}$ data represents an integration over 3- to 6-year periods and reflects groundwater- $\delta^{18}\text{O}$ which tends to smooth the effects of seasonal variations. It may be that this multi-annual $\delta^{18}\text{O}_{\text{p}}$ signal is predominantly influenced by variability in fall and winter precipitation. A similar effect has been observed for inter-annual ice accumulation on Mt. Logan where only winters of high accumulation were found to have a strong connection with atmospheric circulation (Rupper et al., 2004). If this assessment is correct and the limitations of

the isotope time-series are kept in mind, then the correlation can be seen as supporting a relationship between Jellybean Lake- $\delta^{18}\text{O}_{\text{Ca}}$ and AL intensity/position.

Observations between 1976 and 1988 AD show the AL was more intense and shifted eastward, advecting warm moist air along the northwest Pacific coast from the south-southeast, leading to increased coastal precipitation (Cayan and Peterson, 1989; Trenberth and Hurrell, 1994; Mantua et al., 1997). During this period Jellybean Lake $\delta^{18}\text{O}_{\text{Ca}}$ values were relatively depleted. We propose that when the AL is eastward and/or stronger, the effects of Raleigh distillation are enhanced and precipitation reaching the interior is more depleted. An eastward and/or intensified AL (negative NP anomaly) delivers strong southerly winds directly into the mountain barrier trending northwest to southeast along the Alaskan coast. It is possible that such an orientation in moisture flow, directly into the large mountains, would enhance rainout on the coastal side. Consequently, more fractionated vapor is vigorously forced up and over the barrier into the interior. Stronger leeward winds and an enhanced rain shadow effect would lead to further fractionation of the reduced amount of precipitation reaching the interior Yukon (Table 3.4).

In contrast, when the AL is westward and/or weaker, fractionation is decreased during transport and $\delta^{18}\text{O}_{\text{p}}$ is relatively ^{18}O -enriched. Historically, positive NP anomalies represented a weaker and/or westward position of the AL. This causes less vigorous meridional moisture transport from the south-southeast along the northwest Pacific coast and allows more moisture flow from the Bering Sea, to the west, into interior Alaska. During positive NP anomalies, Jellybean Lake $\delta^{18}\text{O}_{\text{Ca}}$ is relatively enriched, reflecting decreased fractionation of precipitation during transport. A more zonal flow pattern and westerly moisture trajectory is able to move more parallel to the coastal mountain barrier and may avoid the same degree of uplift, cooling and rainout than when moisture flow is more directly into the mountain barrier. In this case, less fractionated moisture would be more likely to infiltrate the northeast-southwest trending valleys

leading into the interior of the Yukon (Streten, 1974). We infer that the primary control on $\delta^{18}\text{O}_p$ in the southwest Yukon is temporally changing moisture trajectories into and over the coastal mountains driven by the strength and the position of the AL. Assuming this is correct, the $\delta^{18}\text{O}_{Ca}$ from Jellybean Lake provides a record of Holocene changes in intensity and/or position of the AL (Figure 3.8).

Holocene Paleoclimate

The Jellybean Lake $\delta^{18}\text{O}_{Ca}$ record provides Holocene paleoclimatic information at higher temporal resolution than available from previous work (Figure 3.8). While the comparison of sediment core to instrumental climate data suggest a relationship between lake $\delta^{18}\text{O}_{Ca}$ and characteristics of the AL, such as defined by the NPI, it is important to recognize that data from regional networks of sites are necessary to unambiguously distinguish between changes in AL strength and position over time. Keeping this limitation in mind in interpreting the isotopic record, the data suggests that AL position and strength during the early-to-middle Holocene, 7500 to 4500 cal yr B.P., was generally weaker and/or westward from today's location. Between ~4500 and 3500 cal yr B.P., circulation intensified and was similar to today, with airflow predominantly from the southwest (Wahl et al., 1987). After ~3500 cal yr B.P. a steady trend towards enriched $\delta^{18}\text{O}_{Ca}$ reflects a westward and/or weaker AL. By ~2000 cal yr B.P. the AL position was on average farther west and/or weaker than any time during the last ~7500 years. Other paleoclimatic studies report greater effective moisture in the central and southern Yukon prior to ~2000 cal yr B.P. (Pienitz et al., 2000; Anderson, 2005). These observations are consistent with the isotope results from Jellybean Lake. Previous studies of regional synoptic climatology suggest that a weaker/westward positioned AL is related to increased moisture delivery to interior regions (Edwards et al., 2001).

Our record also suggests that abrupt changes in AL position/strength were more frequent during the last ~2000 years than the preceding period. The decreases in $\delta^{18}\text{O}_{\text{Ca}}$ ~1200 cal yr B.P. represent rapid eastward shifts and/or intensification of the AL. Between ~500 and 300 cal yr B.P., $\delta^{18}\text{O}_{\text{Ca}}$ became relatively enriched again, reflecting a westward shift and/or weakening. Another easterly shift and/or intensification ~1700 AD correspond with cooler spring and summer south coastal land temperatures (Wiles et al., 1998). AL variability since 1900 AD indicates a weak/westward period in the early part of the century that corresponds with the termination of south coastal glacial advances and the end of the Little Ice Age (Wiles et al., 1999).

The oxygen isotope evidence presented here suggests high frequency changes in AL location/strength have occurred throughout the Holocene. However, the largest secular changes occurred after ~3500 cal yr B.P. Large changes in AL intensity and position have been shown to be accompanied by changes in ocean circulation and sea surface temperatures that would likely effect marine ecosystems (Mantua et al., 1997). Salmon catch records during the 20th century suggest a correlation between the eastward shifted and strong AL between 1976 to 1988 AD and increased production of Alaskan salmon (Hare and Francis, 1992; Mann et al., 1998). A reconstruction of Alaskan sockeye salmon abundance indicates a prominent multi-century change from lower to higher average abundance ~1200 cal yr B.P. (Finney et al., 2002; Figure 3.8). This increase corresponds with an eastward and/or intensified AL indicated by Jellybean Lake $\delta^{18}\text{O}_{\text{Ca}}$. Similarly, a multi-decade decline in salmon abundance in the early 19th century (Finney et al., 2000) coincides with a westward and/or weaker AL. The record from Jellybean Lake reflecting changes in AL position/strength is consistent in terms of the timing and direction with late Holocene changes in Alaskan salmon abundance.

Neoglaciation was initiated in the St. Elias and Coast Mountains ~3400 cal yr B.P. (Denton and Karlén, 1977; Calkin et al., 2001; Figure 3.8) and broadly corresponds with a period when the AL was eastward and/or stronger before a shift westwards and/or weakening after

~3000 cal yr B.P. The onset of Neoglaciation may also be attributed to decreasing solar insolation in addition to changes in the seasonality of precipitation. Increased moisture delivery during winter by an intensified/eastward AL could lead to coastal glacier advances (e.g. Heusser et al., 1985). Our results are consistent with other studies that suggest Neoglacial climate corresponds with secular shifts to an intensified/eastward AL and increasing moisture delivery to coastal glaciers and the St. Elias and Coast Mountains (e.g. Heusser et al., 1985; Moore et al., 2002a)

The oxygen isotope data indicates that changes in the intensity of the AL during the early and middle Holocene differed from the late Holocene. Dyke and Savelle (2000) noted a similar circulation change over in the western Arctic Ocean. During the middle and early Holocene, the Beaufort Gyre was positioned either farther west than it is today or had intensified. After ~2000 cal yr B.P., it weakened and contracted or moved. The effect was reduced summer sea-ice extent that may have enticed the eastward migration of bowhead whales and possibly people of the Thule culture (Dyke and Savelle, 2000, 2001). Around ~1200 cal yr B.P. a trend toward an intensified/eastward AL began and subsequent AL variability was rapid and more frequent. When the Beaufort Gyre and associated anticyclonic atmospheric circulation around the polar vortex weakened and contracted, the AL strengthened. The oxygen isotope record presented here is consistent with other regional records of natural climate variability, connecting two prominent high-latitude atmospheric and oceanic circulation features in the western Canadian Arctic and North Pacific region.

Table 3.1 Oxygen and hydrogen isotope values for precipitation in the southern Yukon

Location and description	$\delta^{18}\text{O}$, $\delta^2\text{H}$ (‰ VSMOW)
Whitehorse mean annual, 1962-1964 ¹	-20.4, -160.1
Whitehorse May-Sept, 1961-1965 ¹	-18.3, -142.8
Rain event, August 6, 2000 ²	-22.5, -170

¹ (IAEA/WMO, 2001)

² Sampled at Little Salmon Lake (62.3°N, 134.9 °W)

Table 3.2 General characteristics of surface water and surficial sediments in the southern Yukon region.

Parameter	Jellybean Lake ¹	Spring water ²	Closed Lake ³
<u>Water:</u>			
pH	8.2		9.2
Specific Conductivity (mS)	0.30		0.66
Temperature (°C)	14.8		16.3
Dissolved Oxygen (mgL ⁻¹)	9.5		9.2
Dissolved Carbon Dioxide (ppm)	868		402
Ambient Carbon Dioxide (ppm)	373		377
Alkalinity (mgL ⁻¹)	147	133	339
Na ⁺ (mgL ⁻¹)	4.37	3.93	17.02
K ⁺ (mgL ⁻¹)	2.24	1.49	18.64
Mg ²⁺ (mgL ⁻¹)	7.65	6.85	70.80
Ca ²⁺ (mgL ⁻¹)	49.94	50.84	25.38
Cl ⁻ (mgL ⁻¹)	2.43	1.69	3.37
NO ³⁻ (mgL ⁻¹)	2.16	3.4	1.45
SO ₄ ²⁻ (mgL ⁻¹)	16.87	13.69	30.72
Water δ ¹⁸ O 2000, 2002 (avg) (‰ VSMOW)	-21.0, -19.8 (-20.4)	-21.5	-8.0, -7.6 (-7.8)
Water δ ² H 2000, 2002 (avg) (‰ VSMOW)	-161, -157 (-159)	-162	-106, -105 (-105.5)
<u>Surface sediment</u> δ ¹⁸ O, δ ¹³ C (‰ VPDB)	-19.9, 5.15		-8.21, 4.68
Predicted equilibrium δ ¹⁸ O of calcite (VPDB) ⁴	-20.3		-8.01

¹Jellybean Lake sampled on August 1, 2000.

²Spring water sampled on July 30, 2000 (see Figure 3.1 for location).

³Marcella Lake (60.07°N, 133.81°W) sampled on August 2, 2000.

⁴Epstein et al. (1958)

Table 3.3 Geochronological data for Jellybean Lake

Core Depth (cm)	Material	Lab #	Measured Age (¹⁴ C yr B.P.)	Median Calibrated Age (cal yr B.P.) ¹	1-Sigma Range (cal yr B.P.)
0				2002 AD ²	
15	Wood	OS-38712	240 ± 30	1860 AD ³	
41.5	Wood	CAMS-91761	920 ± 35	825	774-915
59.5	Wood	CAMS-91762	1175 ± 35	1065	1013-1170
64	White River Ash			1150 ⁴	1014-1256 ⁴
87	Charcoal	CAMS-96825	1750 ± 40	1665	1574-1710
170.5	Pollen	CAMS-92155	4000 ± 35	4490	4418-4520
244.5	Wood	CAMS-91763	4800 ± 35	5500	5485-5591
336.5	Pollen	CAMS-92157	6675 ± 50	7525	7505-7585

¹Median intercept, CALIB 4.0 (Stuiver et al., 1998)

²Date when core was taken.

³²¹⁰Pb and ¹³⁷Cs based age

⁴2-sigma range, Clague et al. (1995)

Table 3.4 Relationships between Aleutian Low, $\delta^{18}\text{O}$, Gulf of Alaska, and Alaskan salmon

Aleutian Low Intensity (NP Index ¹)	Strong (-)	Weak (+)
Oxygen isotope fractionation during transport to southern interior Yukon	More	Less
SW-interior Yukon $\delta^{18}\text{O}_p$ Jellybean Lake $\delta^{18}\text{O}_{Ca}$	^{18}O -depleted ^{18}O -depleted	^{18}O -enriched ^{18}O -enriched
Gulf of Alaska boundary currents Gulf of Alaska SST's	Strong Warm	Weak Cold
Alaskan salmon abundance ² Karluk Lake $\delta^{15}\text{N}$ ³	Higher ^{15}N -enriched	Lower ^{15}N -depleted

¹ Trenberth and Hurrell (1994)

² Mantua et al. (1997)

³ Finney et al. (2002)

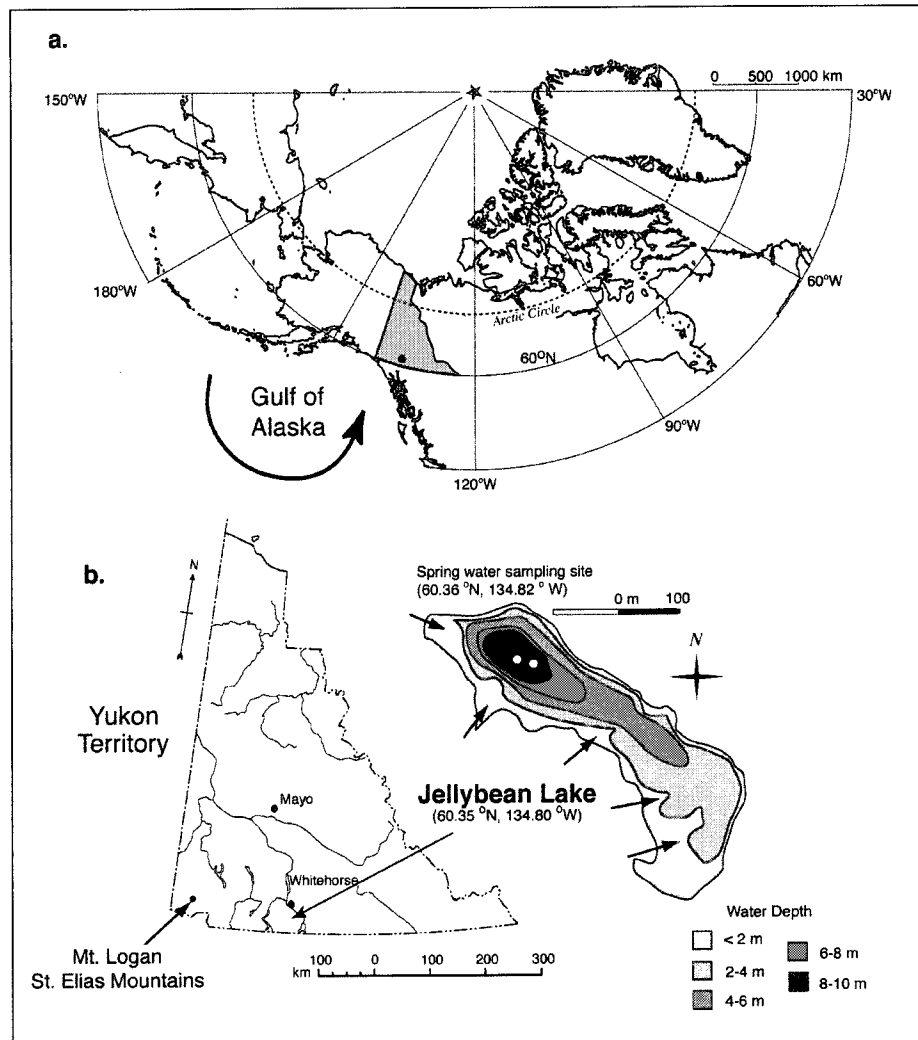


Figure 3.1. (a) Location map showing the Yukon Territory and sites referred to in the text. The general atmospheric circulation around the Aleutian Low in the Gulf of Alaska is indicated by the arrow, (b) bathymetry of Jellybean Lake where arrows indicate the locations of artesian springs and open circles the coring sites

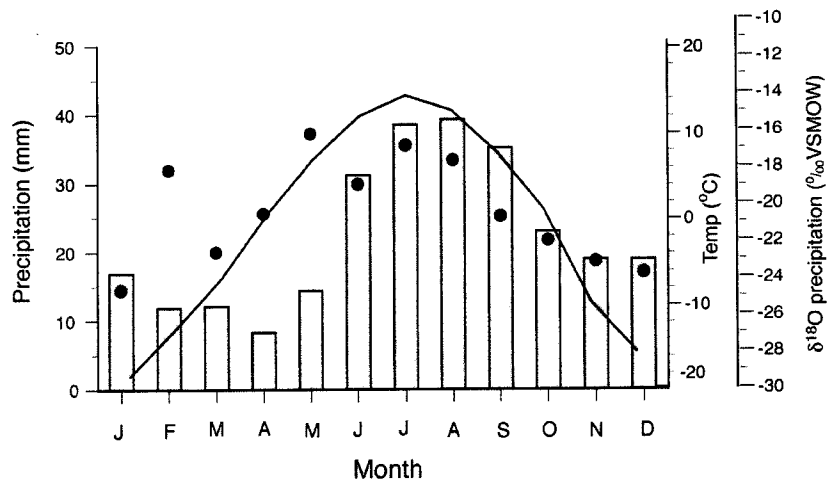


Figure 3.2. Monthly mean temperature (black line) and total precipitation (gray bars) at Whitehorse, Yukon Territory, between 1944 and 1990 AD (Environment Canada, 2003) shown with monthly averages of oxygen isotope ratios of precipitation between 1962 and 1964 AD (filled circle; IAEA/WMO, 2001).

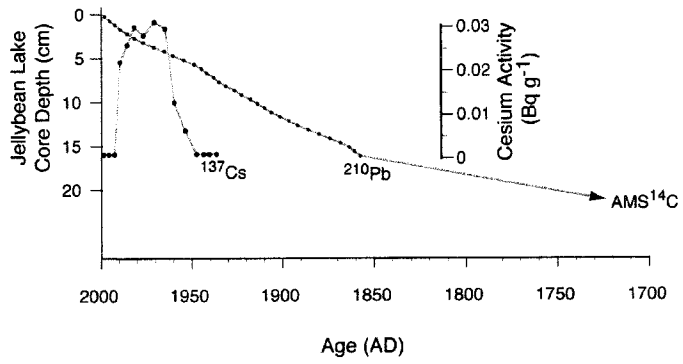


Figure 3.3. Jellybean Lake surface-sediment ^{210}Pb ages from a constant rate of supply (CRS) age model shown with ^{137}Cs activity levels indicating that the site where core C was recovered has a constant sedimentation rate and that surface sediments are undisturbed.

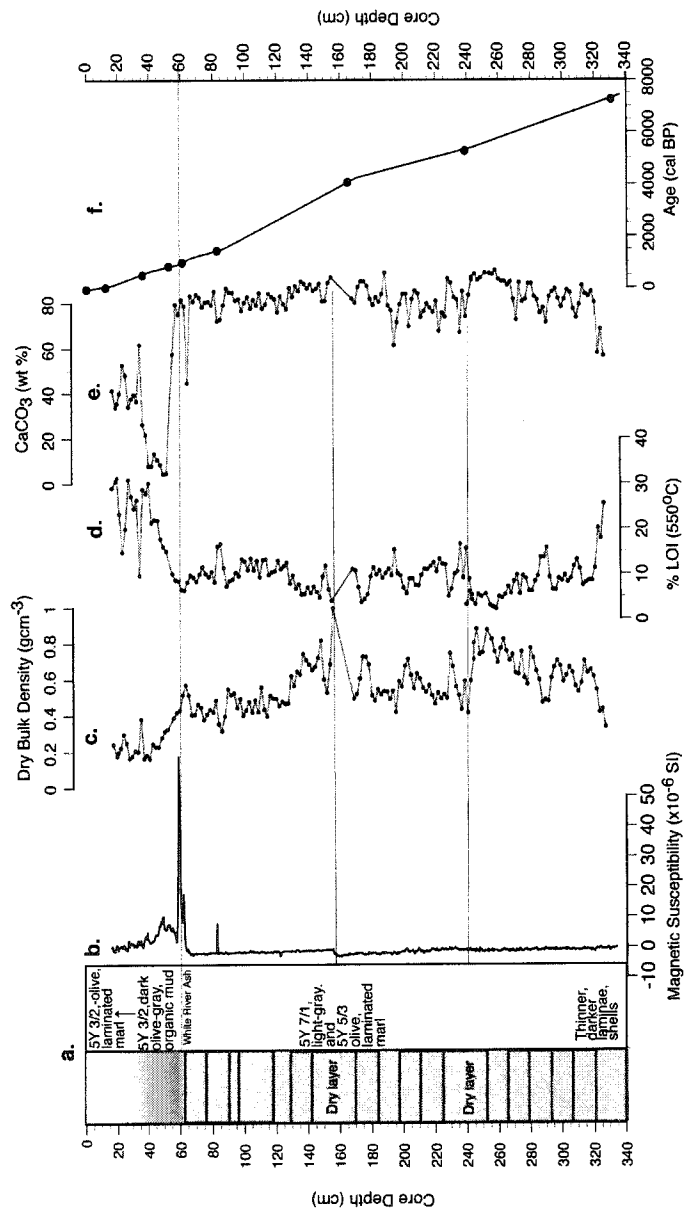


Figure 3.4. Jellybean Lake core properties including (a) magnetic susceptibility, (b) dry bulk density, (c) %LOI at 550°C, (d) weight percent calcium carbonate and (e) median calibrated ages plotted against depth.

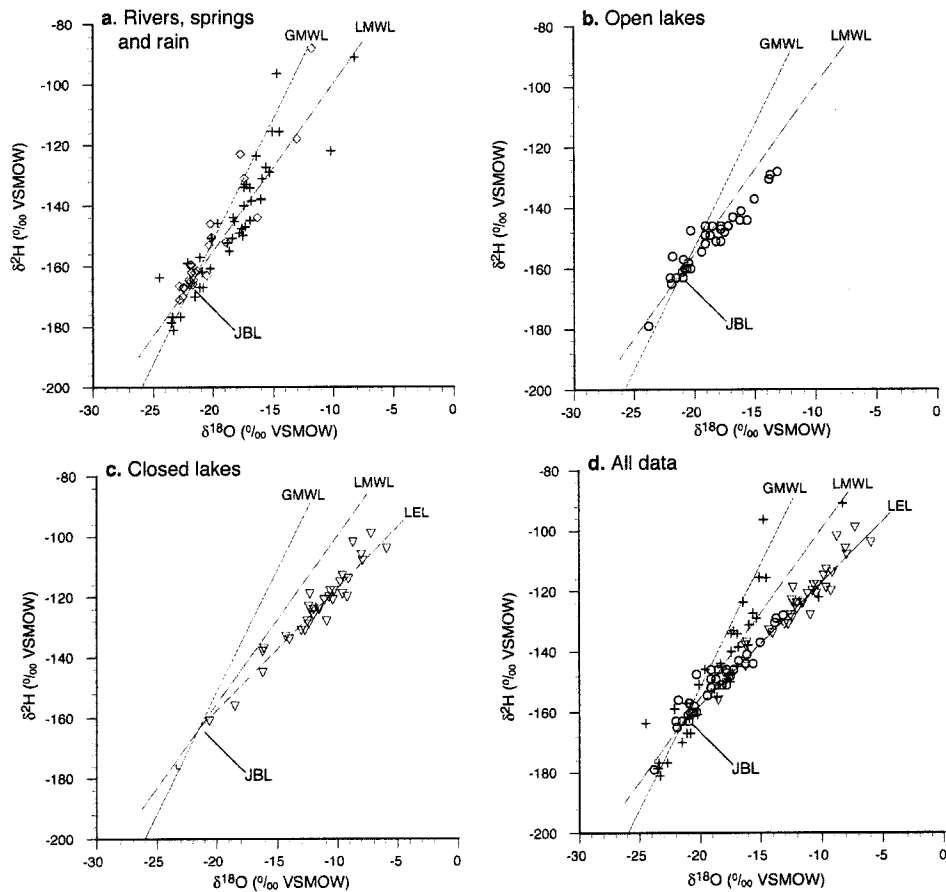


Figure 3.5. Oxygen and hydrogen isotope ratios of 71 surface water and precipitation samples from the southern Yukon Territory including Jellybean Lake (JBL): (a) precipitation from Mayo and Whitehorse (crosses) (IAEA/WMO, 2001), and rivers, groundwater or springs (open diamonds). GMWL is the Global Meteoric Water Line (Rozanski et al., 1992). LMWL is the Local Meteoric Water Line, a linear regression of Mayo and Whitehorse data; (b) hydrologically-open lakes (open circles), (c) hydrologically-closed lakes (open triangles). The LEL is the Local Evaporation Line, a linear regression of the lake data; (d) all data.

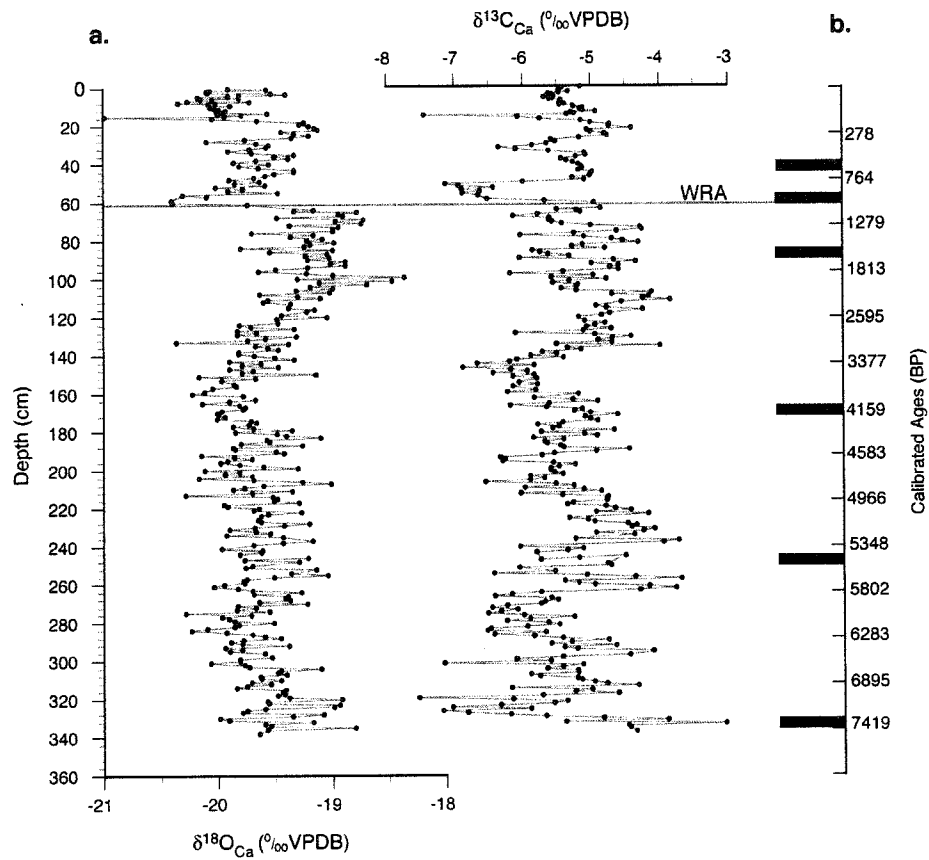


Figure 3.6. Jellybean Lake $\delta^{18}\text{O}_{\text{Ca}}$ and $\delta^{13}\text{C}_{\text{Ca}}$ plotted on a (a) depth scale (cm) and (b) calibrated age scale (cal yr B.P.). Black bars indicate depths of radiocarbon ages. The horizontal line at 64-cm depth is the stratigraphic position of the White River tephra (Clague et al., 1995).

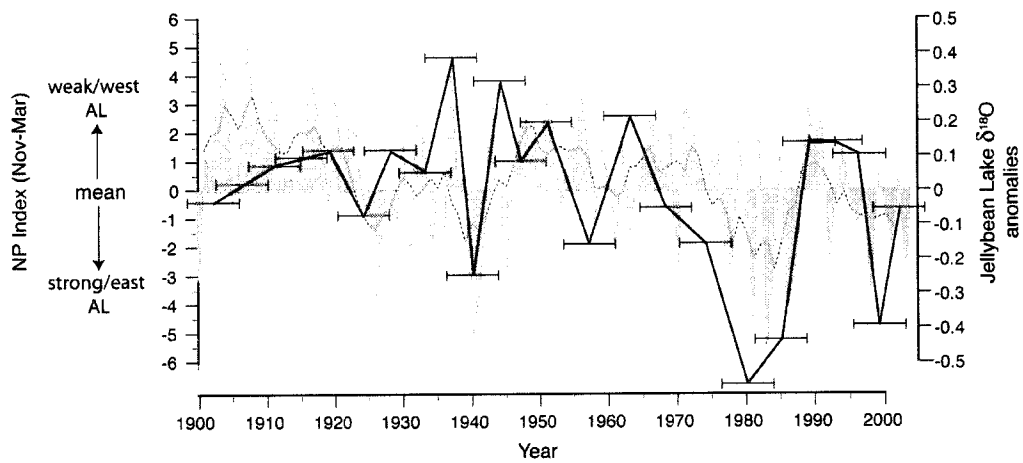


Figure 3.7. Normalized Jellybean Lake $\delta^{18}O_{Ca}$ data (black line) is shown with the NP index since 1900 AD (gray shade is annual data, dashed line is 5-year running average; Trenberth and Hurrell, 1994). Negative NP anomalies represent an strong/eastward Aleutian Low. Error bars on $\delta^{18}O_{Ca}$ data represent \pm 5-yr age uncertainty based on the ^{210}Pb and ^{137}Cs measurements (Figure 3.3).

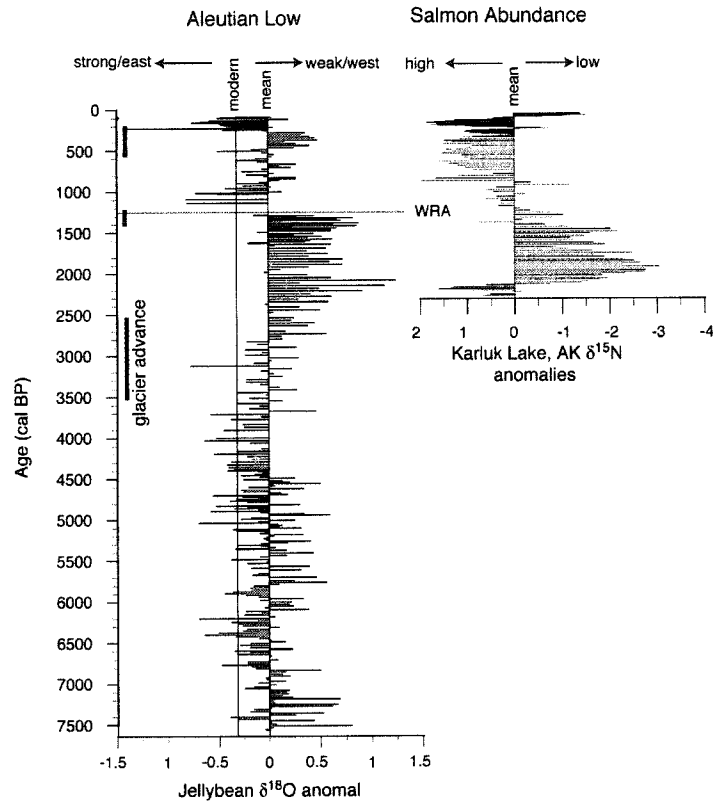


Figure 3.8. Normalized Jellybean Lake $\delta^{18}O_{Ca}$ is shown with sedimentary- $\delta^{15}N$ from Karluk Lake, Alaska since 2200 cal yr B.P. (Finney et al., 2002). $\delta^{15}N$ is a proxy for sockeye salmon abundance where enriched $\delta^{15}N$ records periods of higher salmon abundance (Finney et al., 2000). Note that changes during the 20th century also reflect the influence of commercial fishing in addition to that of climate. Timing of glacier advances in the St. Elias Mountains are indicated by vertical bars (Denton and Karlén, 1977). Vertical line on $\delta^{18}O_{Ca}$ scale labeled 'modern' is an average of the last 30 years of data. WRA indicates the stratigraphic position of the White River tephra.

CHAPTER 4

LATE HOLOCENE HUMIDITY IN THE SOUTHWEST YUKON TERRITORY, CANADA, INFERRED FROM LACUSTRINE CARBONATE STABLE ISOTOPES

Abstract

Analyses of sediment cores from Marcella Lake, a small, evaporation-sensitive lake in the southwest Yukon, provides a record of evaporation and humidity for the last 4500 years at 50- to 200-year resolution. Regional lake-water chemistry and isotope data from the southwest Yukon indicate that Marcella Lake water- $\delta^{18}\text{O}$ is strongly affected by summer evaporation allowing past changes to be reconstructed from sedimentary calcite, $\delta^{18}\text{O}_{\text{Ca}}$. A record of mean-annual precipitation, $\delta^{18}\text{O}_{\text{p}}$, from Jellybean Lake accounts for simultaneous variations related to atmospheric circulation and ambient temperature. The difference between the two isotope records, $\Delta\delta$, represents changes in lake-water $\delta^{18}\text{O}$ due to evaporation which we use in an isotope-hydrology model to estimate ambient humidity. Based on this method we estimate that between 4500 and 3000 cal BP, humidity was about 10% higher than the modern-period estimate of 58%, and reached a maximum of 70% between 3000 and 1200 cal BP. At ~1200 and 200 cal BP humidity abruptly decreased. The timing of these shifts corresponds with other records of effective moisture variability in the interior southwest Yukon that were simultaneous with previously documented late Holocene shifts in North Pacific atmospheric circulation.

Introduction

Airflow trajectories from North Pacific and Arctic regions combined with the immense topography of the St. Elias Mountains create a unique high latitude climate and environment in the southwest Yukon (Figure 4.1; Wahl et al., 1987). Warm/wet maritime air masses originating over the Gulf of Alaska rain out on the coastal side and dry further by adiabatic heating while descending the leeward side of the St. Elias Mountains. Colder/drier air masses originating from the Arctic and sub-Arctic move over the region from the northwest. Moisture in the region is limited. Climate is cold-continental sub-arctic, but local effects within the broad northwest-to-southeast trending valleys in the rain shadow of the mountains are common. Generally, summers are brief, warm and dry and in some locations persistently windy (Wahl et al., 1987). These conditions are favorable for summer growth and cause rapid sedimentation in evaporation-sensitive calcium-rich lakes. This provides an opportunity for sedimentary oxygen isotope studies to document effective moisture change at decadal to century time scales (Anderson, 2005).

Previous paleohydrological and paleolimnological studies in the southwest Yukon provide quantitative estimates of millennial-scale effective moisture variability (Pienitz et al., 2000; Anderson et al., in press). However, relatively little is known about fluctuations in effective moisture at shorter time scales. Previous tree-ring studies in semi-arid central Alaska highlight the impact of effective moisture during the last century (Barber et al., 2000). Little is known about quantitative changes or the relative importance of temperature and effective moisture on shorter time-scales during the Holocene.

We analyzed oxygen and carbon isotopes from Marcella Lake (Figure 4.1) to improve the detail and resolution of the climate history of the southwest Yukon. Marcella Lake is small (0.4 km²), thermally stratified and hydrologically-closed and outflow appears to be limited to evaporation. Calcium-rich lake water contributes to bioinduced calcification above the

thermocline, primarily by Characean algae (*Chara* sp.), allowing the measurement of preserved sedimentary *Chara* oxygen isotope ratios to produce a new climatic history. The sampling resolution and analytical precision of the geochemical data are of sufficient quality to document changes in effective moisture at 50- to 200- year resolution.

Marcella Lake Oxygen Isotopes

Oxygen isotope ratios of water in hydrologically-closed lakes, where outflow is largely restricted to evaporation, are closely related to relative humidity. In such systems, lake-water $\delta^{18}\text{O}$ is influenced by the combined isotopic composition of input water from catchment runoff, groundwater and precipitation falling directly into the lake that is then altered by the preferential evaporation of the lighter ^{16}O isotope in water molecules. In contrast, hydrologically-open lakes that have a large catchments relative to their surface area are typically evaporation-insensitive. In these cases, lake-water- $\delta^{18}\text{O}$ may be primarily controlled by input-water- $\delta^{18}\text{O}$ and/or atmospheric and lake-water temperature. Marcella Lake has a small well-defined watershed relative to the lake's surface area. There is no evidence for surface inflow or outflow and lake water- $\delta^{18}\text{O}$ is notably enriched when compared to other lakes in the southern Yukon (Anderson, 2005; Anderson et al., 2005). Nevertheless, long-term changes in input waters and atmospheric temperature may affect the $\delta^{18}\text{O}$ of lake water. For Marcella Lake these effects can be accounted for by paleo data from Jellybean Lake, located ~75 km northwest of Marcella Lake, of regional mean annual precipitation, $\delta^{18}\text{O}_p$ (Figure 4.1; Anderson et al., 2005). By making the reasonable assumption that $\delta^{18}\text{O}_p$ has been similar at both sites, we removed this effect from Marcella $\delta^{18}\text{O}_{\text{Ca}}$. We are then able to calculate $\Delta\delta$, the ^{18}O -enrichment at Marcella Lake caused by evaporation and use this parameter to estimate changes in humidity.

Field Area

Marcella Lake (60.074 °N, 133.808 °W, 697 a.s.l.) is located within the interior Yukon Plateau physiographic region (Figure 4.1). The lake basin lies ~20m below a broad terrace within a larger southeast to northwest trending depression, interpreted as a former melt-water channel (Dyke et al., 2002). The lake is spring-fed with a small, well-defined watershed (0.8 km²). It is up to 9.7-m deep with a surface area of 0.4 km². Surface inflow is limited to surface run-off during rain events in the surrounding watershed. Outflow appears to be restricted to evaporation. Water column measurements of temperature, specific conductance, pH and dissolved oxygen indicate a thermocline between 5 and 8-m water depth (Anderson, et al., in press). *Chara* dominate a shallow area on the southeast edge but are nearly absent from the rest of the shoreline.

Meteorological data from Whitehorse and Teslin indicate mean annual precipitation totals of ~260 mm/yr (Wahl et al., 1987). Monthly precipitation maximums occur between June and September (Figure 4.2). July mean temperatures are between 10 and 15°C. Mean annual temperatures are between -2 and 0°C (Environment Canada, 2002). Regional lake-ice break-up occurs between April and May and freeze-up typically occurs during October or November. Mean-annual afternoon relative humidity (1500 and 0600 hr) is between 60 and 65%. Mean-annual summer (May-Sept) afternoon relative humidity is between 45 and 50% (Environment Canada 2002; Figure 4.2). Vegetation surrounding Marcella Lake are open stands of lodgepole pine (*Pinus contorta*), trembling aspen (*Populus tremuloides*) and white pine (*Picea glauca*). Sage (*Artemisia*) and grasses (*poaceae*) grow on treeless well-drained south-facing slopes. Cwynar (1988) produced a detailed late-Quaternary pollen record for this site; in his study the lake was called Kettlehole Pond.

Three years of continuous monthly oxygen and hydrogen isotope measurements of precipitation at Whitehorse (1962-1964) show a seasonal $\delta^{18}\text{O}$ cycle ranging from -24.6 to -16.8‰ (Figure 4.2; IAEA/WMO, 2001). More ¹⁸O-enriched precipitation occurs during the

summer months. Mean summer $\delta^{18}\text{O}$ (May through September, 1961-1965) was -18.3‰ while mean annual $\delta^{18}\text{O}$ was -20.4‰. Marcella Lake water $\delta^{18}\text{O}$ is -7.8‰ (Table 4.1).

Methods

A suite of sediment cores 156-cm, 200-cm and 143-cm long, were retrieved from 457, 430 and 451-cm water depth, respectively. The coring location was near the top of a slope gently dipping toward the deepest depth of the lake, located ~3-m from the edge of the Charophyte vegetation in the southeast edge. The cores were retrieved from a floating platform in July 2000 and 2002 using a modified square rod piston corer designed to allow preservation and extrusion of the uppermost sediments. Visual observations and magnetic susceptibility were used to correlate the cores and produce a composite-core sediment stratigraphy labeled C/E. A detailed core description, bulk sedimentary properties and radiocarbon data of composite C/E were presented in Anderson et al., (in press).

Water-column measurements of temperature, pH, conductivity and dissolved oxygen were collected in July of 2000 with a Hydrolab Surveyor 4 and Datasonde 4 from Marcella Lake, Jellybean Lake and six other nearby hydrologically open and closed lakes as part of a modern regional isotope hydrology study (Anderson, 2005; Anderson et al., 2005). Dissolved carbon dioxide ($p\text{CO}_2$) in surface lake water was determined by applying Henry's Law to samples of ambient air and samples of CO_2 gas collected in a head space of known volume from a container of agitated lake water (Plummer and Busenberg, 1982). Surface water samples for cation and anion chemistry were collected in 30-ml HDLP Nalgene bottles and stored in the dark at cool temperatures. Alkalinity was determined by titration in the laboratory. Cation and anion concentrations were determined by ion chromatography and are reported in mgL^{-1} (Table 4.1). Lake-water particulate organic material was collected by filtering 2 L through a glass fiber filter for bulk organic $\delta^{13}\text{C}$ and $\delta^{15}\text{N}$ analyses by an elemental analyzer coupled with a Finnigan Delta-

plus mass spectrometer. Analytical precisions for bulk organic $\delta^{13}\text{C}$ and $\delta^{15}\text{N}$ were $\pm 0.2\text{‰}$ and are expressed as per mil (‰) relative to PDB and Air, respectively (Table 4.1).

$\delta^{18}\text{O}_{\text{Ca}}$ and $\delta^{13}\text{C}_{\text{Ca}}$ from sediment samples were analyzed on more than five individual *Chara* stem encrustations. Samples were picked from water-sieved fractions, freeze dried, ground into a fine powder and subsampled for CO_2 extraction by a Kiel automated device for isotope ratio mass spectrometry on a Finnigan Delta XL mass ratio spectrometer. *Chara* crusts were taken from 0.5-cm increments for the uppermost 32 field-extruded samples, every 1 cm to the White River Ash at 64-cm depth and every 2 cm for the remainder of the core. Duplicate analyses were carried out on select samples and individual stems to assess variations. Sample reproducibility is approximately $\pm 0.5\text{‰}$. Isotope results are reported in δ -notation ($\delta = ([R_{\text{sample}}/R_{\text{standard}}] - 1) \times 1000$ where $R = {}^{18}\text{O}/{}^{16}\text{O}$ or ${}^{13}\text{C}/{}^{12}\text{C}$) and are expressed as per mil (‰) relative to the international standards: Vienna Pee Dee Belemnite (VPDB) for calcite $\delta^{18}\text{O}$ and $\delta^{13}\text{C}$ and Vienna Standard Mean Ocean Water (VSMOW) for water.

The composite core chronology C/E is based on ${}^{210}\text{Pb}$ and ${}^{137}\text{Cs}$, and AMS ${}^{14}\text{C}$ measurements on terrestrial macrofossils (Table 4.2). Terrestrial macrofossils were not present in sufficient quantities at many stratigraphic levels so that an intact aquatic macrofossil was used. Both measured radiocarbon and calibrated ages are reported (median intercept and 1-sigma range), but only calibrated radiocarbon ages are used for discussion. Radiocarbon ages were calibrated using CALIB 4.1 following the methods of Stuiver et al. (1998). ${}^{210}\text{Pb}$ and ${}^{137}\text{Cs}$ activity for Marcella Lake were measured on 0.5-cm slices of the uppermost 16.5 cm extruded in the field (Appleby, 2001). Due to very low ${}^{210}\text{Pb}$ activities and a slightly irregular ${}^{137}\text{Cs}$ peak, only the surface age (2002) and the ${}^{210}\text{Pb}$ -dating horizon at 16.5-cm depth (110 cal BP) were used in the age model.

An age model was constructed from two ${}^{210}\text{Pb}$, six ${}^{14}\text{C}$ measurements and the White River tephra (Clague et al., 1995; Figure 4.3). Linear interpolation between dated depths was used to

determine ages for isotope samples. The chronology indicates a fairly uniform sedimentation rate, ~0.03 to 0.05 mm/year. Oxygen and carbon isotope samples integrate 5 to 10 years in the uppermost 16.5-cm, and 20 to 100 years for the remainder of the core.

Results

Limnology and Hydrology of Marcella Lake

Water chemistry and water column measurements of Marcella Lake indicate that surface waters were slightly oversaturated in CO₂, and had a relatively high specific conductivity and alkalinity (Table 4.1). These observations are consistent with other hydrologically-closed lakes in the region (Anderson et al., 2005). We evaluated the multiple lake-water variables collected from Marcella Lake and six other lakes and three springs from the central and southern Yukon by Principal Component Analyses (PCA) (Figure 4.3). PCA shows relationships between multiple variables and in this case served to highlight the limnochemical contrasts between unmodified spring water, evaporation-insensitive (open lake) and evaporation-sensitive (closed lake) water (e.g. Pienitz et al., 1997).

On a plot of lake-water ion species (Figure 4.3a), positive vector values on the first axis ($\lambda = 64.2\%$) correspond with closed lakes and indicate that high alkalinity and high concentrations of dissolved ions plot with closed lakes. Summer evaporation and long lake-water residence times (years) commonly leads to high dissolved ion concentrations. In contrast, a negative calcium ion vector on the first axis plots with open lakes and spring-water. Open lakes and springs could be characterized by higher calcium ion concentrations because of carbonate dissolution by groundwater within the carbonate-rich tills and outwash deposits throughout the area. Vectors on the second axis ($\lambda = 14.1\%$) distinguish spring water from lake water on the open-lake side of the first axis. Springs plot with the positive calcium ion vector while lakes plot

with negative values on axis 2. Lower dissolved calcium ion concentrations in lake water could be due to summer calcification (McConnaughey et al., 1994).

Another variable set is presented in Figure 4.3b. Here again, vectors with positive values on the first axis ($\lambda = 63.5\%$) plot with closed lakes and include temperature, $\delta^{18}\text{O}$, $\delta^2\text{H}$, conductivity, alkalinity and pH. Conversely, negative vectors on axis one, dissolved gases, group with open lakes. On the closed-lake side of axis one, some lakes plot with positive vectors for temperature and isotope ratios on the second axis ($\lambda = 17.6\%$) while Marcella Lake (ML) group with negative vectors for conductivity, pH and alkalinity. On the open-lake side, two lakes including Jellybean Lake (JBL) plot with a negative vector for dissolved CO_2 on the second axis. In general, these results distinguish limnochemical signatures that reflect the length of lake-water residence times and show that Marcella Lake water is limnochemically and isotopically evolved within the context of other lakes in the area.

Oxygen and carbon Isotopes

Charophytes are macroscopic algae that provide a locus and kinetic advantage for the precipitation of calcite during photosynthesis (bio-induced calcification) (McConnaughey, 1991; McConnaughey et al., 1994). Provided that there is isotopic equilibrium between water and precipitated calcite, *Chara* crust calcite $\delta^{18}\text{O}_{\text{Ca}}$ and $\delta^{13}\text{C}_{\text{Ca}}$ accurately record past lake-water- $\delta^{18}\text{O}$ (modified by any change in temperature) and DIC- $\delta^{13}\text{C}$. Isotopic equilibrium appears to exist in Marcella Lake. By using the temperature equation of Epstein et al. (1953), we found that the predicted $\delta^{18}\text{O}_{\text{Ca}}$ of living *Chara* calcite, -8.01‰ , at 16.3°C (the measured lake water temperature in Marcella Lake) is quite close to the measured $\delta^{18}\text{O}_{\text{Ca}}$ value of -8.21‰ (Table 4.1).

Sediment-core *Chara* oxygen isotope values range between -13.5 and -7.5‰ (Figure 4.4). Assuming a temperature $\sim 16^\circ\text{C}$ for calcite precipitation, this 6‰ range indicates lake waters that

are 5 to 11‰ more positive than the annual range of precipitation measured at Whitehorse (Table 4.1). Below 70-cm depth, $\delta^{18}\text{O}_{\text{Ca}}$ values are more variable and shifts as large as 3‰ occur over 2-cm intervals. In general throughout the core, $\delta^{18}\text{O}_{\text{Ca}}$ is more negative than modern values. Between 144 and 70-cm depth, values vary near -11‰ while above 24 cm, they range from -9.5 to -8‰.

Sediment-core *Chara* Carbon isotope ratios are relatively ^{13}C -enriched (0 to 7‰) and have a slightly larger range of variability than the oxygen isotopes. Shifts as large as ~4.5‰ occur over 2 to 6-cm intervals. Lowermost $\delta^{13}\text{C}_{\text{Ca}}$ values are relatively ^{13}C -depleted (0 to 4.5‰) but values vary across a range centered on core-top values (4.48‰). Between 130 and 98-cm depth, values are persistently more positive-than-modern while between 98 and 64-cm depth they are more often negative-than-modern. Above 64-cm depth values shift again to more positive-than-modern while above 21-cm depth they are generally lower than the preceding interval.

Discussion

Carbon isotopes

Carbon isotope ratios of *Chara* calcite ($\delta^{13}\text{C}_{\text{Ca}}$) record the isotopic composition of lake-water-DIC. DIC in turn is a reflection of the carbon isotope ratios of CO_2 -sources from atmospheric dissolution, biological respiration within the lake and groundwater (McKenzie, 1985; Siegenthaler and Eicher, 1986; Dean and Stuiver, 1993). When a lake is thermally stratified, DIC-pools within the epilimnion and hypolimnion are distinct and evolve in isolation. During peak productivity, *Chara* in the epilimnion grow and calcite precipitates. Aquatic photosynthesis preferentially sequesters ^{12}C -enriched DIC into organic matter, leaving residual DIC- $\delta^{13}\text{C}$ progressively ^{13}C -enriched (*i.e.* McConnaughey et al., 1994). Microbial respiration of ^{12}C -

enriched organic matter in the hypolimnion results in relatively ^{13}C -depleted residual $\text{DIC-}\delta^{13}\text{C}$ below the thermocline. Thus, during stratified periods epilimnion- $\delta^{13}\text{C}_{\text{Ca}}$ values tend to be relatively high compared to the hypolimnion. After lake over-turn, when the DIC pools mix, $\text{DIC-}\delta^{13}\text{C}$ and $\delta^{13}\text{C}_{\text{Ca}}$ values tend to decrease (e.g. Hodell et al., 1998). Thermal stratification develops in wind-protected basins where warm surface waters develop during spring and early summer. For such sites, bulk organic $\delta^{13}\text{C}$ values could be a proxy for changes in thermal stratification regimes, summer temperatures and biological productivity.

Marcella Lake is thermally stratified, being well protected from wind mixing. In sediment cores from the deep basin there is lithologic and isotopic evidence for changes in the thermal stratification regime. Between 4000 and 2000 cal BP well-preserved mm-scale sedimentary laminations and high organic-matter carbon isotope ratios indicates meromixis. This, in addition to other lithologic evidence from a core transect, suggest higher lake levels during this period (Anderson et al., in press). Here, higher-than-modern *Chara*- $\delta^{13}\text{C}_{\text{Ca}}$ in core C/E that occur during the same time period (between 90 and 130 cm depth, Figure 4.4) are consistent with the meromictic high-stand interpretation of the deep core. Equally high *Chara*- $\delta^{13}\text{C}_{\text{Ca}}$ since 2000 cal BP, however, when lake levels were lower, suggest warmer summer temperatures may have been the cause of more persistent stratification over shorter time-intervals. The *Chara*- $\delta^{13}\text{C}_{\text{Ca}}$ are circumstantial evidence in support of this hypothesis but require further investigation. Here we focus on the oxygen isotope data for climatic interpretations

Oxygen isotopes

The limnochemical data, such as high dissolved solids, indicate that variations in evaporation and relative humidity are the primary control of lake-water- $\delta^{18}\text{O}$ and $\delta^{18}\text{O}_{\text{Ca}}$ at Marcella Lake. In addition, any long-term changes in $\delta^{18}\text{O}_{\text{p}}$ will also affect $\delta^{18}\text{O}_{\text{Ca}}$. We can

account for these changes in $\delta^{18}\text{O}$ record using the nearby Jellybean Lake $\delta^{18}\text{O}_{\text{Ca}}$ record which was interpreted in terms of Holocene changes in $\delta^{18}\text{O}_p$ (Anderson et al., 2005). The difference, $\Delta\delta$, between $\delta^{18}\text{O}_{\text{Ca}}$ of Marcella and Jellybean Lake represents the degree of ^{18}O -enrichment in Marcella Lake due to evaporation effects alone. To perform this operation, we: 1) converted both oxygen isotope stratigraphies into time series with equivalent age units using 50-, 100-, and 200-year smoothing of the geochemical data (Figures 4.5a and 4.5b), and 2) subtracted the two smoothed time-series to produce a third time-series, $\Delta\delta$ (Figure 4.5c). The per-mil range of variability of Jellybean Lake $\delta^{18}\text{O}_{\text{Ca}}$ (1.5 to 2‰) is relatively small compared to Marcella Lake, but slight changes emerge in $\Delta\delta$. Based on the mean calibrated radiocarbon ages (1-sigma), the smoothed time-series age error estimates range from ± 20 years from -50 to 400 cal BP, ± 50 to 100 years between 400 and 3000 cal BP, and ± 100 to 300 years for ages older than 3000 cal BP.

Isotopic enrichment and ambient humidity estimates

In general, $\Delta\delta$, isotopic enrichment, is driven by two processes: (1) lighter isotopes are favored in the liquid-to-vapor transition and (2) kinetic isotope effects cause different rates of diffusion through the air-boundary layer (Gat, 1995). According to a steady-state isotope-hydrology model by Gat (1995), the isotopic enrichment ($\Delta\delta$) of a terminal lake is dependent on: (1) ambient humidity, (2) the isotopic composition of atmospheric vapor and (3) the isotopic composition of input water. Using estimates of -34‰ and -22‰ for (2) and (3) respectively (IAEA/WMO, 2002), we applied to this model Marcella Lake $\Delta\delta$ and solved for humidity (Figure 4.5c). Estimated humidity averaged over the last 100 years of data, 58%, is higher than measured mean-summer relative humidity (40 to 45%) but nearer the range of mean-annual relative humidity, ~60%, (Figure 4.2). This result may occur because changes in mixing regimes are not accounted for by this model.

Holocene Paleoclimate

The oxygen isotope ratios from Marcella Lake provide quantitative effective-moisture information at higher temporal resolution than previous work. The following pattern emerges (Figure 4.6). More negative $\Delta\delta$ -anomalies between 4500 and 3000 cal BP indicate that humidity was higher than present with the exception of the ~400-year long period between 3500 and 3100 cal BP when evaporation increased to near modern values. Between 3000 and 1200 cal BP humidity was ~10% higher than the modern era. After ~1200 cal BP, evaporation abruptly increased. This is consistent with higher-than-modern lake levels in Marcella Lake before ~2000 cal BP that were followed by lower lake stands (Anderson et al., in press). A second evaporation increase began ~200 cal BP that lead to the instrumental record, which is characterized today as semi-arid.

Our results are consistent with the record of late Holocene glacial expansion on the northern flank of the St. Elias Mountains. Advances occurred between ~3400 and 2400 cal BP, ~1200 cal BP, and 400 to 90 cal BP (Denton and Karlen, 1977; Figure 4.6). Between 4500 and 1200 cal BP Marcella Lake $\Delta\delta$ -anomalies indicate wetter-than-modern conditions at low elevations which is consistent with increased snow accumulation at higher elevations and glacier expansion. In contrast, after ~200 cal BP, Little Ice Age advances occurred during a period of increasing aridity at Marcella Lake. In many cases coastal advances were the maximum advances since deglaciation (Calkin et al., 2001). Typically, glacial advances are interpreted as indicators of wetter climate and/or regional cooling, but increasing aridity at Marcella Lake suggests a diverging climatic pattern at high and low elevations. This could be explained by shifts in atmospheric circulation that simultaneously favored increasing precipitation at high elevations and aridity in the interior.

Recent studies investigated atmospheric circulation variability in the North Pacific and Gulf of Alaska. Attention has focused on North Pacific atmospheric circulation and Aleutian

Low intensity and/or position as a mechanism for late Holocene paleoclimatic change (Heusser et al., 1985; Mann and Hamilton, 1995; Mock et al., 1998; Edwards et al., 2001). In general an intensified/eastward Aleutian Low leads to stronger meridional storm trajectories that are directed into the ~3000-m high northwest-to-southeast trending St. Elias Mountain barrier. This airflow-to-barrier orientation has been observed to enhance rain out and increase stream flow on the coastal side of the mountains (Cayan and Peterson, 1989; Trenbirth and Hurrell, 1994). As a consequence, down-slope leeward winds intensified, leading to increased adiabatic heating and drying of the moisture-depleted air mass (Streten, 1974; Wahl et al., 1987). In this case, increased rainfall at the coast and snow accumulation at high elevations and intensified leeward winds are consistent with lower ambient humidity at Marcella Lake on the interior side of the mountains. In contrast, more zonal airflow trajectories are associated with a weaker/westward Aleutian Low. This circulation could allow cooler and moister low-level air masses that originated over the Bering Sea to infiltrate the northwest-to-southeast trending valleys in the southwest Yukon (Streten, 1974). Although this trajectory would lead to drying by the continental effect, more moisture might reach the interior than when air masses are more intensely forced up and over the mountains. This scenario may have been more dominant between 3000 and 1200 cal BP, during the time when Jellybean Lake $\delta^{18}\text{O}$ indicates that the Aleutian Low was weaker and/or positioned to the west and Marcella Lake water levels and humidity were higher than modern (Figure 4.6). Today, the Aleutian Low is strongest during the winter and diminishes during the summer. Nevertheless, the most frequent weather pattern affecting the Yukon consists of a persistent low in the western Gulf of Alaska that occurs in all seasons (Wahl et al., 1987). The mountain barrier is a common hinge point during winter and summer and it may be that the long-term circulation variations proposed here would affect winter and summer climate.

We proposed elsewhere that the prominent late Holocene $\delta^{18}\text{O}$ decreases at Jellybean Lake reflect shifts to a more intensified and/or an easterly positioned Aleutian Low leading to

more meridional airflow, increased coastal precipitation and vapor fractionation in the interior (Figure 4.6; Anderson et al., 2005). This hypothesis is now supported by similar isotope shifts in the new Mount Logan summit ice core $\delta^{18}\text{O}$ record (Fisher et al., 2004). Other evidence from coastal and high alpine sites includes the onset of glacial sedimentation after 2000 cal BP at White Pass (Lamoreaux and Cockburn, in press), and late Holocene increases in exotic western Hemlock observed in Northern British Columbia interpreted as more frequent eastward penetration of warm maritime air masses due to Aleutian Low intensification (Spooner et al., 2003). The $\Delta\delta$ shifts at Marcella Lake ~1200 and 200 cal BP indicate more evaporation and lower humidity. This observation is supported by increasing diatom-inferred paleosalinity in a small hyper-saline pond in the central Yukon after 2000 cal BP observed by Pienitz et al. (2000). Based on our new oxygen isotope records, we propose that increasing aridity in the southwest Yukon during the late Holocene was a result of long-term and sustained Aleutian Low intensifications and/or eastward shifts.

The oxygen isotope record presented here supports the evidence from Jellybean Lake that the largest secular climatic changes since the late-middle Holocene have occurred during the last ~3500 years. Previously, these shifts were noted as coinciding with changes in North Pacific Salmon abundance and change in the position and intensity of the Beaufort Gyre (Anderson et al., 2005). Here we propose a mechanism which links these shifts with humidity changes in the interior regions of the northwest sub-Arctic. More remains to be understood about the effects of Aleutian Low intensity/position on Holocene climatic variability in northern Alaska and Yukon where Arctic air mass penetration is more prevalent or about downstream regions such as central British Columbia and northwestern Alberta. Research in these regions which documents late Holocene paleoclimate at decade-to-century time scales will provide a broader view of the hypothesis outlined here. This climatic reconstruction and mechanism provides a framework and hypothesis to be tested by future paleoclimatic investigations.

Table 4.1 Marcella Lake surface water and sediment data

Parameter	Result
pH	9.2
Specific Conductivity (mS)	0.66
Temperature (°C)	16.3
Dissolved Oxygen (mgL ⁻¹)	9.2
Dissolved Carbon Dioxide (ppm)	402
Ambient Carbon Dioxide (ppm)	377
Alkalinity (mgL ⁻¹)	339
Na ⁺ (mgL ⁻¹)	17.02
K ⁺ (mgL ⁻¹)	18.64
Mg ²⁺ (mgL ⁻¹)	70.80
Ca ²⁺ (mgL ⁻¹)	25.38
Cl ⁻ (mgL ⁻¹)	3.37
NO ₃ ⁻ (mgL ⁻¹)	1.45
SO ₄ ²⁻ (mgL ⁻¹)	30.72
Marcella Lake δ ¹⁸ O, δ ² H 2000, 2002 (avg) (‰ VSMOW)	-8.0, -7.6 (-7.8): -106, -105 (-105.5)
Living <i>Chara</i> δ ¹⁸ O _{Ca} , δ ¹³ C _{Ca} (‰ VPDB)	-8.21, 4.68
Predicted-equilibrium δ ¹⁸ O _{Ca} (‰ VPDB) ¹	-8.01

¹ Epstein et al., (1953).

Table 4.2 Marcella Lake core C/E chronostratigraphic data

Core Depth (cm)	Material	Lab #	Measured Age (¹⁴ C yr BP)	Median Calibrated Age (cal BP) ¹	1-Sigma Range (cal BP)
0				2002 ²	
16.5				110 ²	
41	Wood	OS-38713	930 ± 25	830	791-915
44	Wood	CAMS-96826	980 ± 60	925	793-951
64	White River Ash			1150	1014-1256 ³
133	Wood	OS-38714	4080 ± 35	4545	4451-4781

¹ Mean intercept of calibrated radiocarbon ages.

² Surface and ²¹⁰Pb dating horizon.

³ 2-sigma range from Clague et al. (1995).

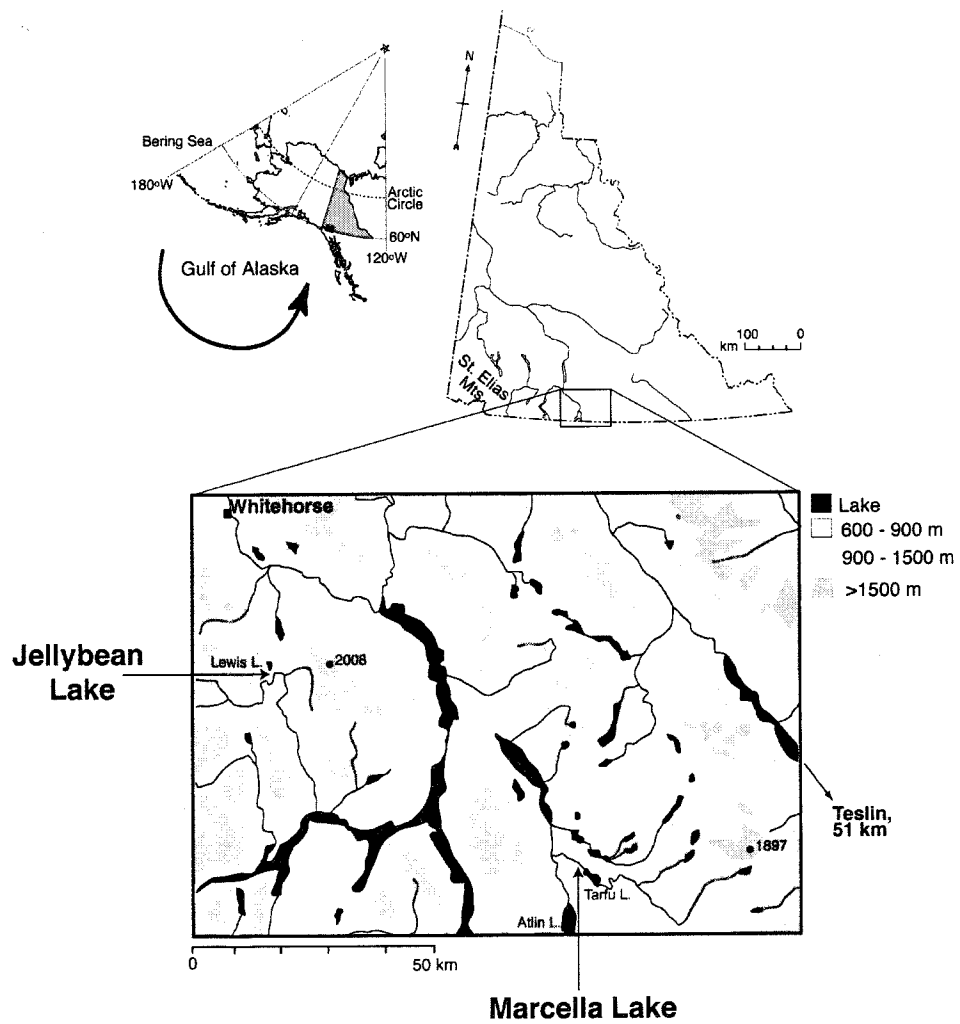


Figure 4.1. Location map that indicates the Yukon Territory, general atmospheric circulation around the Aleutian Low in the Gulf of Alaska, the St. Elias Mountains and the study area including Marcella and Jellybean Lakes, Whitehorse and Teslin.

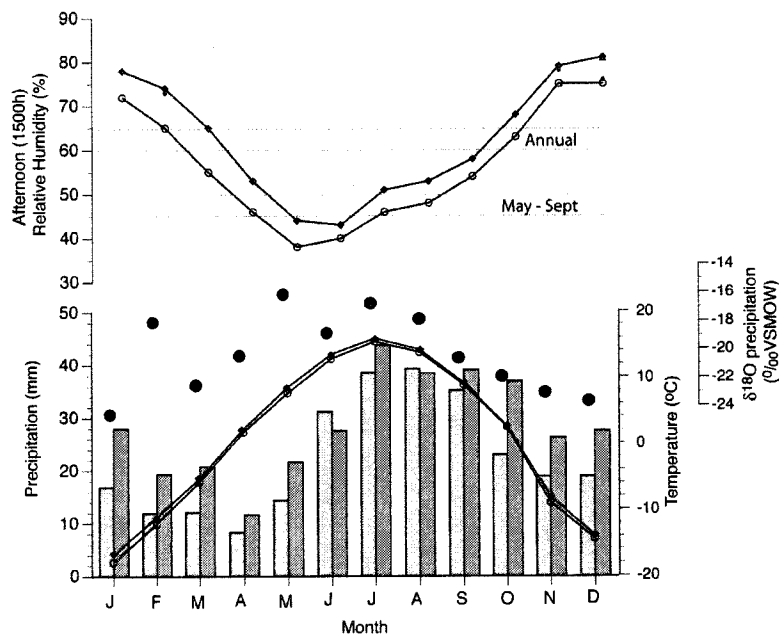


Figure 4.2. Mean-monthly temperature, precipitation, afternoon (1500 hr) relative humidity at Whitehorse (filled diamonds) and Teslin (open), over the period 1944-1990 (Environment Canada, 2003) and mean-monthly oxygen isotope ratios of precipitation (filled circles) at Whitehorse between 1962 and 1964 (IAEA/GNIP, 2002). The instrumental humidity data indicates a May through September humidity range (morning and afternoon) between 45 and 50% while the annual humidity range is between 60 and 63%.

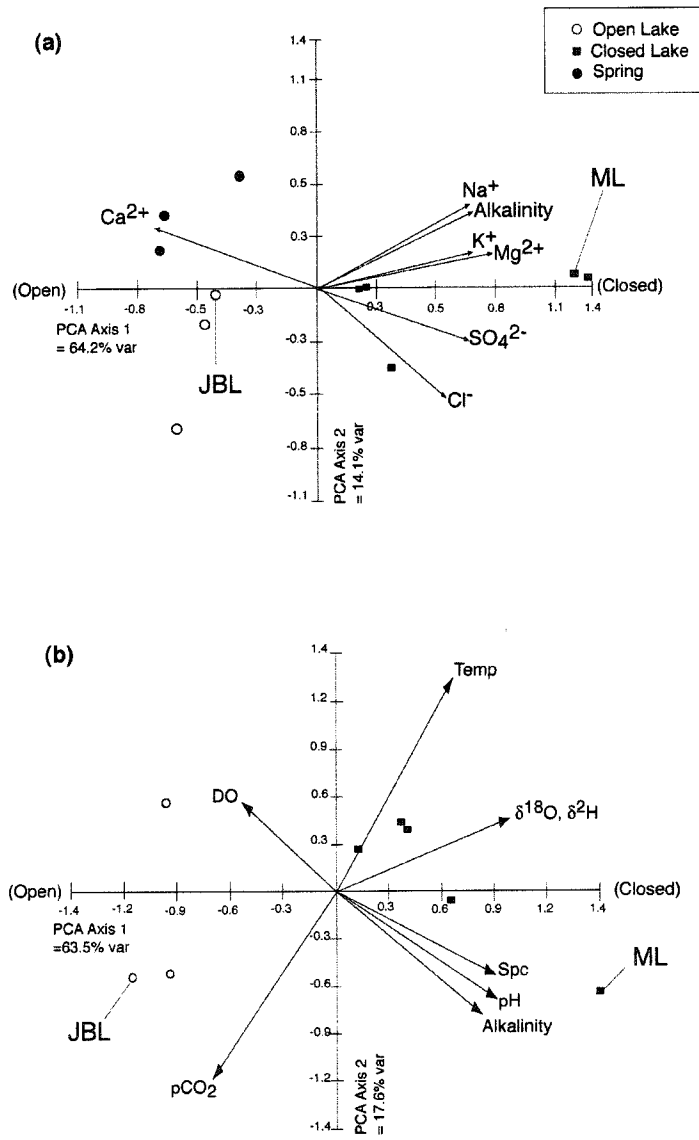


Figure 4.3. PCA bi-plots of (a) limnochemical, and (b) physiolimnological variables of water sampled from eight lakes, including Jellybean Lake (JBL) and Marcella Lake (ML), and three springs located in the southwest and central Yukon Territory (Appendix F).

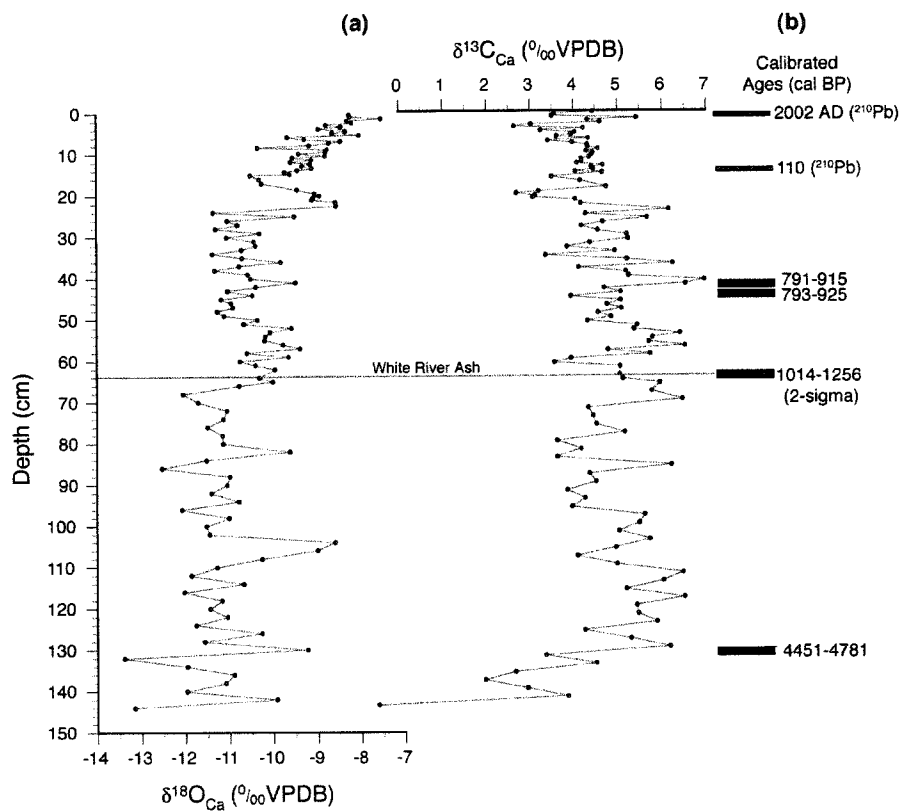


Figure 4.4. Marcella Lake core C/E *Chara* calcite oxygen and carbon isotope ratios ($\delta^{18}\text{O}_{\text{Ca}}$ and $\delta^{13}\text{C}_{\text{Ca}}$) plotted (a) on a depth scale (cm) and (b) with chronostratigraphic data including the surface (2002 AD), the ^{210}Pb dating horizon, the radiocarbon age of the White River tephra (2-sigma range; Clague et al. 1995) and three AMS radiocarbon ages of terrestrial macrofossils (one-sigma range; Table 4.1).

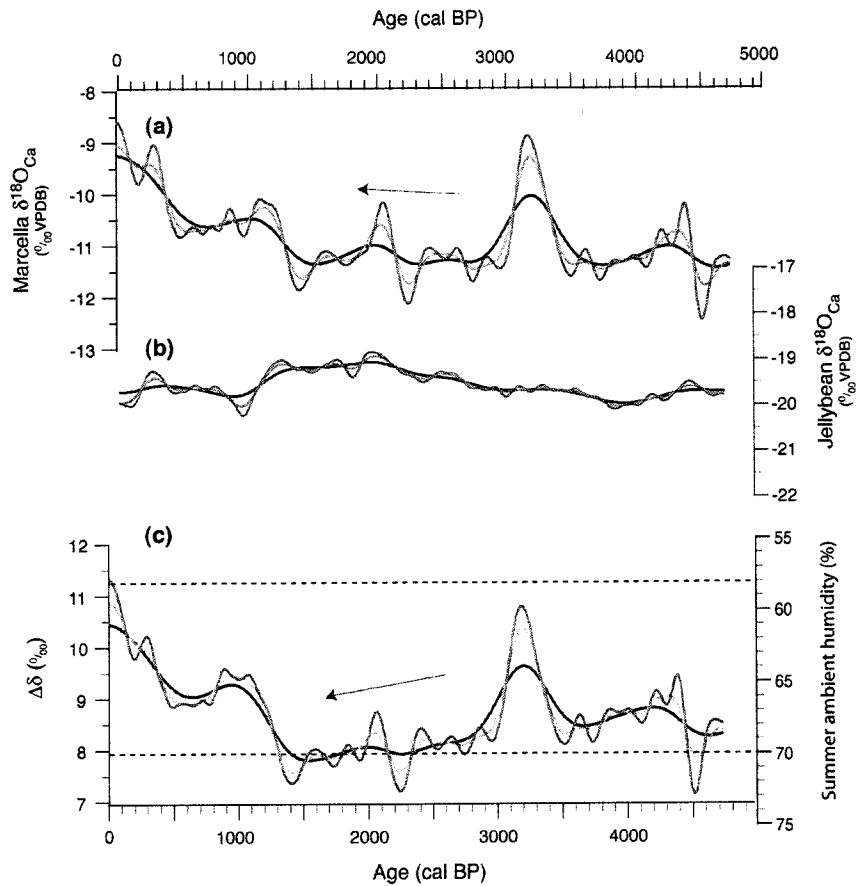


Figure 4.5. Oxygen isotope ratios for (a) Marcella Lake and, (b) Jellybean Lake on a calibrated age scale shown after 200-yr, 100-yr and 50-yr smoothing. The difference between (a) and (b) is (c) $\Delta\delta$, isotopic enrichment due to evaporation and summer ambient humidity, h , also shown as 200-yr, 100-yr and 50-yr smoothed results (Gat, 1995). Arrows indicate the change in trends from (a) to (c) between 3000 and 1200 cal BP. Dashed lines indicate high and low humidity and $\Delta\delta$ values for the record: $\sim 8\text{‰}$ and 70% between 3000 and 1200 cal BP and $\sim 11.4\text{‰}$ and 58%, the average for the last 100 years of data.

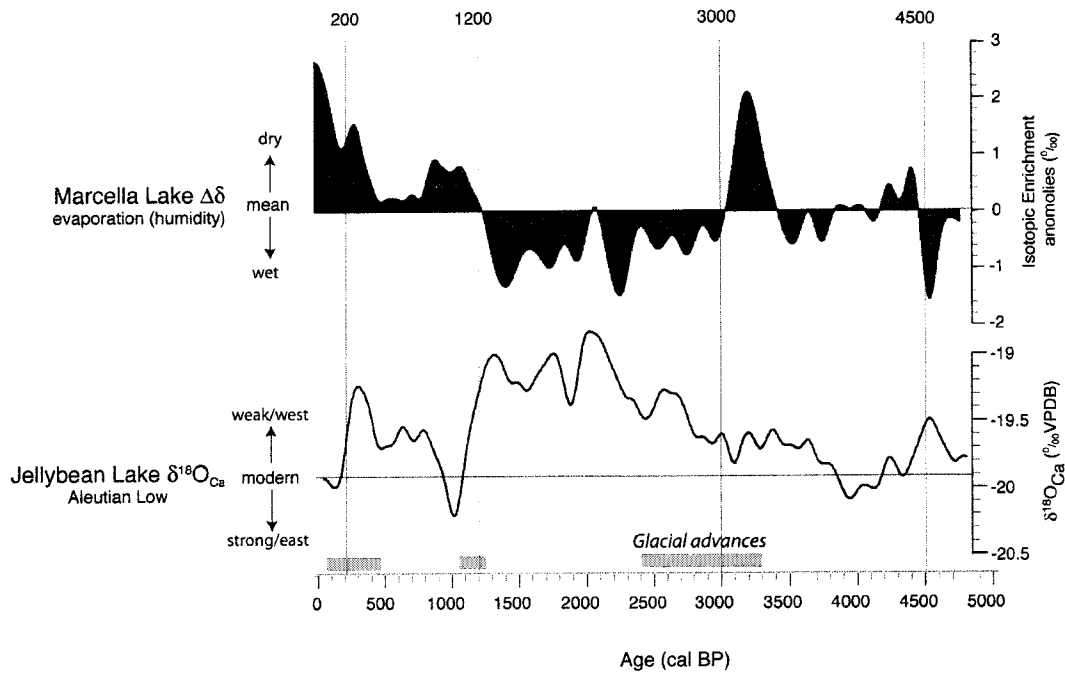


Figure 4.6. Marcella Lake $\Delta\delta$ anomalies (50-yr smooth, difference from the mean for the record) and 50-yr smoothed Jellybean Lake $\delta^{18}\text{O}_{\text{Ca}}$, a record of Aleutian Low intensity and/or position on a calibrated age scale since 5000 cal BP shown with late Holocene glacial activity in the St. Elias Mountains (Denton and Karlén, 1977).

CHAPTER 5

SUMMARY AND CONCLUSIONS

Introduction

This chapter contains a summary of the climatic changes documented by Jellybean and Marcella Lake and a comparison with previous paleoecological, geomorphological and archeological evidence for changes in vegetation, landscape, fauna and humans in the southwest Yukon during the last 10,000 years (Table 5.1).

Holocene Paleoclimate Inferred from Jellybean and Marcella Lake

Jellybean Lake water reflects the oxygen isotope composition of mean annual precipitation. Thus, the oxygen isotope history of Jellybean Lake inferred from sedimentary carbonate oxygen isotope ratios suggests multi-decadal shifts in the oxygen isotope composition of mean annual precipitation superimposed on century and millennial trends. Recent fluctuations correspond to changes in the North Pacific Index, a measure of the intensity and position of the Aleutian Low pressure system over the Gulf of Alaska. This suggests that the Jellybean oxygen isotope record reflects changes in Aleutian Low intensity and position since ~7500 cal BP. Abrupt shifts to an intensified/eastward Aleutian Low occur ~1200 and 400 cal BP after a period of weakening/westward position after 3000 cal BP. These changes correspond with late Holocene glacial advances in the St. Elias Mountains, changes in North Pacific Salmon abundance and shifts in atmospheric circulation over the Beaufort Sea.

Marcella Lake is a small, hydrologically closed, evaporation-sensitive lake. Former water levels, driven by regional paleohydrology, were reconstructed by multi-proxy analyses of

sediment cores from four sites spanning shallow to deep water. Prior to 10,000 cal BP water levels were low. Between 10,000 and 9,000 cal BP they rose to 3- to 4- m below modern levels. Between 7500 and 5000 cal BP water levels were 5- to 6- m below modern but rose by 4000 cal BP. Between 4000 and 2000 cal BP they were higher than modern. During the last 2000 years, water levels lowered to 1- to 2- m below or near modern levels. Marcella Lake water oxygen isotopes are strongly affected by summer evaporation thereby allowing past humidity changes to be reconstructed from sedimentary calcite oxygen isotope ratios at 50 to 200-yr resolution. The record from Jellybean Lake accounts for variations related to atmospheric circulation and ambient temperature allowing the calculation of the difference between Marcella and Jellybean records, a parameter from which we can estimate change in humidity. Between 4500 and 2800 cal BP, summer humidity was higher than the modern average of 58% before reaching a maximum between 2800 and 1200 cal BP near 70%. At ~1200 cal BP humidity abruptly decreased to 65% before decreasing again, to ~60%, around 400 cal BP.

The following climate patterns are emerging. The early Holocene was warm and dry. Between 9000 and 10,000 cal BP there was a rapid increase in lake level suggesting a shift in the precipitation regime. The early aridity may have prevented the establishment of spruce forest. Between 7500 and 4000 cal BP lake levels were relatively stable 5-m below modern levels and Aleutian Low intensity was predominantly weaker and/or westward. Between ~4500 and 3000 cal BP the Aleutian Low intensified and/or shifted eastward before weakening and/or shifting westward further between 3000 and 2000 cal BP. During this interval lake-level and humidity was higher than modern and late Holocene glacial advances began. Rapid Aleutian Low intensification and/or eastward shifts ~1200 and 400 cal BP correspond with humidity decreases in the interior in addition to Little Ice Age glacial advances and increases in North Pacific salmon abundance. Abrupt changes in Aleutian Low intensity/position and humidity were more frequent during the last ~2000 years than the preceding period.

Holocene Vegetation, Landscape and Humans

Vegetation

Wang and Geurts (1991) reviewed the Quaternary vegetation history of the southwest Yukon from. The vegetation summary presented here also includes Keenan and Cwynar (1992), Spear and Cwynar (1997) and Lacourse and Gajewski (2000).

During late glacial and early Holocene times the southwest Yukon supported herb-dominated tundra. By 10,000 cal BP the herb tundra was replaced by birch-dominated shrub tundra. This change is also observed in northern and interior Alaska (Anderson, 1988; Bigelow, 1997). The interval between 9000 to 8500 cal BP marks the regional arrival of white spruce (*Picea Glauca*). Soon afterwards alder appeared and a mixed forest or forest tundra was established by 7500 cal BP and vegetation patterns have remained relatively unchanged since. In some locations black spruce (*Picea mariana*) appearances and green alder (*Alnus*) expansions occurred ~5500 cal BP (Cwynar and Spear, 1995). At ~1300 cal BP herbs and grasses increased at two sites in the center of the dry region around Kluane Lake (Lacourse and Gajewski, 2000) and Lodgepole pine (*Pinus Contorta*) replaced spruce forests locally (eg. Cwynar, 1988).

The vegetation history of the southwest Yukon (Table 5.1b) shows classic Late Pleistocene to early Holocene succession from tundra to birch shrub tundra to mixed spruce forest that is documented in the Northwest Territories to the east and Alaska to the west. Individual localities show some variations in chronology and assemblages, but they are generally small and nevertheless consistent with the Holocene paleoclimate indicated by Jellybean and Marcella Lakes.

Landscape

Early Holocene surficial geology and soils in the southwest Yukon are characteristic of recently de-glaciated high latitude regions. Thick mineral sediment deposits readily available for remobilization or weathering remained after the recession of the northern edge of the Cordilleran ice sheet and the St. Elias ice cap ~11,000 cal BP (Dyke et al., 2002). Numerous glacial lakes formed and drained in the large headwater region of the Yukon River. Early Holocene sedimentation at low elevations is characterized by loess deposition and the remnants of glacial lakes. Loess accumulation eventually slowed as silt source areas were stabilized by vegetation in the early Holocene that was followed by a middle Holocene period of soil development known as the Slims Soil (Workman, 1978; Morlan and Workman, 1980).

Alpine valley glacier growth reoccurred by 3400 and 2000 cal BP in the St. Elias Mountains and Neoglacial loess deposition subsequently reoccurred throughout the region (Denton, 1974). Late Holocene glacial advances and retreats by the Lowell glacier dammed the Alsek River that caused reoccurring formation of Glacial Lake Alsek in the western Dezadeash Valley. Glacial Lake Alsek formed and drained up to four times during the last millennia (Morlan and Workman, 1980). Between 2000 and 1000 cal BP, widespread glacier retreat is suggested by elevated spruce tree-line (Denton and Karlén, 1977). Another brief glacial expansion occurred near the time of the White River tephra. Glacial retreat ~1000 cal BP was followed by another period of expansion ~1600 AD which continued and culminated in Little Ice Age moraine deposits during the late 19th century. Since the early 20th century, glaciers have been retreating.

The east lobe of the White River tephra covers ~540,000 km², extending ~1300 km from its source with a tephra volume of 27 km³ (Robinson, 2001). Two separate lobes are recognized. The earlier, northward trending lobe has been dated at between ~1900 and 1500 ¹⁴C years ago (Lerbekmo and Campbell, 1969). Ash and pumice stratigraphy near the source, Mt. Churchill,

Alaska, suggests a single violent explosion for each lobe (Richter et al., 1995). Although the St. Elias Mountains have been volcanically active throughout the Tertiary, the north and east lobes of the White River Ash are the only known Holocene tephros. The eastern lobe ash fall occurred within days during the winter and has been dated to 1150 cal BP (803 AD; Clague, et al., 1995; West and Donaldson, 2000). This could have caused snow and ice to thaw earlier accelerating erosion by ash choked rivers and streams.

Humans

It is uncertain when humans first arrived in the southwest Yukon but it is possible that they were there as early as 25,000 years ago, the age of settlements in the Old Crow region of the northern Yukon (Morlan and Cinq-Mars, 1982). Evidence for these early inhabitants within late Pleistocene glacial limits, however, is probably lost forever. Thus, the oldest known remains in the southwest Yukon date between 8000 and 7000 years ago, ages obtained from a hunting camp near the Aishihik River, overlooking the former bed of Glacial Lake Champagne (Morlan and Workman, 1980). These people left buffalo bones, small slender sharp-edged stone flakes called microblades, stone tools flaked at one end and on one side only (unifacial), spear points with rounded bases, and crude pebble tools. Little is known of their origins but similar technologies occur in the central Yukon and the District of Mackenzie (Morlan and Workman, 1980). Early to middle Holocene landforms and environments within the upper Yukon watershed region were changing, probably creating a mosaic. Survival would demand a flexible and mobile foraging strategy. Small hunting bands could have relied upon fish, caribou, bison, small game, waterfowl, sheep, elk, moose, and berries (Wright, 2001).

Between 5000 and 4500 years ago, a new and different technology appeared in the southwest Yukon. Spear points had straight or concave ends rather than rounded bases. Blunt ended knives were flaked on both sides (bifacial) and thick unifacially flaked end-scrapers, blunt

skin dressing tools with rounded outlines, and large flat, notched cobbles that may have been used as clubs appear. This technology has been labeled the Teye Lake culture (Morlan and Workman, 1980; Wright, 2001). Workman (1978) speculated that woodland bison were extinct by 3000 year ago possibly making caribou of critical importance for meat, hides, sinew, bone and antler. By 1200 years ago another new technology appears; copper arrowheads, perforators and the bow and arrow (Morlan and Workman, 1980). By the middle 19th century, southwest Yukon inhabitants had direct contact with Europeans, Russians and Canadians.

Climate Change and Humans

How did changes in climate, vegetation and landscape during the Holocene affect people? The small amount of information about early people and the complex interactions between climate, vegetation and fauna only allows speculations about how survival strategies may have changed.

10,000 to 8500 cal BP

An early Holocene moisture regime shift occurred during the transition from herb tundra to a shrub-dominated landscape that would have affected grazing fauna and people. Grazers that prefer grasses, sedges, mosses, and lichen (bison, caribou) could have been displaced. In contrast, the change may have been positive for herbivores that browse woody plants (moose, deer) (Bigelow, 1997). Expanding shrub communities would have impeded overland travel but also made fuel more abundant. This would have been particularly important for winter survival (Bigelow, 1997). The landscape was more exposed, relatively dry and probably dustier and windier than today. Greater seasonal insolation differences caused warmer summers and colder

winters . Humans survival during this period may have been a matter of mobility and the ability to withstand colder winters (Bigelow, 1997).

8500 to 4500 cal BP

The appearance of white spruce and the development of mixed spruce, birch and poplar forests were major vegetation changes. Climate was still drier than today but wetter than the previous two millennia. A brief period of aridity may have occurred ~8000 cal BP. The landscape was stabilizing as vegetation stabilized mineral and loess surface sediments. Spruce forest expansion could have driven grazers such as bison to smaller areas that were still dry enough to sustain herbs and grasses. If the forests supported lichen with good winter forage then the change could have expanded caribou habitats. People may have had to change their subsistence from bison to caribou. It is at this time that the new 'Taye Lake' culture appears. Thus, although the climate of this period was relatively stable and winters were less severe, the archeological record suggests that animals and humans were adapting to the new forest ecosystem, migrating, or in the case of bison, nearing collapse.

4500 to 1500 cal BP

This period marks the beginning of a secular shift in climate from the relatively dry and stable late-early Holocene to a wetter late Holocene. The landscape was changing; glacial advances, glacial lake formation and loess deposition resumed. Increased effective moisture could have lead to peatland formation and paludification (sphagnum accumulation on uplands; Burn, et al., 1986). This could have been a positive change for moose and caribou but may have lead to the extinction of bison (Bigelow, 1997). Higher summer effective moisture and higher lake levels were probably followed by winters with greater snowfall. There is no evidence for a

major technological change coincident with these climatic changes. Human adaptation during this period may have depended upon mobility, to follow caribou migrations. Cultural resilience may have facilitated adaptations to a changing landscape (Wright, 2001).

1500 cal BP to Present

A short climatic respite might have occurred between 2000 and 1000 cal BP but abrupt changes in Aleutian Low intensity and interior humidity mark the last millennia. When Mt. Churchill erupted ~800 BP, up to 15-cm of volcanic tephra fell to the ground. There may have been severe short-term effects. If the tephra harmed caribou, moose and elk populations then humans would have suffered.

North Pacific salmon abundance increased during this period but glacier advances may have blocked migrations up the Alsek River. Increasing summer aridity occurred ~400 cal BP while alpine and coastal glaciers advanced. In the Kluane Lake region, grass and herb vegetation expanded, a positive change for modern grazers such as elk. Despite these relatively severe and unpredictable climate changes, the copper technology appeared. It may indicate that trade and communication facilitated human survival in a rapidly changing landscape.

Recommendations for Future Research

The studies presented here represent a portion of an ongoing research effort. These results have led to the identification of three specific future research goals and recommendations: 1) document the early Holocene with oxygen isotope data, 2) reproduce the Jellybean oxygen isotope record, and 3) document oxygen isotope variations at decade-to-century scales in regions to the north and down-wind of the southwest Yukon.

Early Holocene aridity was far more severe than today. It is important to obtain an early Holocene oxygen isotope record from an evaporation-sensitive lake to verify these new mid-to-late Holocene records. Early Holocene samples from Seven Mile Lake are presented in Appendix A. Due to unresolved questions about the hydrological status of the lake during that period, however, the interpretation is unresolved. The difficulty encountered with early Holocene stable isotope records from Marcella Lake is that lake-level changes disturbed the early sedimentary record. Carbonate preservation was restricted to small mollusks and isotope ratios of biologically produced carbonate have an indirect relationship to climate. Deep lakes, less likely to have experienced early Holocene low water stands, may have avoided sedimentary re-working but tend to be stratified, which inhibits authigenic carbonate preservation. A focus of future investigations should be to identify closed-basin lakes with stratigraphically intact early Holocene carbonate sedimentation. The field investigations carried out for this research indicates that this is a challenging combination, but such a find would expand our knowledge of early Holocene climatic change.

The lake-level and oxygen isotope records presented here have provided new clues about decade-to-century scale changes in the Aleutian Low. The Jellybean Lake record, now supported by similar isotope shifts in the new Mount Logan summit ice core (Fisher et al., 2004), is an important contribution to paleoclimatic studies in the North Pacific region. Nevertheless, it will be significant to verify the record with another evaporation-insensitive lake. I have shown that shifts in Aleutian low intensity and/or position coincide with ecosystem, landscape and climatic change in the southwest Yukon region, but more remains to be understood about the effects in northern Alaska and the Yukon and to the south and east in central and coastal British Columbia and western Alberta. Future research in these regions will provide a broader view of the extent of the climatic effects and provide further insights into the forcing mechanisms.

Table 5.1 Summary of Holocene climate, vegetation, landscape, fauna and human history of the southwestern Yukon Territory (continued on next page)

Age (calibrated)	a. Climate (this study)	b. Vegetation ^{3,4}	c. Glaciations, tree-line, pro-glacial lakes ^{5,6}
2000 AD	Cold continental, subarctic.	Closed canopy forest, white and black spruce, larch,	Widespread retreat continues
1970 AD	-NP anomaly (strong AL)	alpine fir, lodgepole pine, aspen,	
1900 AD	+ NP anomaly (weak AL)	balsam poplar,	Widespread retreat begins
1850 AD		Paper birch. Grasslands restricted to steep, dry, south facing slopes.	Late 'Little Ice Age' Moraines Recent Lake Aisek #5
200 BP (1800 AD)	Long term shift to strong AL Increasing evaporation to present Modern lake levels		'Little Ice Age' Moraines Recent Lake Aisek #4
400 BP (1600 AD)	Shift to weaker AL,		Early 'Little Ice Age' moraines Recent Lake Aisek #3
800 BP			
1000 BP	Long-term shift to strong AL, increasing evaporation lower lake levels		Widespread advance
1200 BP			
1500 BP	Weak AL, Wetter than present		Rise in spruce tree-line, Inferred glacial retreat
2000 BP	Weakest AL of the Holocene	Lodgepole pine and increased grasses and sage locally	Recent Lake Aisek #1-2.
2500 BP	Low evaporation, high humidity. Higher than modern lake levels	Peatland development and paludification?	Widespread advance
3000 BP	Wetter than present		
3500 BP	400 year dry period		
4000 BP	Shift to weaker AL Wetter than present	Spruce Woodland established, Alder present locally	Rise in spruce tree-line, (inferred retreat)
4500 BP	Rising lake levels		
5000 BP	5 to 6 m BML lake levels		
5500 BP			
6000 BP	Weak AL.	Black Spruce abundance increases locally	
6500 BP			
7000 BP	3 to 4 m BML lake levels		Glacial Lake Sekulman, -Aishihik drains?
7500 BP	Weak Aleutian Low (AL)		
8000 BP	Possible lower lake levels	White Spruce invades the region	
8500 BP	3 to 4 m BML lake levels		
9000 BP	Rapidly rising lake levels		Glacial Lake Champagne drains?
9500 BP		Birch tundra or Poplar woodland	
>10,000 BP	Arid	Herb tundra	Wisconsinan ice retreats within Neoglacial limits

Table 5.1 (cont.)

Age (calibrated)	d. Soils ^{1,2} and Geologic Events ⁷	f. Fauna ^{1,8}	g. Culture ^{1,9,10}
2000 AD 1970 AD 1900 AD	Brunisol; midly weathered mineral soil	Moose, caribou, elk, bear, wolf, lynx, fox, salmon, waterfowl.	Modern culture
1850 AD		(Increasing Alaskan salmon)	Fur trade, villages
200 BP (1800 AD) 400 BP (1600 AD) 800 BP	Neoglacial Loess, glacial lake sediments locally: recent Lake Alek	(Low Alaskan salmon)	
1000 BP 1200 BP	White River Ash Fall: Explosive volcanism	(Decreasing Alaskan salmon)	New Technology: copper arrowheads, bow and arrow, small seasonal camps, moose, caribou, fish, small mammals. Aishihik Culture.
1500 BP 2000 BP	Glacial lake sediments locally: recent Lake Alek	(High Alaskan salmon) passage to interior blocked?	
2500 BP 3000 BP 3500 BP	Neoglacial loess deposition,	Woodland bison (<i>B.b</i> <i>athabaskae</i>) extinct.	
4000 BP	Soil formation: Slims soil, oxidized reddish brown layer.		New Technology (bifacial flaking, notched spear points, small group hunters of bison, caribou, moose. Taye Lake Culture
4500 BP 5000 BP 5500 BP 6000 BP 6500 BP 7000 BP	Little soil deposition, weathering		Little Arm Culture (unifacial flaking, rounded base of spear points, large bison bones). Oldest archeological dates
8000 BP		Extinction of late Pleistocene fauna.	
8500 BP 9000 BP 9500 BP	Loess deposition		
>10,000 BP	Kluane Lake drains to Pacific?	Salmon access to interior via Alek River?	

¹Workman, 1978; ²Smith, 2001; ³Oswald and Senyk, 1977; ⁴Wang and Geurts, 1991; ⁵Denton and Karlén, 1977; ⁶Calkin, 1988; ⁷Clague et al., 1995; ⁸Finney et al., 2000, 2002; ⁹Morlan and Workman, 1980; ¹⁰Wright, 2001.

APPENDIX A

TABLE OF SEDIMENT CORES RETRIEVED

Month/ Year	Lake Name	Water Depth (cm)	Core	Drive	Depth (cm)	Drive Length (cm) ¹
Jul-99	Seven Mile (7.5)Lake	1258	A	1	1258-1334	72-polycarb ²
				2	1308-1408	91
				3	1408-1508	92
				4	1508-1608	109
				5	1608-1672	63
Jul-99	Seven Mile (7.5) Lake	1258	B	1	1330-1430	94
				2	1430-1527	94
				3	1527-1626	96
				4	1626-1696	73
				5	1696-1773	65
Jul-99	Seven Mile (7.0) Lake	1220	A	1	1225-1325	84
				2	1310-1370	57
				3	1310-1396	86.5
Jul-99	Seven Mile (7.0) Lake	723	B	1	723-823	99
				2	823-923	86
				3	750-850	100
				4	850-877	26.5
Jul-99	Seven Mile (7.0) Lake	585	C	1	585-685	97
				2	685-785	94
Jul-00	Waddington Pond	479	A	1	469-577	76-polycarb
				2	495-591	98
				3	575-671	97
				4	655-751	95
				5	745-841	96

Month/ Year	Lake Name	Water Depth (cm)	Core	Drive	Depth (cm)	Drive Length (cm) ¹
				6	845-941	62
				7	907-1003	83
				8	1007-1051	39
Jul-00	Waddington Pond	548	B	1	580-676	96
				2	630-726	99
				3	710-806	97
				4	800-896	94
				5	890-968	72
				6	972-1068	92
				7	1072-1123	55
				8	568-636	72-polycarb
Jul-00	Waddington Pond	290	C	1	300-396	79
				2	380-476	98
				3	460-556	94
				4	540-636	97
Jul-00	Waddington Pond	123	D	1	123-217	98
				2	213-307	97
				3	313-407	90
				4	411-487	82
Aug-00	Jellybean Lake	1000	A	1	1010-1091	81-polycarb
				2	1008-1090	82-polycarb
Aug-00	Marcella Lake	960	A	1	955-1051	96-polycarb
				2	980-1076	95
				3	1040-1136	99
Aug-00	Marcella Lake	960	A	4	1120-1216	98
				5	1210-1306	94
				6	1300-1396	93
				7	1390-1486	91
				8	1490-1501	15

Month/ Year	Lake Name	Water Depth (cm)	Core	Drive	Depth (cm)	Drive Length (cm) ¹
Aug-00	Marcella Lake	970	B	1	970-1066	98
				2	1060-1156	97
				3	1150-1246	100
				4	1240-1336	93
				5	1330-1426	90
				6	1420-1506	63
Aug-00	Marcella Lake	430	C	1	440-536	98
				2	520-516	99
				3	600-643	47
Aug-00	Marcella Lake	200	D	1	200-296	94
				2	280-376	97
				3	360-456	99
				4	440-536	100
				5	520-556	37
Aug-00	Seven Mile (7.5) Lake	1285	C	1	1280-1347	67-polycarb
				2	1290-1353	63-polycarb
				3	1355-1451	96
Aug-00	Seven Mile (7.5) Lake	1280	D	1	1280-1329	54-polycarb
				2	1343-1437	84
Aug-00	Seven Mile (7.5) Lake	1345	E	1	1330-1413	83-polycarb
				2	1410-1506	70
Aug-00	(7.5) Lake	1345	E	3	1426-1522	86
Aug-00	Seven Mile (7.5) Lake	800	F	1	790-845	55-polycarb

Month/ Year	Lake Name	Water Depth (cm)	Core	Drive	Depth (cm)	Drive Length (cm) ¹
Jul-02	Marcella Lake	457	E	1	457-613	156-polycarb
				2	451-594	143-polycarb
Jul-02	Marcella Lake	697	F	1	697-892	195-polycarb
				2	870-970	96
				3	970-1038	68
				4	950-1037	90
Jul-02	Jellybean Lake	1162	C	"1"	Not retrieved	
				1	1162-1333	171-polycarb
				2	1310-1411	100
				3	1400-1501	100

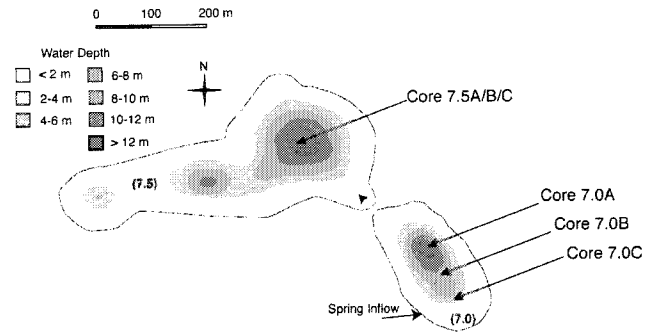
¹ Extruded Livingstone core

² Livingstone square rod and piston used with a polycarbonate core barrel.

APPENDIX B

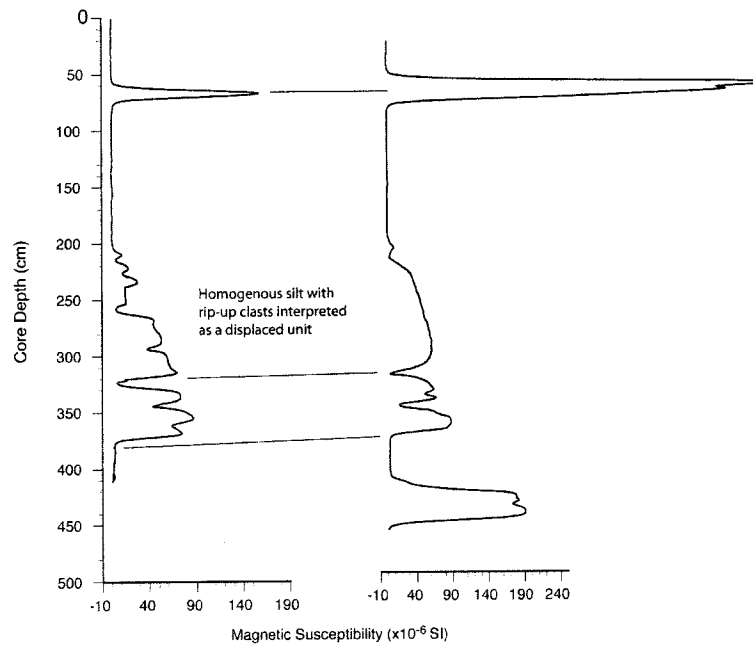
SEVEN MILE LAKE DATA

(a) Seven Mile (7.0 and 7.5) Lake bathymetry and core locations

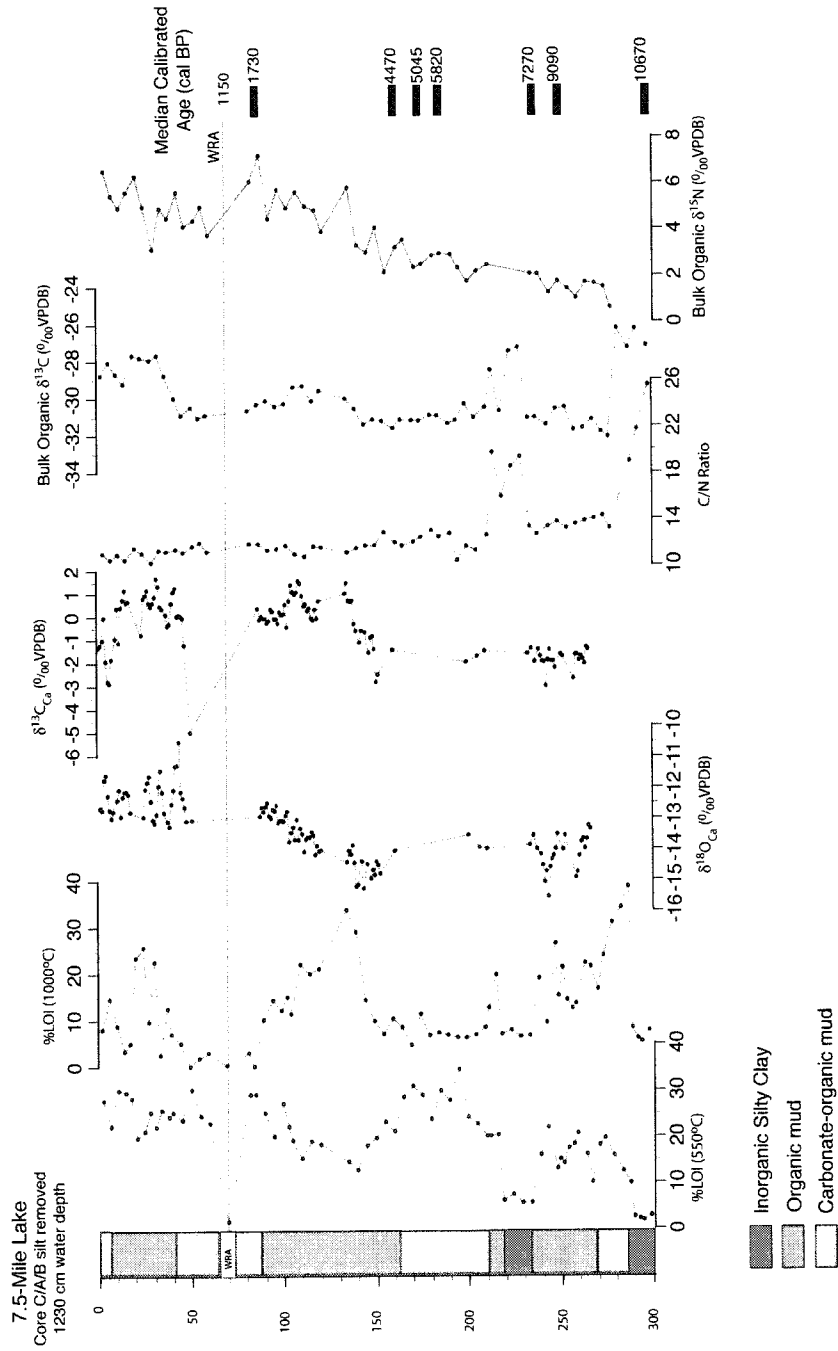


(b) Seven (7.5) Mile Core A

(c) Seven Mile (7.5) Core B

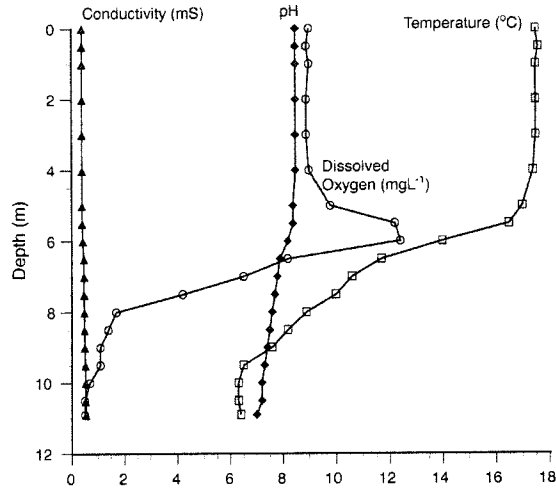


Bathymetric map, coring locations and magnetic susceptibility of core A and B from 7.5 Mile Lake. A composite core C/A/B was based on visual correlation and magnetic susceptibility. Core C extended from the surface to the ash. A silt unit 133-cm thick between 233 and 366 cm depth contained rip-up clasts (shaded). It was interpreted as a displaced unit and removed from the composite C/A/B stratigraphy.

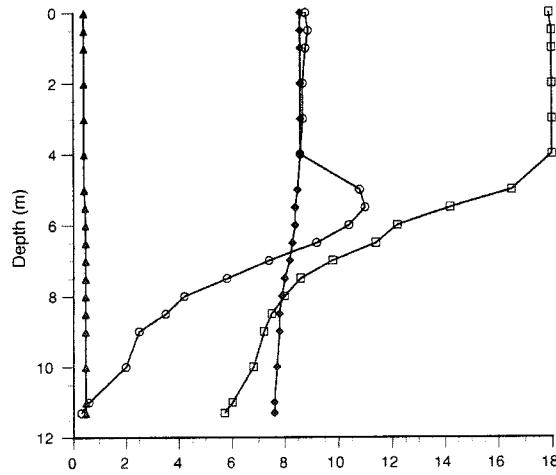


7.5-Mile Lake core C/A/B stratigraphy after removal of the 133-cm silt unit between 233 and 336-cm depth including %LOI, bulk calcite $\delta^{18}\text{O}$ and $\delta^{13}\text{C}$, bulk organic C/N ratio, $\delta^{13}\text{C}$ and $\delta^{15}\text{N}$, and median calibrated ages.

(a) 7.0 Mile Lake



(b) 7.5 Mile Lake



7.0-Mile (a) and 7.5-Mile (b) water column measurements including conductivity (triangle), pH (filled circle), dissolved oxygen (open circle) and temperature (open square).

Seven Mile (7.5) Lake Water and Surface Sediment Analyses

Parameter	Result
pH	8.6
Specific Conductivity (mS)	0.42
Temperature (°C)	17.9
Dissolved Oxygen (mgL ⁻¹)	8.8
Dissolved Carbon Dioxide (ppm)	382
Ambient Carbon Dioxide (ppm)	381
Alkalinity (mgL ⁻¹)	177
Na ⁺ (mgL ⁻¹)	13.54
K ⁺ (mgL ⁻¹)	5.24
Mg ²⁺ (mgL ⁻¹)	34.71
Ca ²⁺ (mgL ⁻¹)	29.03
Cl ⁻ (mgL ⁻¹)	2.13
NO ₃ ⁻ (mgL ⁻¹)	1.38
SO ₄ ²⁻ (mgL ⁻¹)	23.95
Lake water δ ¹⁸ O, δ ² H (VSMOW)	-10.4, -121
Living <i>Chara</i> δ ¹⁸ O _{Ca} , δ ¹³ C _{Ca} (‰ VPDB)	-10.69, 2.1
Predicted-equilibrium δ ¹⁸ O _{Ca} (‰ VPDB) ¹	-10.66
Particulate organic matter δ ¹³ C, δ ¹⁵ N (‰ VPDB)	-26.3, 5.3

¹ Epstein et al., (1953).

Seven Mile (7.0) Lake Water and Surface Sediment Analyses

Parameter	Result
pH	8.5
Specific Conductivity (mS)	0.40
Temperature (°C)	17.5
Dissolved Oxygen (mgL ⁻¹)	9.0
Dissolved Carbon Dioxide (ppm)	400.8
Ambient Carbon Dioxide (ppm)	381
Alkalinity (mgL ⁻¹)	180
Na ⁺ (mgL ⁻¹)	12.48
K ⁺ (mgL ⁻¹)	4.49
Mg ²⁺ (mgL ⁻¹)	32.48
Ca ²⁺ (mgL ⁻¹)	30.51
Cl ⁻ (mgL ⁻¹)	2.57
NO ₃ ⁻ (mgL ⁻¹)	2.44
SO ₄ ²⁻ (mgL ⁻¹)	28.79
Lake water δ ¹⁸ O, δ ² H (VSMOW)	-13, -131
Living <i>Chara</i> δ ¹⁸ O _{Ca} , δ ¹³ C _{Ca} (‰ VPDB)	-12.92, 2.39
Predicted-equilibrium δ ¹⁸ O _{Ca} (‰ VPDB) ¹	-11.95

¹ Epstein et al., (1953).

Seven Mile Lake Composite Core C/A/B Geochronological Data

Core	Core Depth (cm)	Core Depth -133-cm silt ¹ (cm)	Material	Lab #	Measured Age (¹⁴ C yr BP)	Median Calibrated Age (cal BP) ²	1-Sigma Range
7.5C	0	0	²¹⁰ Pb			2002 AD ³	
7.5C	15.25	0	²¹⁰ Pb			192 ³	
7.5C	65	65	White River			1150 ⁴	1014-1256 ⁴
			Ash				
7.5C	84	84	Wood	CAMS-73157	1820 ± 40	1730	1707-1819
7.5B	155	155	Pollen	CAMS-92158	4505 ± 35	5130 ⁵	5048-5295
7.5B	155	155	Macros	CAMS-92159	4020 ± 45	4470	4419-4565
7.5A	165	165	Wood	CAMS-73170	4450 ± 40	5045	4973-5260
7.5A	179	179	Wood	CAMS-73171	5070 ± 40	5820	5745-5905
7.5B	232.5	232.5	pollen	CAMS-92160	5870 ± 35	6700 ⁵	6643-6729
7.5B	232.5	232.5	Macros	CAMS-92161	6365 ± 35	7270	7316-7523
7.5B	365.5	232.5	Pollen	CAMS-92162	15625 ± 45	18660 ⁵	18379-18959
7.5B	377	244	Pollen	CAMS-92163	8170 ± 163	9090	9027-9251
7.5B	423.5	290.5	Pollen	CAMS-92164	12060 ± 60	14090 ⁵	12843-15021
7.5B	444.25	311.25	Pollen	OS-26714	9370 ± 50	10670	10503-10672

¹ Depths after removal of the 133-cm of homogenous silt containing rip-up clasts between 233 and 366-cm depths.

² Mean intercept of calibrated radiocarbon ages.

³ Year core retrieved and ²¹⁰Pb-based age based on constant Rate of Supply (CRS) model (Appleby, 2001).

⁴ 2-sigma range from Clague et al. (1995).

7.5-Mile Lake Bulk Carbonate Oxygen and Carbon Isotope Data

Core-Drive ¹	Sediment-Water Interface Depth (cm)	Sediment-Water Interface Depth with silt removed (cm)	$\delta^{13}\text{C}_{\text{Ca}}$ (‰)	$\delta^{18}\text{O}_{\text{Ca}}$ (‰)
Core C-Drive 1	1	1	-1.33	-12.66
Core C-Drive 1	2	2	-1.23	-12.73
Core C-Drive 1	3	3	-1.02	-11.74
Core C-Drive 1	4	4	-0.03	-11.58
Core C-Drive 1	5	5	-1.91	-12.25
Core C-Drive 1	6	6	-2.79	-12.72
Core C-Drive 1	7	7	-2.88	-12.99
Core C-Drive 1	8	8	-1.83	-12.77
Core C-Drive 1	10	10	-0.94	-12.40
Core C-Drive 1	11	11	0.37	-12.06
Core C-Drive 1	12	12	-1.12	-12.93
Core C-Drive 1	13	13	0.41	-12.29
Core C-Drive 1	14	14	0.74	-12.13
Core C-Drive 1	15	15	1.16	-12.12
Core C-Drive 1	16	16	0.63	-12.21
Core C-Drive 1	17	17	0.67	-12.79
Core C-Drive 1	24	24	-0.78	-12.94
Core C-Drive 1	25	25	0.80	-12.04
Core C-Drive 1	26	26	0.94	-11.81
Core C-Drive 1	27	27	1.16	-11.62
Core C-Drive 1	28	28	0.60	-12.43
Core C-Drive 1	29	29	0.44	-13.04
Core C-Drive 1	30	30	0.60	-13.15
Core C-Drive 1	31	31	0.86	-12.86
Core C-Drive 1	32	32	1.67	-11.94
Core C-Drive 1	33	33	1.33	-11.43
Core C-Drive 1	34	34	0.46	-12.13
Core C-Drive 1	35	35	0.35	-12.81
Core C-Drive 1	37	37	0.11	-13.10
Core C-Drive 1	38	38	-0.38	-13.26
Core C-Drive 1	39	39	-0.31	-12.52
Core C-Drive 1	40	40	0.59	-12.07
Core C-Drive 1	41	41	1.09	-11.29
Core C-Drive 1	42	42	1.25	-11.27
Core C-Drive 1	43	43	0.03	-10.51
Core C-Drive 1	44	44	0.08	-12.13

Core-Drive ¹	Sediment-Water Interface Depth (cm)	Sediment-Water Interface Depth with silt removed (cm)	$\delta^{13}\text{C}_{\text{Ca}}$ (‰)	$\delta^{18}\text{O}_{\text{Ca}}$ (‰)
Core C-Drive 1	45	45	0.04	-12.33
Core C-Drive 1	46	46	-0.05	-12.63
Core C-Drive 1	47	47	-1.22	-13.08
Core C-Drive 1	50	50	-5.00	-13.06
Core B-Drive 2	87	87	0.35	-12.93
Core B-Drive 2	88	88	-0.13	-12.64
Core B-Drive 2	89	89	0.01	-12.78
Core B-Drive 2	90	90	-0.06	-12.62
Core B-Drive 2	91	91	-0.06	-12.49
Core B-Drive 2	92	92	-0.27	-12.92
Core B-Drive 2	93	93	-0.18	-12.99
Core B-Drive 2	94	94	0.32	-12.71
Core B-Drive 2	95	95	0.23	-12.76
Core B-Drive 2	96	96	-0.09	-12.57
Core B-Drive 2	97	97	-0.09	-13.14
Core B-Drive 2	98	98	-0.28	-13.07
Core B-Drive 2	99	99	0.21	-13.07
Core B-Drive 2	100	100	0.09	-13.10
Core B-Drive 2	101	101	0.11	-12.90
Core B-Drive 2	102	102	0.53	-12.77
Core B-Drive 2	103	103	-0.45	-13.76
Core B-Drive 2	104	104	0.68	-13.46
Core B-Drive 2	105	105	1.38	-13.29
Core B-Drive 2	106	106	1.07	-13.69
Core B-Drive 2	107	107	0.97	-13.03
Core B-Drive 2	108	108	1.05	-13.70
Core B-Drive 2	109	109	1.55	-13.32
Core B-Drive 2	110	110	1.45	-13.51
Core B-Drive 2	111	111	0.91	-14.08
Core B-Drive 2	112	112	0.47	-13.67
Core B-Drive 2	113	113	0.54	-13.60
Core B-Drive 2	114	114	0.25	-13.61
Core B-Drive 2	115	115	0.37	-13.44
Core B-Drive 2	116	116	-0.06	-13.55
Core B-Drive 2	117	117	-0.15	-14.18
Core B-Drive 2	118	118	0.31	-13.89
Core B-Drive 2	119	119	-0.08	-14.07

Core-Drive ¹	Sediment-Water Interface Depth (cm)	Sediment-Water Interface Depth with silt removed (cm)	$\delta^{13}\text{C}_{\text{Ca}}$ (‰)	$\delta^{18}\text{O}_{\text{Ca}}$ (‰)
Core B-Drive 2	120	120	0.68	-14.04
Core B-Drive 3	134	134	1.00	-14.42
Core B-Drive 3	135	135	1.45	-14.05
Core B-Drive 3	136	136	0.69	-14.17
Core B-Drive 3	137	137	0.66	-13.87
Core B-Drive 3	138	138	0.69	-14.44
Core B-Drive 3	139	139	-0.32	-15.21
Core B-Drive 3	140	140	-0.62	-15.15
Core B-Drive 3	142	142	-1.12	-14.39
Core B-Drive 3	143	143	-0.61	-15.27
Core B-Drive 3	145	145	-0.68	-14.48
Core B-Drive 3	147	147	-1.55	-14.95
Core B-Drive 3	148	148	-0.91	-14.67
Core B-Drive 3	149	149	-0.84	-14.84
Core B-Drive 3	150	150	-1.40	-14.40
Core B-Drive 3	151	151	-2.82	-14.51
Core B-Drive 3	152	152	-2.50	-14.79
Core B-Drive 3	160	160	-1.44	-14.05
Core B-Drive 4	341	200	-1.97	-13.54
Core B-Drive 4	348	206	-1.72	-13.95
Core B-Drive 4	352	210	-1.49	-13.99
Core B-Drive 4	375	233	-1.60	-13.87
Core B-Drive 4	377	235	-1.38	-13.56
Core B-Drive 4	379	237	-1.96	-14.00
Core B-Drive 4	381	239	-1.43	-14.18
Core B-Drive 4	382	240	-1.73	-14.53
Core B-Drive 4	383	241	-1.94	-15.08
Core B-Drive 4	384	242	-1.97	-14.73
Core B-Drive 4	385	243	-3.01	-15.55
Core B-Drive 4	386	244	-1.89	-14.60
Core B-Drive 4	387	245	-1.44	-14.34
Core B-Drive 4	388	246	-1.93	-14.22
Core B-Drive 4	389	247	-1.93	-14.00
Core B-Drive 4	390	248	-2.23	-13.52
Core B-Drive 4	393	251	-1.64	-14.02
Core B-Drive 4	395	252	-1.72	-13.57
Core B-Drive 5	395	258	-2.68	-14.93

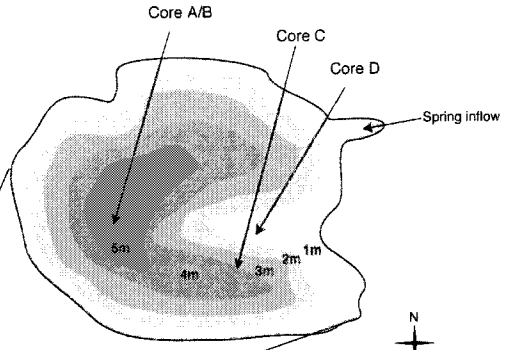
Core-Drive ¹	Sediment-Water Interface Depth (cm)	Sediment-Water Interface Depth with silt removed (cm)	$\delta^{13}\text{C}_{\text{Ca}}$ (‰)	$\delta^{18}\text{O}_{\text{Ca}}$ (‰)
Core B-Drive 5	396	259	-1.65	-14.75
Core B-Drive 5	397	260	-1.64	-14.23
Core B-Drive 5	398	261	-1.90	-13.77
Core B-Drive 5	399	262	-1.71	-13.67
Core B-Drive 5	400	263	-1.85	-13.99
Core B-Drive 5	401	264	-2.04	-13.68
Core B-Drive 5	402	265	-1.34	-13.25
Core B-Drive 5	403	266	-1.42	-13.35

¹See Appendix A

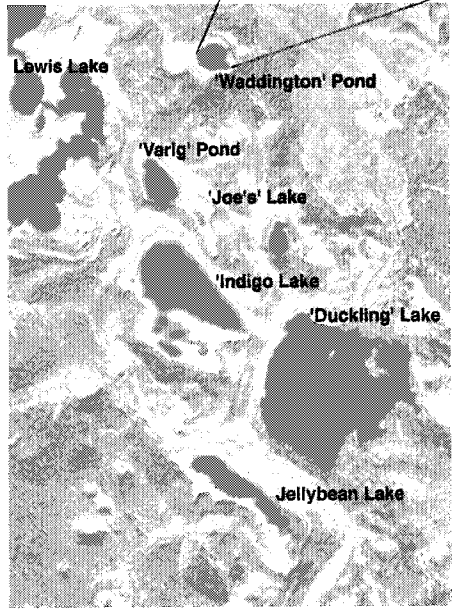
APPENDIX C

WADDINGTON POND DATA

(a) Waddington Pond bathymetry and core locations

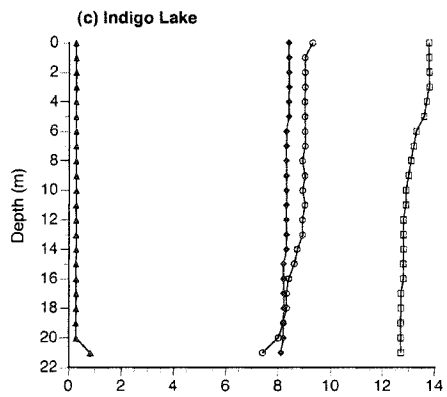
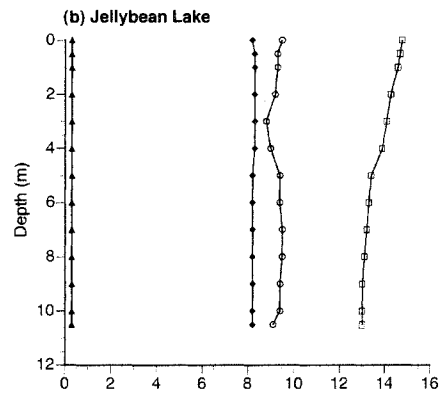
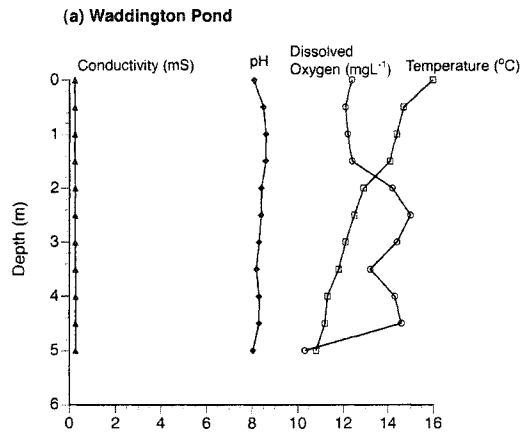


(b) Lewis Lake and surrounding region



Air photograph A27666-45, copyright 1990 by Her Majesty the Queen in Right of Canada, reproduced from the collection of the National Air Photo Library, with permission Natural Resources Canada

Lewis Lake and surrounding lakes including Jellybean Lake, Indigo Lake and Waddington Pond location, bathymetry and coring loations



Water column measurements of Waddington Pond (a), Jellybean Lake (b) and Indigo Lake (c) including conductivity (solid triangle), pH (filled circle), dissolved oxygen (open circle) and temperature (open square).

Waddington Pond Water and Surface Sediment Analyses

Parameter	Result
pH	8.1
Specific Conductivity (mS)	0.24
Temperature (°C)	16.0
Dissolved Oxygen (mgL ⁻¹)	12.40
Dissolved Carbon Dioxide (ppm)	409
Ambient Carbon Dioxide (ppm)	369
Alkalinity (mgL ⁻¹)	99
Na ⁺ (mgL ⁻¹)	4.70
K ⁺ (mgL ⁻¹)	2.08
Mg ²⁺ (mgL ⁻¹)	8.90
Ca ²⁺ (mgL ⁻¹)	35.74
Cl ⁻ (mgL ⁻¹)	2.16
NO ³⁻ (mgL ⁻¹)	3.87
SO ₄ ²⁻ (mgL ⁻¹)	20.85
Lake water δ ¹⁸ O, δ ² H (VSMOW)	-18.5, -146
Living <i>Chara</i> δ ¹⁸ O _{Ca} , δ ¹³ C _{Ca} (‰ VPDB)	--18.41, -0.27
Predicted-equilibrium δ ¹⁸ O _{Ca} (‰ VPDB) ¹	-18.36
Particulate organic matter δ ¹³ C, δ ¹⁵ N (‰ VPDB)	-26.32, 2.22

¹ Epstein et al., (1953).

Indigo Lake Water and Surface Sediment Analyses

Parameter	Result
pH	8.4
Specific Conductivity (mS)	0.28
Temperature (°C)	13.8
Dissolved Oxygen (mgL ⁻¹)	9.30
Dissolved Carbon Dioxide (ppm)	610
Ambient Carbon Dioxide (ppm)	401
Alkalinity (mgL ⁻¹)	130
Na ⁺ (mgL ⁻¹)	4.09
K ⁺ (mgL ⁻¹)	1.62
Mg ²⁺ (mgL ⁻¹)	7.75
Ca ²⁺ (mgL ⁻¹)	46.28
Cl ⁻ (mgL ⁻¹)	2.38
NO ³⁻ (mgL ⁻¹)	1.66
SO ₄ ²⁻ (mgL ⁻¹)	14.58
Lake water δ ¹⁸ O, δ ² H (VSMOW)	-20.8, -160
Particulate organic matter δ ¹³ C, δ ¹⁵ N (‰ VPDB)	-24.57, 2.74

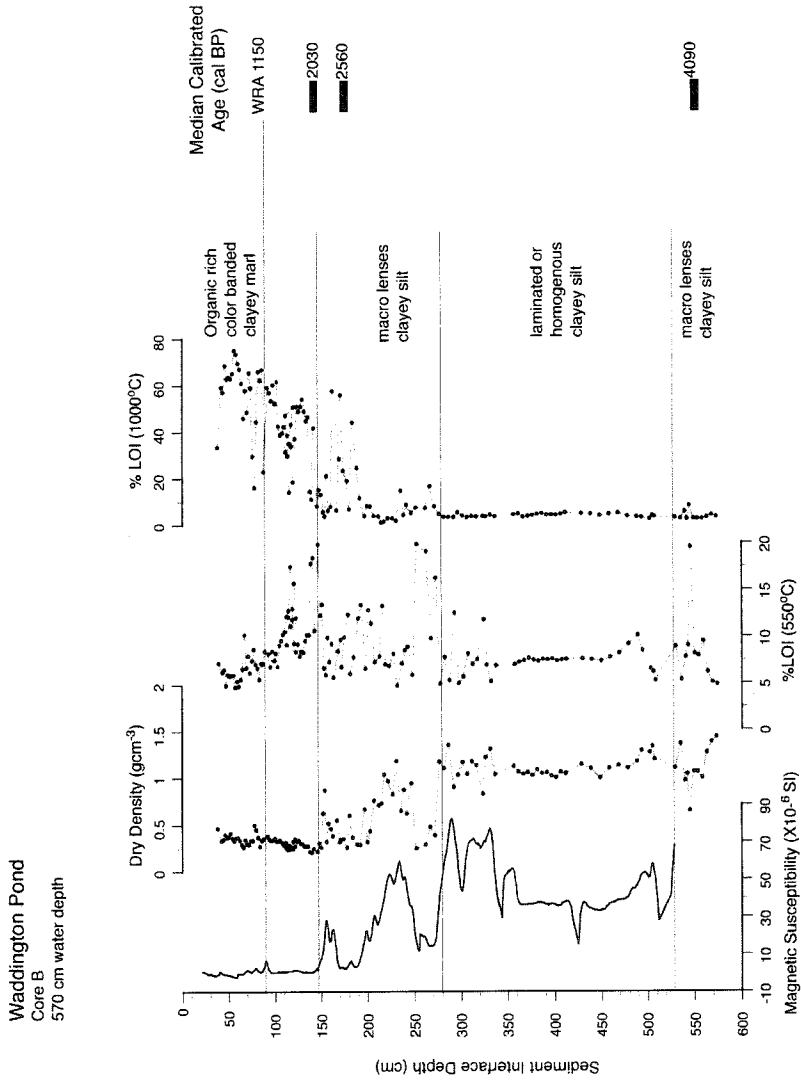
¹ Epstein et al., (1953).

Waddington Pond Geochronological Data

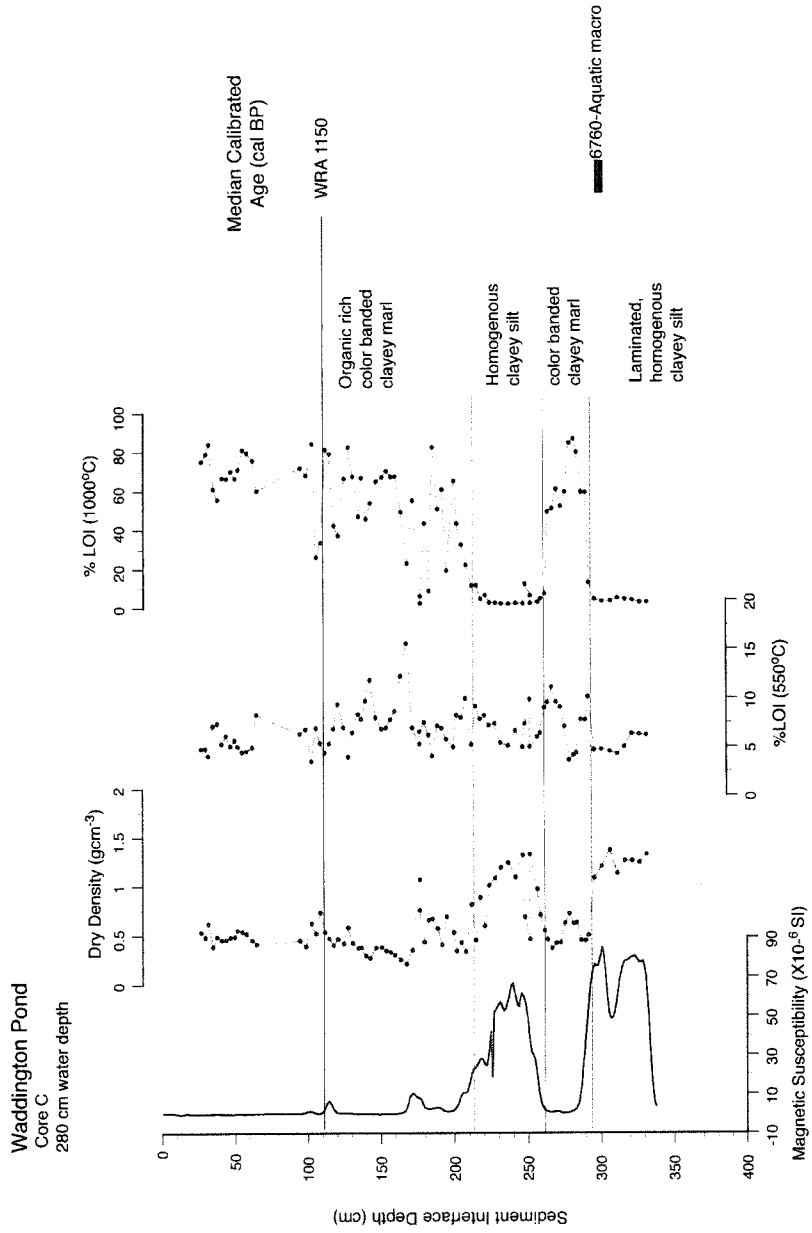
Core	Core Depth (cm)	Material	Lab #	Measured Age (¹⁴ C yr BP)	Median Calibrated Age (cal BP) ¹	1-Sigma Range
A	90-100	White River Ash			1150 ²	1014-1256 ²
A	476	Wood	CURL-5206	3860 ± 60	4290	4158-4405
B	90	White River Ash			1150 ²	1014-1256 ²
B	139.5	Wood	CAMS-73141	2070 ± 40	2030	1951-2112
B	178	Wood	CAMS-73155	2500 ± 50	2560	2469-2736
B	559	Wood	CURL-5390	3730 ± 35	4090	3989-4146
C	114	White River Ash			1150 ²	1014-1256 ²
C	291	Aquatic macro	CAMS-73142	6830 ± 45	7670	7510-7835
D	25	White River Ash			1150 ²	1014-1256 ²
D	62	Aquatic macro	CAMS-73156	2080 ± 50	2020	1952-2119
D	170	Charcoal	CAMS-73143	2780 ± 60	2870	2783-2949
D	305.5	Wood/spruce needle	OS-12128	4070 ± 35	4560	4777-4449

¹ Mean intercept of calibrated radiocarbon ages using Stuiver et al (1998).

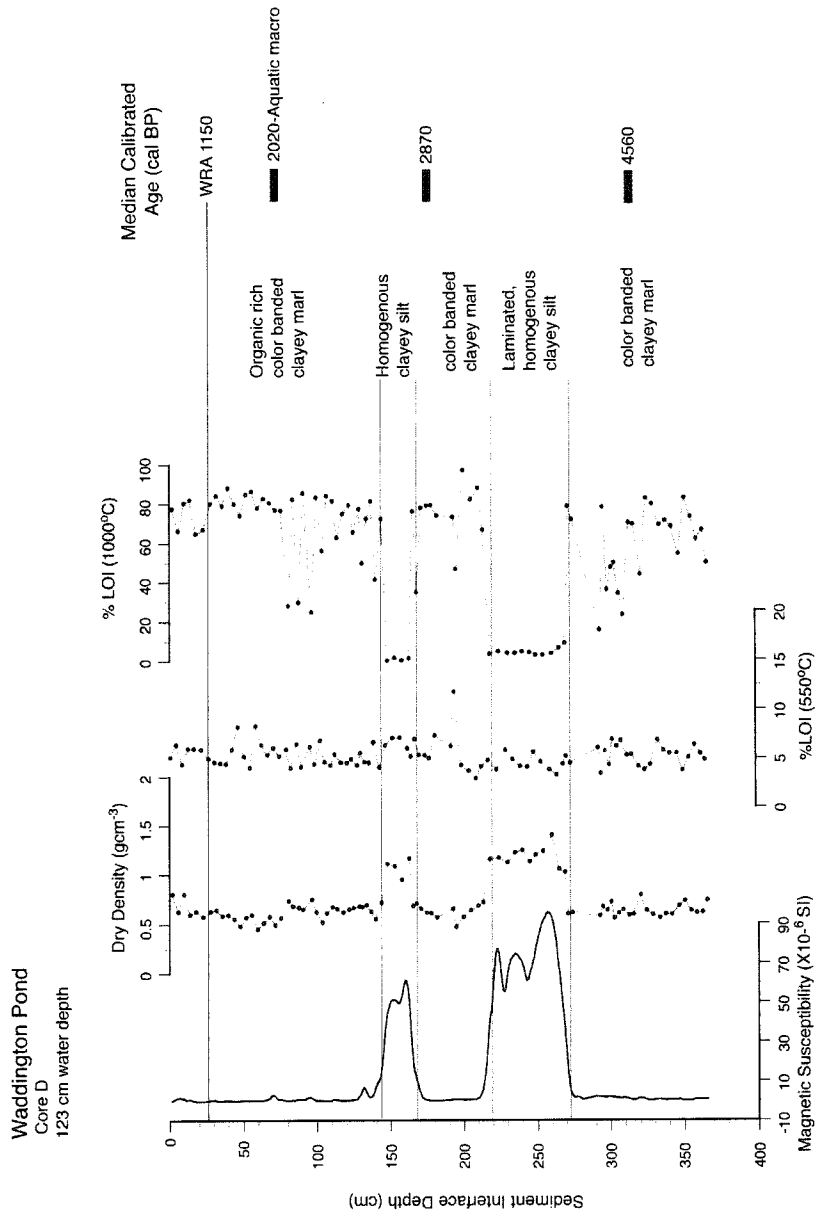
² 2-sigma range from Clague et al. (1995).



Waddington Pond Core B magnetic susceptibility, dry density, %LOI and median calibrated ages.



Waddington Pond core C magnetic susceptibility, dry density, %LOI and median calibrated ages.



Waddington Pond core D magnetic susceptibility, dry density, %LOI and median calibrated ages.

APPENDIX D

JELLYBEAN LAKE DATA

Jellybean Lake Core C/A Bulk Carbonate Oxygen and Carbon Isotope Data

Core-Drive ¹	Sediment- Water Interface Depth (cm)	Age (cal BP)	$\delta^{13}\text{C}_{\text{Ca}}$ (‰)	$\delta^{18}\text{O}_{\text{Ca}}$ (‰)	Duplicates
Core C-Drive 1	0.25	-52	-5.15	-19.91	
Core C-Drive 1	0.75	-49	-5.42	-19.57	
Core C-Drive 1	1.25	-46	-5.46	-20.07	
Core C-Drive 1	1.75	-43	-5.47	-20.10	
Core C-Drive 1	2.25	-39	-5.47	-20.09	
Core C-Drive 1	2.75	-35	-5.33	-19.53	
Core C-Drive 1	3.25	-30	-5.47	-19.40	
Core C-Drive 1	3.75	-24	-5.62	-19.81	
Core C-Drive 1	4.25	-18	-5.58	-19.91	
Core C-Drive 1	4.75	-13	-5.64	-20.18	
Core C-Drive 1	5.25	-7	-5.54	-19.81	
Core C-Drive 1	5.75	-1	-5.69	-20.15	
Core C-Drive 1	6.25	3	-5.56	-20.05	-5.27 -20.31
Core C-Drive 1	6.75	6	-5.61	-20.27	
Core C-Drive 1	7.25	10	-5.44	-19.72	
Core C-Drive 1	7.75	13	-5.45	-20.35	
Core C-Drive 1	8.25	17	-5.45	-20.02	
Core C-Drive 1	8.75	22	-5.46	-20.08	
Core C-Drive 1	9.25	26	-5.39	-19.89	
Core C-Drive 1	9.75	31	-5.46	-20.07	
Core C-Drive 1	10.25	35	-5.26	-20.06	
Core C-Drive 1	10.75	39	-5.25	-20.03	
Core C-Drive 1	11.25	43	-5.11	-19.99	-5.02 -19.52
Core C-Drive 1	11.75	48	-5.16	-19.93	
Core C-Drive 1	12.25	53	-5.13	-20.01	
Core C-Drive 1	12.75	58	-5.11	-19.95	
Core C-Drive 1	13.25	64	-4.92	-19.56	
Core C-Drive 1	13.75	70	-5.29	-20.00	
Core C-Drive 1	14.25	76	-5.24	-19.79	
Core C-Drive 1	14.75	82	-5.35	-19.94	
Core A-Drive 1	15	95	-7.44*	-20.99*	-7.82, - -21.03, 7.07 -20.96
Core A-Drive 1	16	110	-6.07*	-20.05*	-5.67, - -20.01, 6.47 -20.09
Core A-Drive 1	17	121	-5.75	-19.65	
Core A-Drive 1	18	144	-5.14	-19.24	
Core A-Drive 1	19	166	-5.00	-19.28	
Core A-Drive 1	20	188	-4.72	-19.20	
Core A-Drive 1	21	211	-4.73	-19.15	

Core-Drive ¹	Sediment- Water Interface	Age	$\delta^{13}\text{C}_{\text{Ca}}$ (‰)	$\delta^{18}\text{O}_{\text{Ca}}$ (‰)	Duplicates
	Depth (cm)	(cal BP)			
Core A-Drive 1	22	233	-4.40	-19.12	
Core A-Drive 1	23	256	-5.05	-19.44	
Core A-Drive 1	24	278	-5.00	-19.33	
Core A-Drive 1	25	300	-4.79*	-19.20*	-4.92, - -19.11, 4.66 -19.29
Core A-Drive 1	26	323	-4.75*	-19.35*	-4.59, - -18.78, 4.91 -19.92
Core A-Drive 1	27	345	-5.17*	-19.76*	-4.87, - -19.45, 5.47 -20.07
Core A-Drive 1	28	368	-5.58*	-20.10*	-5.35, - -20.32, 5.81 -19.55
Core A-Drive 1	29	390	-5.52	-19.66	
Core A-Drive 1	30	412	-5.65	-19.55	
Core A-Drive 1	31	435	-5.86	-19.57	
Core A-Drive 1	32	457	-6.35	-19.72	
Core A-Drive 1	33	480	-6.10	-19.91	
Core A-Drive 1	34	502	-5.62	-19.70	
Core A-Drive 1	35	524	-5.09	-19.33	
Core A-Drive 1	36	547	-5.07	-19.50	
Core A-Drive 1	37	569	-5.22	-19.38	
Core A-Drive 1	38	592	-5.44	-19.66	
Core A-Drive 1	39	614	-5.36	-19.86	
Core A-Drive 1	40	636	-5.26	-19.55	
Core A-Drive 1	41	659	-5.18	-19.81	
Core A-Drive 1	42	677	-5.14	-19.64	
Core A-Drive 1	43	692	-5.12	-19.33	
Core A-Drive 1	44	706	-5.18	-19.33	
Core A-Drive 1	45	721	-4.97	-19.50	
Core A-Drive 1	46	735	-4.99	-19.58	
Core A-Drive 1	47	749	-5.01	-19.68	
Core A-Drive 1	48	764	-5.27	-19.90	
Core A-Drive 1	49	778	-5.09	-19.63	
Core A-Drive 1	50	793	-6.00	-19.85	
Core A-Drive 1	51	807	-7.13	-19.58	
Core A-Drive 1	52	822	-6.94	-20.02	
Core A-Drive 1	53	836	-6.43	-19.78	
Core A-Drive 1	54	851	-6.89	-19.91	
Core A-Drive 1	55	865	-6.62	-19.47	
Core A-Drive 1	56	879	-6.88	-20.31	
Core A-Drive 1	57	894	-6.65	-20.10	
Core A-Drive 1	59	923	-6.52	-20.41	
Core A-Drive 1	60	954	-5.68	-20.40	

Core-Drive ¹	Sediment- Water Interface Depth (cm)	Age (cal BP)	$\delta^{13}\text{C}_{\text{Ca}}$ (‰)	$\delta^{18}\text{O}_{\text{Ca}}$ (‰)	Duplicates
Core A-Drive 1	61	1003	-4.95	-19.74	
Core C-Drive 1	64	1150	-4.85	-19.16	
Core C-Drive 1	64.5	1158	-5.50	-19.33	
Core C-Drive 1	65	1166	-5.21	-18.78	
Core C-Drive 1	66	1182	-5.15	-18.94	
Core C-Drive 1	67	1198	-5.78	-18.90	
Core C-Drive 1	68	1214	-6.14	-19.48	
Core C-Drive 1	69	1230	-5.61	-18.72	
Core C-Drive 1	70	1247	-5.62	-18.97	
Core C-Drive 1	71	1263	-5.57	-18.74	
Core C-Drive 1	72	1279	-5.43	-19.37	
Core C-Drive 1	73	1295	-5.00	-18.94	
Core C-Drive 1	74	1311	-4.27	-18.99	
Core C-Drive 1	75	1327	-4.25	-18.99	
Core C-Drive 1	76	1343	-4.62	-19.70	
Core C-Drive 1	77	1359	-5.25	-19.16	
Core C-Drive 1	78	1375	-6.04	-19.36	
Core C-Drive 1	79	1391	-5.10	-19.08	
Core C-Drive 1	80	1407	-4.69	-19.22	
Core C-Drive 1	81	1423	-4.53	-18.98	
Core C-Drive 1	82	1440	-4.30	-19.19	
Core C-Drive 1	83	1456	-5.12	-19.24	
Core C-Drive 1	84	1472	-5.28	-19.80	
Core C-Drive 1	85	1488	-4.79	-18.99	
Core C-Drive 1	86	1504	-5.86	-19.54	
Core C-Drive 1	87	1520	-5.75	-19.04	
Core C-Drive 1	88	1553	-5.63	-19.23	
Core C-Drive 1	89	1585	-5.32	-19.02	
Core C-Drive 1	90	1618	-6.05	-19.21	
Core C-Drive 1	91	1650	-4.66	-18.88	
Core C-Drive 1	92	1683	-4.34	-19.01	
Core C-Drive 1	93	1715	-4.99	-18.88	
Core C-Drive 1	94	1748	-4.59	-19.21	
Core C-Drive 1	95	1781	-4.72	-19.49	
Core C-Drive 1	96	1813	-4.59	-19.64	
Core C-Drive 1	97	1846	-5.41	-19.22	
Core C-Drive 1	98	1878	-6.19	-18.99	
Core C-Drive 1	99	1911	-4.96	-18.36	
Core C-Drive 1	100	1943	-5.58	-19.30	
Core C-Drive 1	101	1976	-4.77	-18.47	-4.67 -18.85
Core C-Drive 1	102	2009	-5.32	-19.11	

Core-Drive ¹	Sediment- Water Interface Depth (cm)	Age (cal BP)	$\delta^{13}\text{C}_{\text{Ca}}$ (‰)	$\delta^{18}\text{O}_{\text{Ca}}$ (‰)	Duplicates
Core C-Drive 1	103	2041	-5.56	-18.69	
Core C-Drive 1	104	2074	-5.19	-19.19	
Core C-Drive 1	105	2106	-5.22	-18.99	
Core C-Drive 1	106	2139	-5.44	-19.31	
Core C-Drive 1	107	2171	-5.22	-19.02	
Core C-Drive 1	108	2204	-4.11	-19.63	
Core C-Drive 1	109	2237	-4.69	-19.30	
Core C-Drive 1	110	2269	-4.15	-19.10	
Core C-Drive 1	111	2302	-4.24	-19.56	
Core C-Drive 1	112	2334	-3.84	-19.60	
Core C-Drive 1	113	2367	-4.55	-19.36	
Core C-Drive 1	114	2400	-4.53	-19.60	
Core C-Drive 1	115	2432	-4.92	-19.38	
Core C-Drive 1	116	2465	-4.77	-19.15	
Core C-Drive 1	117	2497	-4.24	-19.22	
Core C-Drive 1	119	2562	-4.72	-19.44	
Core C-Drive 1	120	2595	-4.84	-19.04	
Core C-Drive 1	121	2628	-5.18	-19.48	
Core C-Drive 1	122	2660	-4.37	-19.39	
Core C-Drive 1	123	2693	-5.09	-19.47	
Core C-Drive 1	124	2725	-4.79	-19.81	
Core C-Drive 1	125	2758	-4.94	-19.71	
Core C-Drive 1	126	2790	-5.06	-19.33	
Core C-Drive 1	127	2823	-4.70	-19.83	
Core C-Drive 1	128	2856	-5.11	-19.66	
Core C-Drive 1	129	2888	-6.11	-19.83	
Core C-Drive 1	130	2921	-4.94	-19.31	
Core C-Drive 1	131	2953	-4.41	-19.58	
Core C-Drive 1	132	2986	-4.68	-19.74	
Core C-Drive 1	133	3018	-4.89	-20.37	
Core C-Drive 1	134	3051	-4.69	-19.38	
Core C-Drive 1	135	3084	-5.51	-19.67	
Core C-Drive 1	136	3116	-3.99	-19.56	
Core C-Drive 1	137	3149	-5.35	-19.47	
Core C-Drive 1	138	3181	-5.15	-19.82	
Core C-Drive 1	139	3214	-5.72	-19.82	
Core C-Drive 1	140	3246	-5.51	-19.68	
Core C-Drive 1	141	3279	-5.89	-19.50	
Core C-Drive 1	142	3312	-5.41	-19.33	
Core C-Drive 1	143	3344	-6.09	-19.90	
Core C-Drive 1	144	3377	-6.20	-19.62	

Core-Drive ¹	Sediment- Water Interface Depth (cm)	Age (cal BP)	$\delta^{13}\text{C}_{\text{Ca}}$ (‰)	$\delta^{18}\text{O}_{\text{Ca}}$ (‰)	Duplicates
Core C-Drive 1	145	3409	-6.67	-19.79	
Core C-Drive 1	146	3442	-5.84	-19.47	
Core C-Drive 1	147	3474	-6.88	-19.90	
Core C-Drive 1	148	3507	-6.18	-19.69	
Core C-Drive 1	149	3540	-5.94	-19.79	
Core C-Drive 1	150	3572	-6.44	-19.14	
Core C-Drive 1	151	3605	-5.84	-20.17	-6.75 -19.42
Core C-Drive 1	152	3637	-6.15	-19.67	
Core C-Drive 1	153	3670	-5.80	-19.97	
Core C-Drive 1	154	3703	-5.93	-19.70	
Core C-Drive 1	155	3735	-6.06	-19.86	
Core C-Drive 1	156	3768	-5.79	-19.84	
Core C-Drive 1	157	3800	-6.15	-20.05	
Core C-Drive 1	159	3865	-5.82	-20.12	
Core C-Drive 1	160	3898	-6.23	-20.23	
Core C-Drive 1	161	3931	-5.19	-19.78	
Core C-Drive 1	162	3963	-6.22	-20.06	
Core C-Drive 1	163	3996	-5.55	-20.02	
Core C-Drive 1	164	4028	-5.27	-19.90	
Core C-Drive 1	165	4061	-4.90	-20.14	
Core C-Drive 1	166	4093	-5.58	-19.59	
Core C-Drive 1	167	4126	-6.19	-19.76	
Core C-Drive 1	168	4159	-5.66	-19.78	
Core C-Drive 2	168	4159	-5.67	-19.71	
Core C-Drive 2	169	4191	-5.13	-19.97	
Core C-Drive 2	170	4224	-5.25	-20.01	
Core C-Drive 2	171	4248	-5.01	-20.00	
Core C-Drive 2	172	4264	-4.61	-19.94	
Core C-Drive 2	173	4280	-5.09	-20.01	
Core C-Drive 2	174	4296	-5.01	-19.71	
Core C-Drive 2	175	4312	-4.90	-19.66	
Core C-Drive 2	176	4328	-5.42	-19.73	
Core C-Drive 2	177	4344	-5.79	-19.87	
Core C-Drive 2	178	4360	-5.48	-19.69	
Core C-Drive 2	179	4376	-5.57	-19.35	
Core C-Drive 2	180	4391	-4.66	-19.85	
Core C-Drive 2	181	4407	-5.74	-19.48	
Core C-Drive 2	182	4423	-5.10	-19.40	
Core C-Drive 2	183	4439	-4.91	-19.10	
Core C-Drive 2	184	4455	-5.85	-19.57	
Core C-Drive 2	185	4471	-5.41	-19.55	

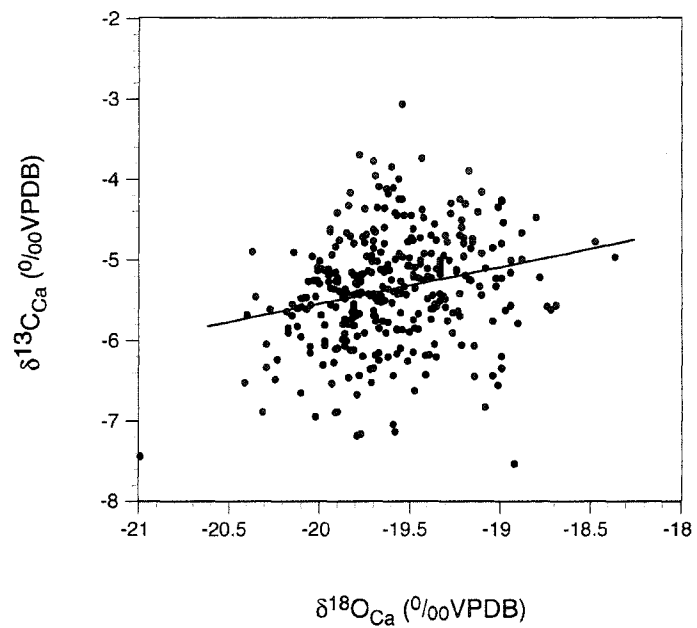
Core-Drive ¹	Sediment- Water	Age (cal BP)	$\delta^{13}\text{C}_{\text{Ca}}$ (‰)	$\delta^{18}\text{O}_{\text{Ca}}$ (‰)	Duplicates	
	Interface Depth (cm)					
Core C-Drive 2	186	4487	-5.69	-19.80		
Core C-Drive 2	187	4503	-5.65	-19.26	-5.79	-19.51
Core C-Drive 2	188	4519	-5.46	-19.87		
Core C-Drive 2	189	4535	-5.41	-19.85		
Core C-Drive 2	190	4551	-4.44	-19.49		
Core C-Drive 2	191	4567	-4.92	-19.42		
Core C-Drive 2	192	4583	-5.55	-20.15		
Core C-Drive 2	193	4599	-5.73	-19.86		
Core C-Drive 2	194	4615	-6.34	-19.70		
Core C-Drive 2	195	4631	-6.27	-19.92		
Core C-Drive 2	196	4647	-6.30	-19.98		
Core C-Drive 2	197	4663	-5.56	-19.81		
Core C-Drive 2	198	4679	-5.24	-19.60		
Core C-Drive 2	199	4694	-5.48	-19.30		
Core C-Drive 2	200	4710	-5.60	-20.12		
Core C-Drive 2	201	4726	-5.60	-19.81		
Core C-Drive 2	202	4742	-5.55	-19.94		
Core C-Drive 2	203	4758	-5.42	-19.70		
Core C-Drive 2	204	4774	-5.90	-20.17		
Core C-Drive 2	205	4790	-5.69	-19.69		
Core C-Drive 2	206	4806	-5.90	-19.26		
Core C-Drive 2	207	4822	-6.55	-19.01		
Core C-Drive 2	208	4838	-5.53	-19.60		
Core C-Drive 2	209	4854	-5.26	-19.77		
Core C-Drive 2	210	4870	-5.98	-19.87		
Core C-Drive 2	211	4886	-5.11	-19.35	-5.10	-19.58
Core C-Drive 2	212	4902	-4.85	-19.70		
Core C-Drive 2	213	4918	-6.04	-20.29		
Core C-Drive 2	214	4934	-5.43	-19.52		
Core C-Drive 2	215	4950	-4.75	-19.48		
Core C-Drive 2	216	4966	-4.77	-19.51		
Core C-Drive 2	217	4981	-4.77	-19.29		
Core C-Drive 2	218	4997	-5.27	-19.95		
Core C-Drive 2	219	5013	-5.36	-19.92		
Core C-Drive 2	220	5029	-4.79	-19.64		
Core C-Drive 2	221	5045	-4.65	-19.69		
Core C-Drive 2	222	5061	-4.42	-19.27		
Core C-Drive 2	223	5077	-4.93	-19.56		
Core C-Drive 2	224	5093	-4.17	-19.62		
Core C-Drive 2	225	5109	-5.25	-19.63		
Core C-Drive 2	226	5125	-5.33	-19.65		

Core-Drive ¹	Sediment- Water Interface Depth (cm)	Age (cal BP)	$\delta^{13}\text{C}_{\text{Ca}}$ (‰)	$\delta^{18}\text{O}_{\text{Ca}}$ (‰)	Duplicates
Core C-Drive 2	227	5141	-5.05	-19.62	
Core C-Drive 2	228	5157	-4.95	-19.20	
Core C-Drive 2	229	5173	-4.47	-19.42	
Core C-Drive 2	230	5189	-4.34	-19.68	
Core C-Drive 2	231	5205	-4.41	-19.90	
Core C-Drive 2	232	5221	-4.08	-19.67	
Core C-Drive 2	233	5237	-4.24	-19.54	
Core C-Drive 2	234	5253	-4.93	-19.93	
Core C-Drive 2	235	5269	-4.37	-19.43	
Core C-Drive 2	237	5300	-5.24	-19.17	
Core C-Drive 2	238	5316	-3.73	-19.43	
Core C-Drive 2	239	5332	-3.95	-19.69	
Core C-Drive 2	240	5348	-5.03	-19.63	
Core C-Drive 2	241	5364	-6.05	-19.97	
Core C-Drive 2	242	5380	-5.12	-19.61	
Core C-Drive 2	243	5396	-5.36	-19.62	
Core C-Drive 3	244	5412	-5.81	-19.81	
Core C-Drive 3	245	5431	-4.24	-19.64	
Core C-Drive 3	246	5453	-4.50	-19.21	
Core C-Drive 3	247	5475	-5.18	-19.77	
Core C-Drive 3	248	5496	-5.75	-19.29	-5.71 -19.37
Core C-Drive 3	249	5518	-4.92	-19.82	
Core C-Drive 3	250	5540	-4.76	-19.70	
Core C-Drive 3	251	5562	-4.71	-19.76	
Core C-Drive 3	252	5584	-6.06	-19.14	
Core C-Drive 3	253	5606	-7.03	-19.40	
Core C-Drive 3	254	5628	-5.54	-19.36	
Core C-Drive 3	255	5649	-6.43	-19.04	
Core C-Drive 3	256	5671	-5.07	-19.51	
Core C-Drive 3	257	5693	-4.36	-19.75	
Core C-Drive 3	258	5715	-3.69	-19.78	
Core C-Drive 3	259	5737	-5.40	-19.77	
Core C-Drive 3	260	5759	-5.19	-19.95	
Core C-Drive 3	261	5780	-4.95	-20.04	
Core C-Drive 3	262	5802	-4.16	-19.83	
Core C-Drive 3	263	5824	-3.77	-19.70	
Core C-Drive 3	264	5846	-4.29	-19.27	
Core C-Drive 3	265	5868	-5.75	-19.69	
Core C-Drive 3	266	5890	-6.17	-19.39	
Core C-Drive 3	267	5912	-6.42	-19.41	
Core C-Drive 3	268	5933	-5.60	-19.37	

Core-Drive ¹	Sediment- Water Interface	Age	$\delta^{13}\text{C}_{\text{Ca}}$ (‰)	$\delta^{18}\text{O}_{\text{Ca}}$ (‰)	Duplicates
	Depth (cm)	(cal BP)			
Core C-Drive 3	269	5955	-5.50	-19.64	
Core C-Drive 3	270	5977	-5.69	-19.22	
Core C-Drive 3	271	5999	-5.75	-19.83	
Core C-Drive 3	272	6021	-6.24	-19.67	
Core C-Drive 3	273	6043	-6.46	-19.84	
Core C-Drive 3	274	6065	-6.09	-19.55	
Core C-Drive 3	275	6086	-6.33	-20.29	
Core C-Drive 3	276	6108	-6.52	-19.71	
Core C-Drive 3	277	6130	-6.00	-19.97	
Core C-Drive 3	278	6152	-5.26	-19.91	
Core C-Drive 3	279	6174	-5.91	-19.86	
Core C-Drive 3	280	6196	-6.25	-19.51	
Core C-Drive 3	281	6217	-5.64	-19.82	
Core C-Drive 3	282	6239	-5.48	-19.86	
Core C-Drive 3	283	6261	-5.95	-20.10	
Core C-Drive 3	284	6283	-6.48	-20.24	
Core C-Drive 3	285	6305	-6.53	-19.93	
Core C-Drive 3	286	6327	-5.68	-19.70	
Core C-Drive 3	287	6349	-6.43	-19.59	
Core C-Drive 3	288	6370	-5.85	-19.45	
Core C-Drive 3	289	6392	-5.43	-19.78	
Core C-Drive 3	290	6414	-4.75	-19.89	
Core C-Drive 3	291	6436	-5.30	-19.79	
Core C-Drive 3	292	6458	-5.60	-19.38	
Core C-Drive 3	293	6480	-4.64	-19.94	
Core C-Drive 3	294	6501	-5.41	-19.79	
Core C-Drive 3	295	6523	-5.22	-19.90	
Core C-Drive 3	296	6545	-4.10	-19.59	
Core C-Drive 3	297	6567	-3.84	-19.52	
Core C-Drive 3	298	6589	-4.44	-19.53	
Core C-Drive 3	299	6611	-5.43	-19.81	
Core C-Drive 3	300	6633	-6.11	-19.81	-5.96 -19.81
Core C-Drive 3	301	6654	-5.61	-20.07	
Core C-Drive 3	302	6676	-7.16	-19.77	
Core C-Drive 3	303	6698	-5.13	-19.73	
Core C-Drive 3	304	6720	-5.43	-19.10	
Core C-Drive 3	305	6742	-5.66	-19.45	
Core C-Drive 3	306	6764	-5.21	-19.48	
Core C-Drive 3	307	6785	-5.20	-19.40	
Core C-Drive 3	308	6807	-5.90	-19.63	
Core C-Drive 3	309	6829	-5.77	-19.62	

Core-Drive ¹	Sediment- Water Interface Depth (cm)	Age (cal BP)	$\delta^{13}\text{C}_{\text{Ca}}$ (‰)	$\delta^{18}\text{O}_{\text{Ca}}$ (‰)	Duplicates
Core C-Drive 3	310	6851	-5.22	-19.45	
Core C-Drive 3	311	6873	-5.15	-19.71	
Core C-Drive 3	312	6895	-4.96	-19.54	
Core C-Drive 3	313	6917	-4.78	-19.75	
Core C-Drive 3	314	6938	-4.32	-19.84	
Core C-Drive 3	315	6960	-6.18	-19.41	
Core C-Drive 3	316	6982	-5.00	-19.44	
Core C-Drive 3	317	7004	-5.25	-19.42	
Core C-Drive 3	318	7026	-4.61	-19.48	
Core C-Drive 3	319	7048	-5.73	-19.38	
Core C-Drive 3	320	7070	-7.53	-18.92	
Core C-Drive 3	321	7091	-6.16	-19.57	
Core C-Drive 3	322	7113	-5.37	-19.56	
Core C-Drive 3	323	7135	-5.56	-18.94	
Core C-Drive 3	324	7157	-6.34	-18.99	
Core C-Drive 3	325	7179	-7.04	-19.59	
Core C-Drive 3	326	7201	-5.90	-19.75	
Core C-Drive 3	327	7222	-7.18	-19.79	
Core C-Drive 3	328	7244	-6.82	-19.08	
Core C-Drive 3	329	7266	-6.20	-19.35	
Core C-Drive 3	330	7288	-5.68	-19.99	
Core C-Drive 3	331	7310	-4.83	-19.91	
Core C-Drive 3	332	7332	-3.89	-19.17	
Core C-Drive 3	333	7354	-5.39	-19.59	
Core C-Drive 3	334	7375	-3.06	-19.54	
Core C-Drive 3	335	7397	-4.47	-18.80	
Core C-Drive 3	336	7419	-4.44	-19.57	
Core C-Drive 3	338	7463	-4.35	-19.64	

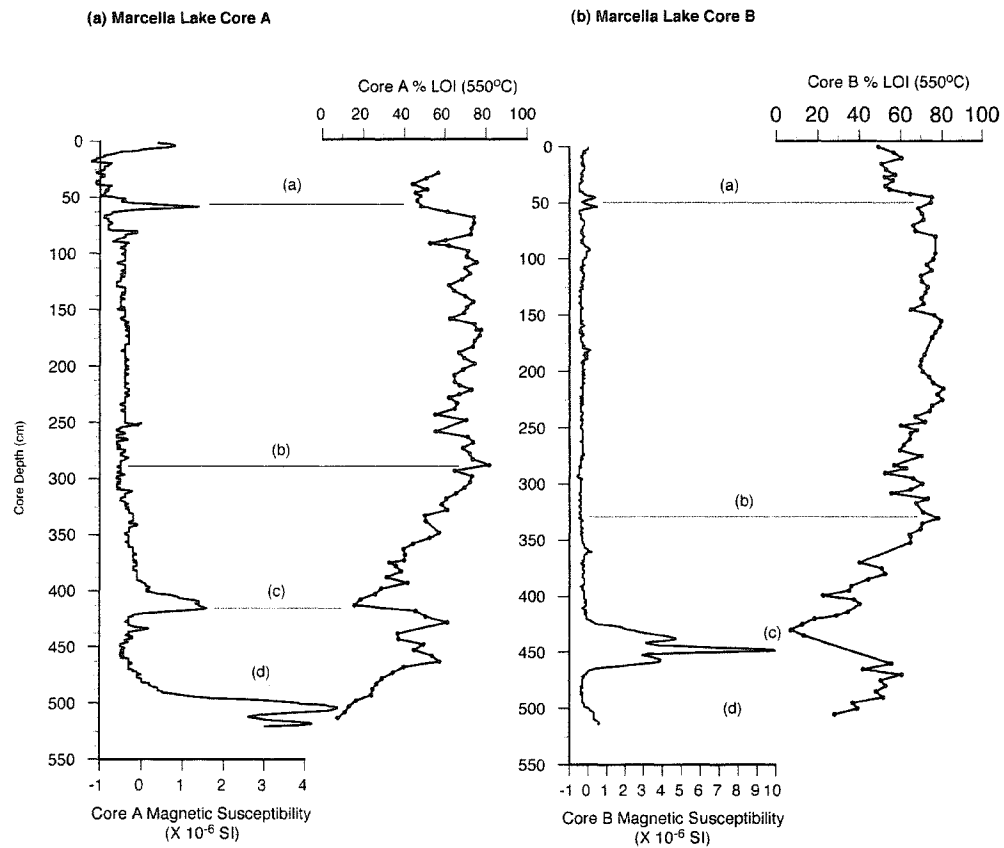
¹ See Table of Cores in Appendix A



Biplot of Jellybean Lake bulk carbonate oxygen and carbon isotope ratios, $r=0.24$.

APPENDIX E

MARCELLA LAKE DATA



Magnetic susceptibility and %LOI (550°C) for Marcella Lake core A (a) and core B (b). Lines marked (a), (b), (c) and (d) mark notable peaks and shifts. A composite core stratigraphy A/B was created using the tie-points and visual color and structure matching.

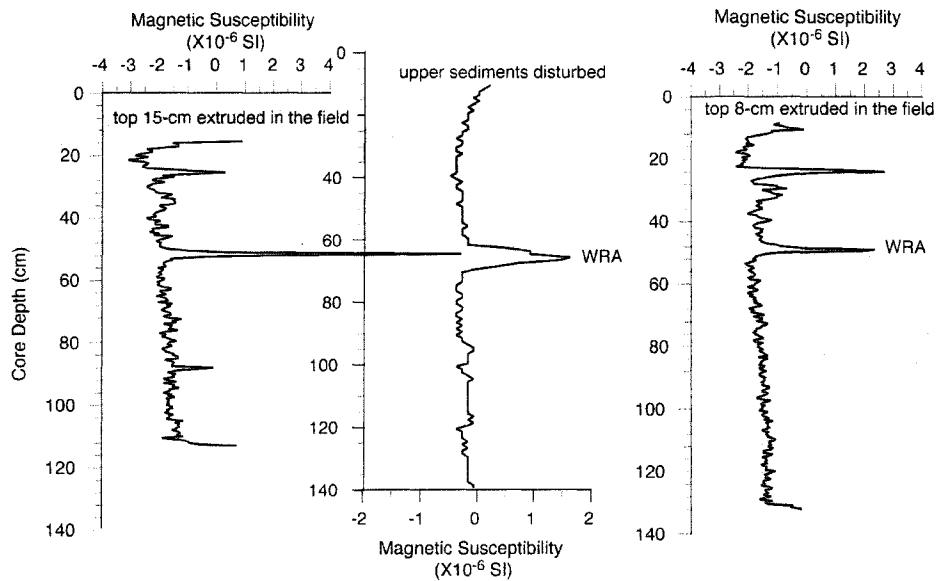
Marcella Lake Composite Core A/B Depth Scale

Core A Drive #	Core A Drive Depth (cm)	Core A Depth BML (cm)	Core A Sediment-Water Interface Depth (cm)	Corresponding Core B Drive Depth (cm)	Core B Drive #
2	10	990	30	13	1
2	15	995	35	18	1
2	20	1000	40	23	1
2	25	1005	45	28	1
2	28	1008	48	31	1
2	31	1011	51	34	1
2	35	1015	55	38	1
2	40	1020	60	43	1
WRA	42-43	1022-1023	62-63	45-46	WRA
2	45	1025	65	48	1
2	50	1030	70	53	1
2	55	1035	75	58	1
2	60	1040	80	63	1
2	65	1045	85	68	1
2	70	1050	90	73	1
2	75	1055	95	78	1
2	80	1060	100	0	2
2	85	1065	105	5	2
3	30	1070	110	10	2
3	35	1075	115	15	2
3	40	1080	120	20	2
3	45	1085	125	25	2
3	50	1090	130	30	2
3	55	1095	135	35	2
3	60	1100	140	40	2
3	65	1105	145	45	2
3	70	1110	150	50	2
3	75	1115	155	55	2
3	80	1120	160	60	2
3	85	1125	165	65	2
3	90	1130	170	70	2
4	15	1135	175	75	2
4	20	1140	180	80	2
4	25	1145	185	85	2
4	30	1150	190	0	3
4	35	1155	195	5	3
4	40	1160	200	10	3
4	45	1165	205	15	3
4	50	1170	210	20	3
4	55	1175	215	25	3

Core A Drive #	Core A Drive Depth (cm)	Core A Depth BML (cm)	Core A Sediment-Water Interface Depth (cm)	Corresponding Core B Drive Depth (cm)	Core B Drive #
4	60	1180	220	30	3
4	65	1185	225	35	3
4	70	1190	230	40	3
4	75	1195	235	45	3
4	80	1200	240	50	3
4	85	1205	245	55	3
4	90	1210	250	60	3
5	5	1215	255	65	3
5	10	1220	260	70	3
5	15	1225	265	75	3
5	20	1230	270	80	3
5	25	1235	275	85	3
5	30	1240	280	90	3
5	35	1245	285	5	4
5	40	1250	290	10	4
5	45	1255	295	15	4
5	50	1260	300	20	4
5	55	1265	305	25	4
5	60	1270	310	30	4
5	65	1275	315	35	4
5	70	1280	320	40	4
5	75	1285	325	45	4
5	80	1290	330	50	4
5	85	1295	335	55	4
5	90	1300	340	60	4
6	5	1305	345	65	4
6	10	1310	350	70	4
6	15	1315	355	75	4
6	20	1320	360	80	4
6	25	1325	365	85	4
6	30	1330	370	90	4
6	35	1335	375	5	5
6	40	1340	380	10	5
6	45	1345	385	15	5
6	50	1350	390	20	5
6	55	1355	395	25	5
6	60	1360	400	30	5
6	65	1365	405	35	5
6	70	1370	410	40	5
6	75	1375	415	45	5
6	80	1380	420	50	5
6	85	1385	425	55	5

Core A Drive #	Core A Drive Depth (cm)	Core A Depth BML (cm)	Core A Sediment-Water Interface Depth (cm)	Corresponding Core B Drive Depth (cm)	Core B Drive #
6	90	1390	430	60	5
7	5	1395	435	65	5
7	10	1400	440	70	5
7	15	1405	445	22	6
7	20	1410	450	27	6
7	25	1415	455	32	6
7	30	1420	460	37	6
7	35	1425	465	42	6
7	40	1430	470	47	6
7	45	1435	475	52	6
7	50	1440	480	57	6
7	55	1445	485	62	6
7	60	1450	490		
7	65	1455	495		
7	70	1460	500		
7	75	1465	505		
7	80	1470	510		
7	85	1475	515		
8	4	1480	520		

(a) Marcella Lake Core E-D2 (451-cm water depth) (b) Marcella Lake Core C (440-cm water depth) (c) Marcella Lake Core E-D1 (457-cm water depth)



□ Core sections used for composite isotope stratigraphy

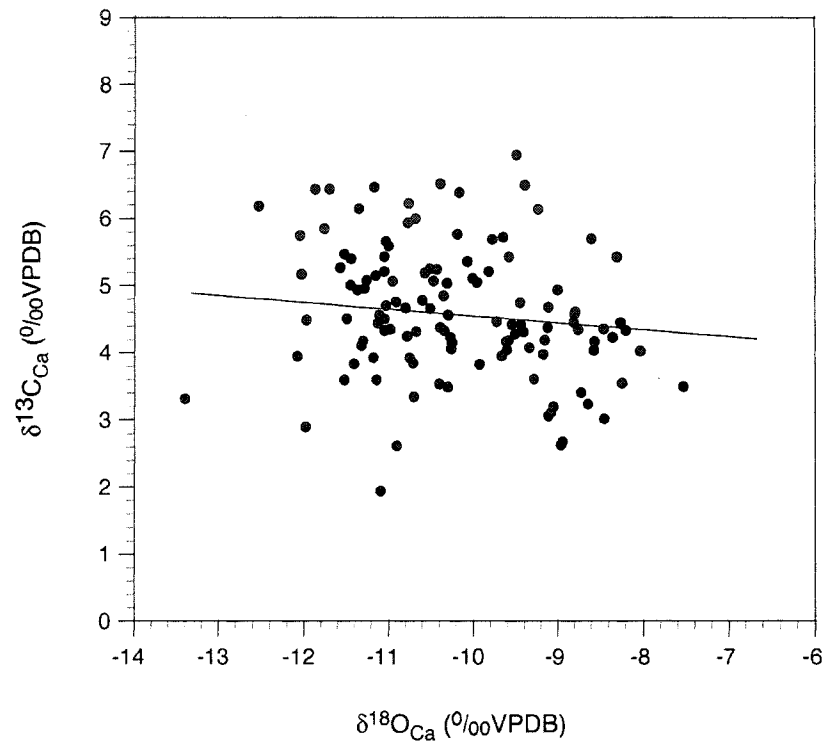
Magnetic susceptibility from Marcella Lake core E-D2 (a), core C (b) and core E-D1 (c). The peaks in susceptibility at the White River tephra are aligned and the shaded regions in each stratigraphy indicate the depths which samples were taken for the composite isotope stratigraphy C/E. Note the differences in the magnetic susceptibility scales.

Marcella Lake Core C/E *Chara* Oxygen and Carbon Isotope Data

Core-Drive ²	Sediment-Water Interface Depth (cm)	Age (cal B.P.) ¹	$\delta^{13}\text{C}_{\text{Ca}}$ (‰)	$\delta^{18}\text{O}_{\text{Ca}}$ (‰)	Duplicates
Core E-Drive 2	0.25	-52	4.45	-8.26	
Core E-Drive 2	0.75	-49	3.55	-8.24	
Core E-Drive 2	1.25	-46	3.50	-7.53	
Core E-Drive 2	1.75	-43	5.43	-8.30	
Core E-Drive 2	2.25	-39	4.33	-8.20	
Core E-Drive 2	2.75	-35	4.61	-8.79	
Core E-Drive 2	3.25	-30	3.02	-8.45	
Core E-Drive 2	3.75	-24	2.63	-8.96	
Core E-Drive 2	4.25	-18	4.23	-8.35	
Core E-Drive 2	4.75	-13	3.24	-8.64	
Core E-Drive 2	5.25	-7	4.03	-8.03	
Core E-Drive 2	5.75	-1	3.95	-9.67	
Core E-Drive 2	6.25	3	3.61	-9.28	
Core E-Drive 2	6.75	6	4.35	-8.46	
Core E-Drive 2	7.25	10	3.41	-8.72	
Core E-Drive 2	7.75	13	3.98	-9.17	
Core E-Drive 2	8.25	17	4.33	-10.34	
Core E-Drive 2	8.75	22	4.34	-8.76	
Core E-Drive 2	9.25	26	4.57	-8.80	
Core E-Drive 2	9.75	31	4.31	-9.41	
Core E-Drive 2	10.25	35	4.45	-8.81	
Core E-Drive 2	10.75	39	4.42	-9.55	
Core E-Drive 2	11.25	43	4.37	-9.12	
Core E-Drive 2	11.75	48	4.18	-9.59	
Core E-Drive 2	12.25	53	4.19	-9.15	
Core E-Drive 2	12.75	58	4.08	-9.34	
Core E-Drive 2	13.25	64	4.68	-9.11	
Core E-Drive 2	13.75	70	4.42	-9.44	
Core E-Drive 2	14.25	76	4.46	-9.73	
Core E-Drive 2	14.75	82	4.04	-9.61	
Core C-Drive 1	15.75	103	4.66	-10.51	
Core C-Drive 1	16.75	112	3.49	-10.30	
Core C-Drive 1	17	125	4.15	-10.25	
Core C-Drive 1	18.5	169	4.75	-9.45	
Core C-Drive 1	19.5	198	3.20	-9.05	
Core C-Drive 1	20	213	2.68	-8.94	
Core C-Drive 1	20.5	228	3.11	-9.08	
Core C-Drive 1	21	242	3.06	-9.11	
Core C-Drive 1	21.5	257	4.04	-8.57	

Core-Drive ²	Sediment-Water Interface Depth (cm)	Age (cal B.P.) ¹	$\delta^{13}\text{C}_{\text{Ca}}$ (‰)	$\delta^{18}\text{O}_{\text{Ca}}$ (‰)	Duplicates	
Core C-Drive 1	22.5	287	4.17	-8.56		
Core C-Drive 1	24	331	6.15	-11.35	6.27	-11.31
Core C-Drive 1	25	360	4.28	-9.51		
Core C-Drive 1	26	390	5.66	-11.03		
Core C-Drive 1	27	419	4.67	-10.80		
Core C-Drive 1	28	448	4.18	-11.30		
Core C-Drive 1	29	478	4.56	-10.30	4.55	-10.18
Core C-Drive 1	30	507	5.21	-11.05		
Core C-Drive 1	31	537	5.24	-10.43		
Core C-Drive 1	32	566	4.38	-10.39		
Core C-Drive 1	33	596	3.85	-10.71	4.02	-10.70
Core C-Drive 1	34	625	4.94	-11.37	5.13	-10.43
Core C-Drive 1	35	654	3.35	-10.70		
Core C-Drive 1	36	684	5.21	-9.82		
Core C-Drive 1	37	713	6.23	-10.76		
Core C-Drive 1	38	743	4.11	-11.32	4.25	-11.09
Core C-Drive 1	39	772	5.19	-10.57		
Core C-Drive 1	40	802	5.25	-10.51		
Core C-Drive 1	41	831	6.95	-9.49		
Core C-Drive 1	42	862	6.52	-10.39	6.84	-9.99
Core C-Drive 1	43	894	4.70	-11.03		
Core C-Drive 1	44	925	5.07	-10.47		
Core C-Drive 1	45	936	3.93	-11.18		
Core C-Drive 1	46	947	5.07	-10.95		
Core C-Drive 1	47	958	4.76	-10.91	4.70	-11.30
Core C-Drive 1	48	969	5.08	-11.26		
Core C-Drive 1	49	981	4.56	-11.11		
Core C-Drive 1	50	992	4.85	-10.35	4.16	-10.57
Core C-Drive 1	51	1003	4.32	-10.67		
Core C-Drive 1	52	1014	5.43	-9.58		
Core C-Drive 1	53	1025	5.36	-10.07		
Core C-Drive 1	54	1036	6.39	-10.17		
Core C-Drive 1	55	1047	5.77	-10.19		
Core C-Drive 1	56	1058	5.69	-9.78		
Core C-Drive 1	57	1069	6.50	-9.39		
Core C-Drive 1	58	1080	4.78	-10.60		
Core C-Drive 1	59	1092	5.72	-9.65		
Core C-Drive 1	60	1103	3.93	-10.75		
Core C-Drive 1	61	1114	3.54	-10.40		
Core C-Drive 1	62	1125	5.05	-9.96		
					Core E-D2	
						-10.24, -
Core C-Drive 1	64	1147	5.04	-10.31	5.23, 5.30	10.56

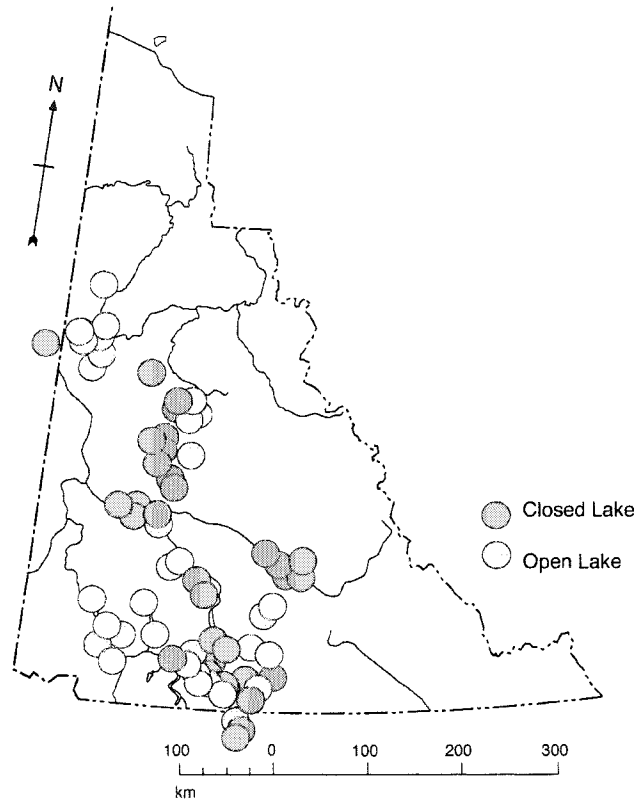
Core-Drive ²	Sediment-Water		$\delta^{13}\text{C}_{\text{Ca}}$ (‰)	$\delta^{18}\text{O}_{\text{Ca}}$ (‰)	Duplicates	
	Interface Depth (cm)	Age (cal B.P.) ¹				
Core E-Drive 1	65	1196	5.11	-10.01		
Core E-Drive 1	66	1245	5.94	-10.77		
Core E-Drive 1	68	1344	5.75	-12.05		
Core E-Drive 1	70	1442	6.44	-11.70		
Core E-Drive 1	72	1541	4.33	-11.05		
Core E-Drive 1	74	1639	4.44	-11.13		
Core E-Drive 1	76	1738	4.51	-11.49		
Core E-Drive 1	78	1836	5.15	-11.15		
Core E-Drive 1	80	1935	3.60	-11.14		
Core E-Drive 1	82	2033	4.16	-9.62		
Core E-Drive 1	84	2132	3.60	-11.52	3.71	-11.20
Core E-Drive 1	86	2230	6.19	-12.53		
Core E-Drive 1	88	2329	4.35	-10.98		
Core E-Drive 1	90	2427	4.50	-11.05		
Core E-Drive 1	92	2526	3.84	-11.41		
Core E-Drive 1	94	2624	4.25	-10.78		
Core E-Drive 1	96	2723	3.95	-12.08		
Core E-Drive 1	98	2821	5.59	-11.00		
Core E-Drive 1	100	2920	5.47	-11.52		
Core E-Drive 1	102	3018	5.01	-11.45		
Core E-Drive 1	104	3117	5.70	-8.60		
Core E-Drive 1	106	3215	4.94	-9.00		
Core E-Drive 1	108	3314	4.06	-10.26		
Core E-Drive 1	110	3412	4.96	-11.28		
Core E-Drive 1	112	3511	6.44	-11.87		
Core E-Drive 1	114	3609	6.00	-10.68		
Core E-Drive 1	116	3708	5.17	-12.03		
Core E-Drive 1	118	3806	6.47	-11.17	6.32	-11.60
Core E-Drive 1	120	3905	5.40	-11.44		
Core E-Drive 1	122	4003	5.43	-11.05		
Core E-Drive 1	124	4102	5.85	-11.76		
Core E-Drive 1	126	4200	4.23	-10.27		
Core E-Drive 1	128	4299	5.27	-11.57		
Core E-Drive 1	130	4397	6.14	-9.23		
Core E-Drive 1	132	4496	3.32	-13.40		
Core E-Drive 1	134	4562	4.49	-11.97		
Core E-Drive 1	136	4596	2.62	-10.90		
Core E-Drive 1	138	4630	1.94	-11.09		
Core E-Drive 1	140	4664	2.90	-11.98		
Core E-Drive 1	142	4698	3.83	-9.93		
Core E-Drive 1	144	4732	-0.47	-13.17		



Biplot of Marcella Lake bulk carbonate oxygen and carbon isotope ratios, $r=0.29$.

APPENDIX F

SURFACE WATER DATA



Lake water locations sampled July-August 1999, 2000 and 2002.

Surface Water Samples by Location

Sample #-Year (July/August)	Sample Name	Latitude (°N)	Longitude (°W)	Elevation (m)	$\delta^{18}\text{O}$ (‰)	$\delta^2\text{H}$ (‰)
Y1-99	7.5 mile Lake	62.18	136.39	503	-10.4	-120.5
Y2-99	7.0 mile Lake	62.18	136.39	503	-11.7	-127
Y3-99	7 mile lake spring			503	-21.9	-159.5
Y4-99	Six mile Lake	62.12	136.33	542	-11	-122
Y5-99	Eight mile Lake	62.19	136.39	489	-10.5	-118.5
Y6-99	Tatchum Lake	62.26	136.16	579	-20.9	-161
Y7-99	Wrong Lake	63.15	136.50	575	-12.1	-125
Y8-99	Jackfish Lake	63.02	136.47	655	-10.6	-115.5
Y9-99	Ethel Lake	63.38	136.08	747	-18.7	-149
Y10-99	Rock Island Lake	62.7	136.68	579	-11.6	-121.5
Y11-99	Bleached Tree Lake	62.77	136.68	564	-7.6	-106
Y12-99	Five Mile Lake "East"	63.65	135.85	594	-11.5	-124
Y13-99	Five Mile Lake "West"	63.65	135.9	579	-11.6	-124
Y14-99	Halfway Lake West	63.78	136.8	762	-13.8	-130.5
Y15-99	Hanson Lake	63.98	135.4	701	-16.8	-143
Y16-99	McQuestion Lake	64.18	135.38	701	-20.3	-147.5
Y17-99	Barlow Lake	63.75	137.72	671	-11.5	-123.5
Y18-99	Gravel Lake	63.85	138.03	610	-12.4	-123
Y19-99	Chapman Lake	64.85	138.33	610	-16.1	-141
Y20-99	Two Moose Lake	64.73	138.36	1006	-15	-137
Y21-99	#19 Ogilvie Mts.	64.69	138.38	1128	-20.5	-158
Y22-99	"Scooter" Pond	64.61	138.33	1173	-19.1	-151.8
Y23-99	"Surf" Lake	64.61	138.32	1204	-19.4	-154.5
Y24-99	"Surf" Pond inflow	64.61	138.32	1204	-22	-164.5
Y25-99	"Fold" Lake Cirque	64.49	138.3	1500	-22.8	-166.5
Y26-99	Fold Lake I	64.46	138.28	1387	-21.8	-156
Y27-99	"Fold" Lake II	64.47	138.28	1448	-22	-163
Y28-99	"Fold" Lake outflow	64.46	138.28	1387	-20.5	-163
Y29-99	Ogilvie precip I	64.6	138.4	~1200	-17.4	-131
Y30-99	Ogilvie precip II	64.6	138.4	~1200	-17.7	-123
Y31-99	Yukon River, Carmacks	62.09	136.28	~500	-20.1	-150.5
Y32-99	Pelly River, Pelly Crossing	62.82	136.58	~500	-21.8	-159.5

Sample #-Year (July/August)	Sample Name	Latitude (°N)	Longitude (°W)	Elevation (m)	$\delta^{18}\text{O}$ (‰)	$\delta^2\text{H}$ (‰)
Y33-99	Stewart River, Stewart Crossing	63.2	136.5	~500	-21.8	-162
Y34-99	Mayo River, Mayo	63.75	135.8	~600	-21.6	-164.5
Y35-99	Klondike River, Dawson	64.1	139.5	~500	-22.4	-167
AK1-99	S Fork Forty Mile River	64.2	141.3	~400	-21.3	-161.5
Y36-99	N Klondike River, Tombstone	64.6	138.4	~1000	-22.5	-167
AK2-99	Chicken Lake, Chicken Alaska	64.08	141.77	472	-20.6	-161
AK3-99	Chicken Lake AK spring inflow	64.08	141.77	472	-21.9	-165
AK4-99	Eagle, Alaska, well water	64.9	141.3	~400	-22.8	-171
Y01-00	Two Dog Lake	60.60	134.87	~600	-10.3	-118
Y02-00	Kookatsoon Lake	60.56	134.88	~600	-14.3	-133
Y03-00	Buck's Lake	60.30	134.77	~550	-7.2	-99
Y04-00	Emerald Lake	60.26	134.75	~600	-12.3	-119
Y05-00	Waddington Pond	60.36	134.81	~720	-18.5	-146
Y06-00	Lewis Lake	60.37	134.82	720	-17.8	-146
Y08-00	Waddington Pond Spring	60.37	134.81	725	-18.9	-152
Y11-00	Varig Pond	60.36	134.81	725	-20.6	-160
Y12-00	Joe's Lake	60.36	134.81	725	-21	-161
Y13-00	Indigo Lake	60.36	134.81	725	-20.8	-160
Y13A-00	Indigo Lake Spring	60.36	134.81	~725	-21.5	-162
Y14-00	Duckling Lake	60.35	134.80	~725	-21.5	-163
Y15-00	Jellybean Lake	60.35	134.81	727	-21	-161
Y16-00	Judas Lake	60.38	134.13	746	-12	-126
Y17-00	Marcella Lake	60.07	133.81	454	-8	-106
Y18-00	Tarfu Lake	60.06	133.75	~450	-17.5	-148
Y19-00	Atlin Lake B.C.	59.91	133.81	~400	-19.1	-146
Y20-00	Davie Hall Lake B.C.	59.68	133.71	~400	-12.3	-124
Y21-00	Como Lake B.C.	59.61	133.68	~400	-8.7	-102
Y22-00	Tarfu Creek	60.10	133.82	~400	-16.3	-144
Y23-00	Squanga Lake	60.45	133.60	~500	-18.2	-151
Y24-00	Salmo Lake	60.44	133.56	~500	-16.2	-145
Y25-00	Silver Dollar Lake	60.49	133.42	~500	-13.7	-129

Sample #-Year (July/August)	Sample Name	Latitude (°N)	Longitude (°W)	Elevation (m)	$\delta^{18}\text{O}$ (‰)	$\delta^2\text{H}$ (‰)
Y26-00	Teslin River	60.48	133.30	~500		
Y27-00	Haircut Lake	60.52	133.21	~700	-16.2	-144
Y28-00	Quiet Lake	60.99	133.03	~750	-21	-161
Y29-00	Rose Lake	61.60	133.08	~750	-21.9	-165
Y30-00	Coffee Lake	61.91	132.44	~750	-9.1	-114
Y31-00	Cream Pond	61.87	132.36	~750	-9.2	-120
Y32-00	Snipe Lake	61.87	132.36	~750	-5.9	-104
Y33-00	Stinko Lake	61.95	132.46	~750	-9.6	-119
Y34-00	Whiskers Lake	61.97	132.51	~750	-9.8	-115
Y35-00	Rock Island Lake	62.72	136.70	579	-12.3	-127
Y36-00	Bleached Tree Lake	62.77	136.62	564	-8.1	-110
Y37-00	Wrong Lake	63.15	136.50	575	-12.8	-131
Y38-00	Jackfish Lake	63.02	136.47	655	-10.6	-120
Y39-00	Pond Next to Jackfish Pelly River at xing	63.02	136.47	655	-12.7	-131
Y40-00	Klondike Hwy Yukon River	62.83	136.58	~500	-21.7	-166
Y41-00	Carmacks	62.09	136.28	~500	-20.3	-153
Y42-00	Tatchun Lake	62.30	136.18	~500	-21	-165
Y43-00	Six Mile Lake	62.12	136.36	542	-14.9	-140
Y44-00	Eight Mile Lake	62.19	136.39	489	-10.8	-121
Y45-00	8.5 Mile Lake	62.19	136.39	500	-14	-134
Y46A-00	7.5 Mile Lake	62.18	136.38	503	-10.4	-121
Y46B-00	7.0 Mile Lake	62.18	136.38	503	-13	-131
Y46C-00	7.0 Mile Lake Spring	62.18	136.38	503	-21.9	-166
Y47-00	Twin Lake	61.70	135.93	~500	-17.8	-151
Y47A-00	Risen Lake	61.70	135.94	~500	-10.2	-121
Y47B-00	Twin Lake East	61.70	135.94	~500	-15.6	-144
Y48-00	Mat Lake	61.09	135.28	~500	-18.5	-156
Y49-00	Long Lake	60.74	135.05	~500	-11.1	-121
Y50-00	Hidden Lake #2	60.69	135.01	~500	-16.2	-138
Y50A-00	Hidden Lake #1	60.69	135.01	~500	-16.1	-137
Y51-00	Scout Lake	60.79	135.42	~500	-9.6	-113
Y52-00	Takhini River	60.86	135.74	~500	-20.2	-146
Y53-00	Atthilu Lake	61.23	136.96	~600	-20.3	-160
Y54-00	Lacelle Lake	61.39	137.01	~700	-10	-114
Y55-00	Aishihik Lake	61.20	137.00	~700	-17.8	-147

Sample #-Year (July/August)	Sample Name	Latitude (°N)	Longitude (°W)	Elevation (m)	$\delta^{18}\text{O}$ (‰)	$\delta^2\text{H}$ (‰)
Y56-00	Pine Lake	60.80	137.48	~600	-17.2	-146
Y57-00	Kathleen Lake	60.58	137.22	~600	-20.9	-157
Y58-00	Dezdeash Lake	60.40	137.04	~600	-19.1	-149
Y59-00	Sulphur Lake	60.94	137.98	~600	-13.1	-128
Y60-00	Kluane Lake	61.15	138.55	~600	-23.8	-179
Y62-00	Precip, Little Salmon Lake	62.30	134.90	~600	-22.5	-170
Y63-00	Precip, Aishihik Lake	61.60	137.80	~700	-13	-118
Total Samples: 105						

Surface Water Samples by Hydrologic Category

Open Lakes

Sample #-year (July, August)	Name	$\delta^{18}\text{O}$ (‰)	$\delta^2\text{H}$ (‰)	Avg. $\delta^{18}\text{O}$ (‰)	Avg. $\delta^2\text{H}$ (‰)
Y6-99	Tatchun Lake	-20.9	-161	-20.95	-163
Y42-00	Tatchun Lake	-21	-165		
Y9-99	Ethel Lake	-18.7	-149		
Y14-99	Halfway Lake West	-13.8	-130.5		
Y15-99	Hanson Lake	-16.8	-143		
Y16-99	McQuestion Lake	-20.3	-147.5		
Y20-99	Two Moose Lake	-15	-137		
Y21-99	#19, Ogilvie Mts.	-20.5	-158		
Y22-99	"Scooter" Pond	-19.1	-151.8		
Y23-99	"Surf" Lake	-19.4	-154.5		
Y26-99	Fold Lake I	-21.8	-156		
Y27-99	"Fold" Lake II	-22	-163		
Y19-99	Chapman Lake	-16.1	-141		
Y05-00	Waddington Pond	-18.5	-146		
Y06-00	Lewis Lake	-17.8	-146		
Y11-00	Varig Pond	-20.6	-160		
Y12-00	Joe's Lake	-21	-161		
Y13-00	Indigo Lake	-20.8	-160		
Y14-00	Duckling Lake	-21.5	-163		
Y15-00	Jellybean Lake	-21	-161		
Y18-00	Tarfu Lake	-17.5	-148		
Y19-00	Atlin Lake B.C.	-19.1	-146		
Y23-00	Squanga Lake	-18.2	-151		
Y25-00	Silver Dollar Lake	-13.7	-129		
Y27-00	Haircut Lake	-16.2	-144		
Y28-00	Quiet Lake	-21	-161		
Y29-00	Rose Lake	-21.9	-165		
Y47-00	Twin Lake	-17.8	-151		
Y47B-00	Twin Lake East	-15.6	-144		
Y53-00	Atthilu Lake	-20.3	-160		
Y55-00	Aishihik Lake	-17.8	-147		
Y56-00	Pine Lake	-17.2	-146		
Y57-00	Kathleen Lake	-20.9	-157		
Y58-00	Dezdeash Lake	-19.1	-149		
Y59-00	Sulphur Lake	-13.1	-128		
Y60-00	Kluane Lake	-23.8	-179		
Total Open Lakes: 36					

Closed Lakes

Sample #-year (July, August)	Name	$\delta^{18}\text{O}$ (‰)	$\delta^2\text{H}$ (‰)	Average $\delta^{18}\text{O}$ (‰)	Average $\delta^2\text{H}$ (‰)
Y1-99	7.5 mile lake	-10.4	-120.5	-10.4	-121
Y46A-00	7.5 Mile Lake	-10.4	-121		
Y2-99	7.0 mile Lake	-11.7	-127	-12.4	-129
Y46B-00	7.0 Mile Lake	-13	-131		
Y4-99	Six Mile Lake	-11	-122	-13.0	-131
Y43-00	Six Mile Lake	-14.9	-140		
Y5-99	Eight mile Lake	-10.5	-118.5	-10.7	-120
Y44-00	Eight Mile Lake	-10.8	-121		
Y7-99	Wrong lake	-12.1	-125	-12.5	-128
Y37-00	Wrong Lake	-12.8	-131		
Y8-99	Jackfish Lake	-10.6	-115.5	-10.6	-118
Y38-00	Jackfish Lake	-10.6	-120		
Y10-99	Rock Island Lake	-11.6	-121.5	-12.0	-124
Y35-00	Rock Island Lake	-12.3	-127		
Y11-99	Bleached Tree Lake	-7.6	-106	-7.9	-108
Y36-00	Bleached Tree Lake	-8.1	-110		
Y12-99	Five Mile Lake "East"	-11.5	-124		
Y13-99	Five Mile Lake "West"	-11.6	-124		
Y17-99	Barlow Lake	-11.5	-123.5		
Y18-99	Gravel Lake	-12.4	-123		
AK2-99	Chicken Lake, Alaska	-20.6	-161		
Y01-00	Two Dog Lake	-10.3	-118		
Y02-00	Kookatsoon Lake	-14.3	-133		
Y03-00	Buck's Lake	-7.2	-99		
Y04-00	Emerald Lake	-12.3	-119		
Y16-00	Judas Lake	-12	-126		
Y17-00	Marcella Lake	-8	-106		
Y20-00	Davie Hall Lake B.C.	-12.3	-124		
Y21-00	Como Lake B.C.	-8.7	-102		
Y24-00	Salmo Lake	-16.2	-145		
Y30-00	Coffee Lake	-9.1	-114		
Y31-00	Cream Pond	-9.2	-120		
Y32-00	Snipe Lake	-5.9	-104		
Y33-00	Stinko Lake	-9.6	-119		
Y34-00	Whiskers Lake	-9.8	-115		
Y39-00	Pond Next to Jackfish	-12.7	-131		
Y45-00	8.5 Mile Lake	-14	-134		
Y48-00	Mat Lake	-18.5	-156		
Y49-00	Long Lake	-11.1	-121		
Y50-00	Hidden Lake #2	-16.2	-138		
Y50A-00	Hidden Lake #1	-16.1	-137		
Y51-00	Scout Lake	-9.6	-113		
Total Closed	Lakes: 42				

Rivers

Sample #-year (July, August)	Name	$\delta^{18}\text{O}$ (‰)	$\delta^2\text{H}$ (‰)	Average $\delta^{18}\text{O}$ (‰)	Average $\delta^2\text{H}$ (‰)
Y28-99	"Fold" Lake Yukon outflow	-20.5	-163		
Y31-99	Yukon River, Carmacks	-20.1	-150.5	-20.2	-152
Y41-00	Yukon River, Carmacks	-20.3	-153		
Y32-99	Pelly River, Pelly Crossing	-21.8	-159.5	-21.8	-163
Y40-00	Pelly River, Pelly Crossing	-21.7	-166		
Y33-99	Stewart River, Stewart Crossing	-21.8	-162		
Y34-99	Mayo River, Mayo	-21.6	-164.5		
Y35-99	Klondike River Yukon	-22.4	-167		
AK1-99	S. Fork Forty Mile River	-21.3	-161.5		
Y36-99	N Klondike River, Tombstone	-22.5	-167		
Y22-00	Tarfu Creek	-16.3	-144		
Y52-00	Takhini River	-20.2	-146		

Total Rivers: 12

Precipitation and Springs

Sample #-year (July, August)	Name	$\delta^{18}\text{O}$ (‰)	$\delta^2\text{H}$ (‰)
Y3-99	7 mile lake spring water	-21.9	-159.5
Y24-99	"Surf" Pond inflow	-22	-164.5
Y25-99	"Fold" Lake Cirque	-22.8	-166.5
Y29-99	Ogilvie ppt I	-17.4	-131
Y30-99	Ogilvie ppt II	-17.7	-123
AK3-99	Chicken Lake AK spring inflow	-21.9	-165
AK4-99	Eagle, Alaska, well water	-22.8	-171
Y08-00	Waddington Pond Spring	-18.9	-152
Y13A-00	Indigo Lake Spring	-21.5	-162
Y46C-00	7.0 Mile Lake Spring	-21.9	-166
Y62-00	Little Salmon Lake	-22.5	-170
Y63-00	Aishihik Lake	-13	-118

Total Precipitation and Springs: 12

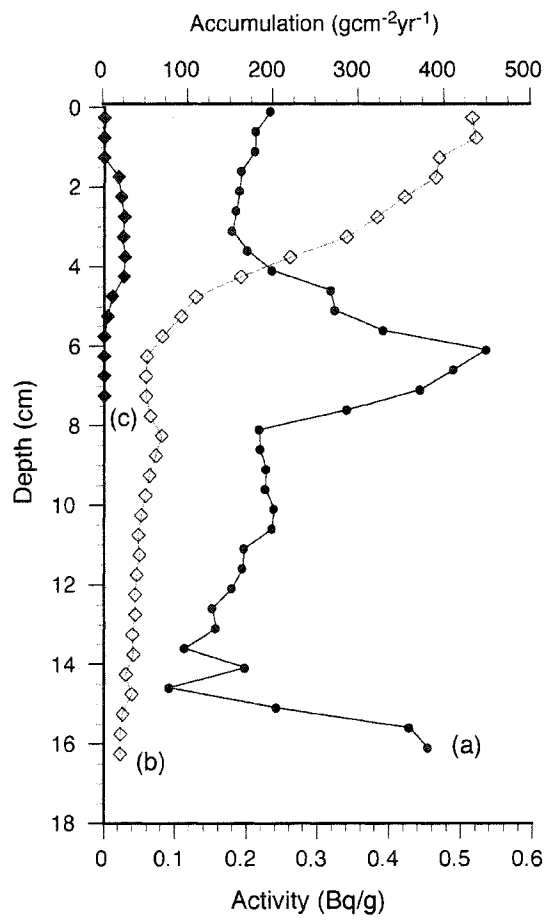
APPENDIX G

LEAD AND CESIUM RADIOGENIC DATA

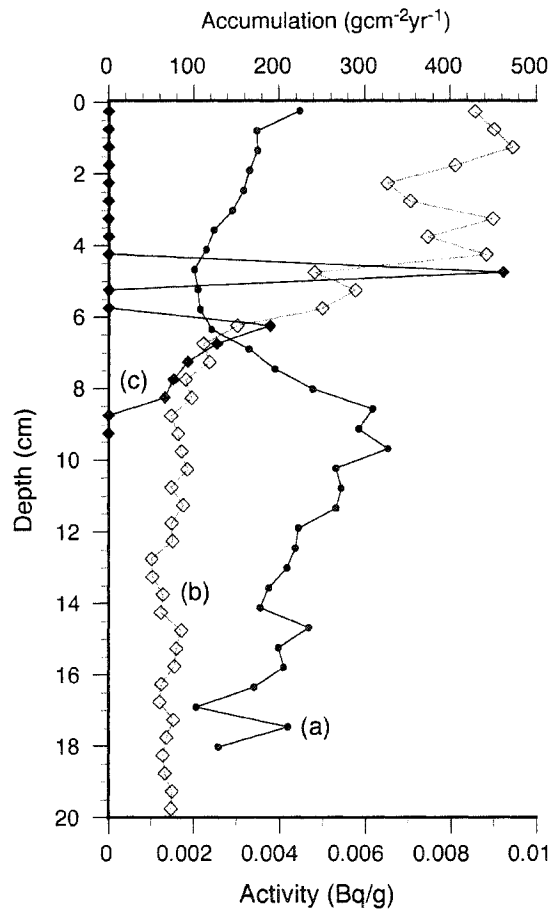
Jellybean and Marcella Lake ^{210}Pb CRS¹ Age Models and ^{137}Cs Activities

Depth (cm)	Jellybean Age (AD) (CRS ¹)	Jellybean ^{137}Cs Activity (Bq/g \pm 1sd)	Marcella Age (AD) (CRS ¹)	Marcella ^{137}Cs Activity (Bq/g \pm 1sd)
0.25	2002		2002	
0.75	1999		2001	
1.25	1996		2001	
1.75	1993	0.0210 \pm 0.001	2000	
2.25	1989	0.0249 \pm 0.00487	1999	
2.75	1985	0.0290 \pm 0.00448	1998	
3.25	1980	0.0271 \pm 0.00442	1997	
3.75	1974	0.0302 \pm 0.00346	1997	
4.25	1968	0.0286 \pm 0.00271	1995	
4.75	1963	0.0118 \pm 0.00229	1994	0.0328 \pm 0.00923
5.25	1957	0.00546 \pm 0.00111	1992	0
5.75	1951		1990	0
6.25	1947		1987	0.0185 \pm 0.00379
6.75	1944		1984	0.00617 \pm 0.00255
7.25	1940		1980	0.00734 \pm 0.00186
7.75	1937		1975	0.004.47 \pm 0.00152
8.25	1933		1971	0.00373 \pm 0.00132
8.75	1928		1966	
9.25	1924		1962	
9.75	1919		1958	
10.25	1915		1954	
10.75	1911		1950	
11.25	1907		1945	
11.75	1902		1939	
12.25	1897		1932	
12.75	1892		1923	
13.25	1886		1915	
13.75	1880		1908	
14.25	1874		1901	
14.75	1868		1893	
15.25	1863		1878	
15.75	1860		1862	
16.25	1857		1854	

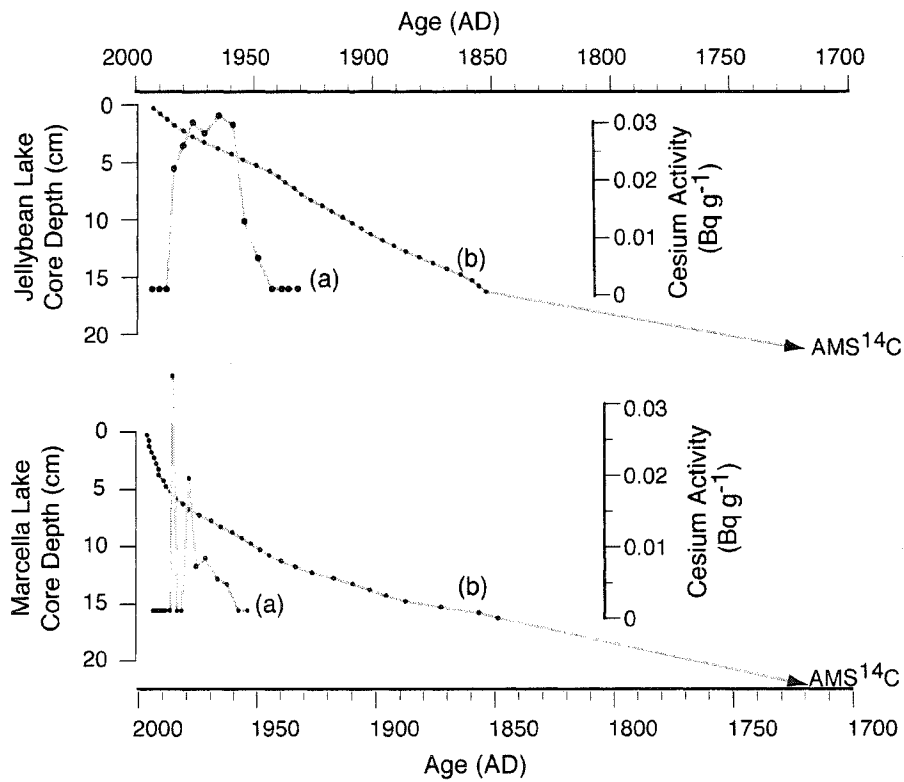
¹Constant Rate of Supply (Appleby, 2001)



Jellybean Lake sediment accumulation (a), ^{210}Pb activity (b) and ^{137}Cs activity (c) from the sediment-water interface to 16.5 cm depth.



Marcella Lake sediment accumulation(a), ²¹⁰Pb activity (b) and ¹³⁷Cs activity (c) from the sediment-water interface to 20-cm depth.



Constant Rate of Supply (CRS) age models based on ^{210}Pb activity and sediment accumulation for Jellybean and Marcella Lake. Peaks in ^{137}Cs ~1963 are used to verify the age model. Marcella Lake has low ^{210}Pb accumulation rates and an irregular ^{137}Cs peak indicating the site was non-depositional for lead and is slightly disturbed. Only the surface (2002 AD) and the onset of ^{210}Pb activity (16.5 cm) were used in the Marcella core C/E age model.

APPENDIX H

PRINCIPLE COMPONENT DATA

Principle Component Variable Loadings and Eigenvalues

Run #1
Analysing 9 variable
and 11 case scores
Tolerance of
eigenanalyses set at
10⁻⁷
Vector scaling: 2.05

Eigenvalues		
	Axis 1	Axis 2
Eigenvalues (l)	5.782	1.27
Percent of variation	64.241	14.115
PCA Variable Loadings		
	Axis 1	Axis 2
CaCO ₃ (mgl-1)	0.373	0.217
Na ⁺ (mgl-1)	0.36	0.218
NH ₄ ⁺ (mgl-1)	0.148	0.635
K ⁺ (mgl-1)	0.365	0.099
Mg ²⁺ (mgl-1)	0.409	0.095
Ca ²⁺ (mgl-1)	-0.373	0.156
Cl ⁻ (mgl-1)	0.304	-0.288
NO ₃ ⁻ (mgl-1)	-0.224	-0.598
SO ₄ ²⁻ (mgl-1)	0.356	-0.138
PCA Case Scores		
	Axis 1	Axis 2
Waddington Pond	-0.514	-0.175
Waddington Spring	-0.7	0.389
Indigo Lake	-0.648	-0.728
Indigo Spring	-0.723	0.203
Jellybean Lake	-0.475	-0.018
Marcella Lake	1.279	0.082
Jackfish Lake	0.341	-0.402
Eight Mile Lake	1.375	0.066
7.5 Mile Lake	0.198	-0.009
7.0 Mile Lake	0.225	0.006
7.0 Mile Spring	-0.357	0.586

Run #2
Analysing 9 variable and
8 case scores
Tolerance of
eigenanalyses set at 10⁻⁷
Vector scaling: 2.41

Eigenvalues		
	Axis 1	Axis 2
Eigenvalues (l)	5.716	1.581
Percent of variation	63.517	17.571
PCA Variable Loadings		
	Axis 1	Axis 2
pH	0.371	-0.272
Specific conductivity (spc)	0.372	-0.215
Temperature (°C)	0.271	0.552
Dissolved Oxygen (mgl- 1)	-0.213	0.225
Lake Water pCO ₂ (ppm)	-0.281	-0.482
Atmospheric pCO ₂ (ppm)	0.289	-0.348
Lake Water δ ¹⁸ O (VSMOW)	0.404	0.192
Lake Water δ ² H (VSMOW)	0.405	0.185
Alkalinity (mgl-1)	0.341	-0.316
PCA Case Scores		
	Axis 1	Axis 2
Waddington Pond	-0.933	0.535
Indigo Lake	-0.907	-0.495
Jellybean Lake	-1.111	-0.525
Marcella Lake	1.446	-0.583
Jackfish Lake	0.361	0.432
Eight Mile Lake	0.636	-0.056
7.5 Mile Lake	0.384	0.393
7.0 Mile Lake	0.125	0.3

REFERENCES CITED

- Abbott, M.B., Finney, B.P., Edwards, M.E. and Kelts, K.R. 2000. Lake-level reconstructions and paleohydrology of Birch Lake, Central Alaska, based on seismic reflection profiles and core transects. *Quaternary Research* 53, 154-166.
- Anderson, L., Abbott, M.B., and Finney, B.P. 2001. Holocene climate inferred from oxygen isotope ratios in lake sediments, Central Brooks Range, Alaska. *Quaternary Research* 55, 313-321.
- Anderson, P.M. and Brubaker, L.B. 1994. Vegetation history of north central Alaska: a mapped summary of late-Quaternary pollen data. *Quaternary Science Reviews* 13, 71-92.
- Appleby, P.G. 2001. Chronostratigraphic techniques in recent sediments. In: Last, W. and Smol, J.P. (Eds.), *Tracking Environmental Change Using Lake Sediments, Volume 1: Basin Analysis, Coring, and Chronological Techniques*. Kluwer Academic Press, Dordrecht, pp.171-203.
- Barber, V., and Finney, B.P. 2000. Late Quaternary paleoclimatic reconstructions for interior Alaska based on paleolake-level data and hydrologic models. *Journal of Paleolimnology* 24, 29-41.
- Barber, V., Juday, G.P. and Finney, B.P. 2000. Reduced growth of Alaskan white spruce in the twentieth century from temperature-induced drought stress. *Nature* 405, 668-673.
- Bengtsson, L., and Enell, M., 1986. Chemical Analyses. In: Berglund, B.E. (Ed.), *Handbook of Holocene Paleoecology and Paleohydrology*. J.Wiley, Chichester. pp.423-451.
- Berger, A. and Loutre, M.F. 1991. Insolation values for the climate of the last 10 million years. *Quaternary Science Reviews* 10, 297-317.
- Bigelow, N.H. 1997. Late Quaternary vegetation and lake level changes in central Alaska. Unpublished Ph.D. Dissertation. University of Alaska Fairbanks. pp. 212.
- Bigelow, N. and Edwards, M.E. 2001. A 14,000 yr paleoenvironmental record from Windmill Lake, Central Alaska: late glacial and Holocene vegetation in the Alaska Range. *Quaternary Science Reviews* 20, 203-215.

- Biondi, F., Gershunov, A., and Cayan, D.R. 2001. North Pacific decadal climate variability since 1661. *Journal of Climate* 14, 5-10.
- Bitz, C.M., and Battisti, D.S. 1999. Interannual to decadal variability in climate and the glacier mass balance in Washington, Western Canada and Alaska. *Journal of Climate* 12, 3181-3196.
- Bowen, G.J., and Wilkinson, B. 2002. Spatial distribution of $\delta^{18}\text{O}$ in meteoric precipitation. *Geology* 30, 315-318.
- Brown, T.A., Nelson, D.E., Mathewes, R.W., Vogel, J.S., and Southon, J.R. 1989. Radiocarbon dating of pollen by accelerator mass spectrometry. *Quaternary Research* 32, 205-212.
- Burn, C.R. 1997. Cryostratigraphy, paleogeography, and climate change during the early Holocene warm interval, western Arctic coast, Canada. *Canadian Journal of Earth Sciences* 34, 912-925.
- Burn, C.R., Michel, F.A. and Smith, M.W. 1986. Stratigraphic, isotopic, and mineralogical evidence for an early Holocene thaw unconformity at Mayo, Yukon Territory. *Canadian Journal of Earth Sciences* 23, 794-803.
- Calkin, P.E., Wiles, G. C., and Barclay, D.J. 2001. Holocene coastal glaciation of Alaska. *Quaternary Science Reviews* 20, 449-461.
- Cayan, D.R. and Peterson, D.H. 1989. The influence of North Pacific atmospheric circulation on streamflow in the west. *Geophysical Monograph* 55, 375-397
- Clague, J.J., Evans, S.G., Rampton, V.N., and Woodsworth, G.J. 1995. Improved age estimates for the White River and Bridge River tephtras, western Canada. *Canadian Journal of Earth Sciences* 32, 1172-1179.
- Cwynar, L.C. 1988. Late Quaternary vegetation history of Kettlehole Pond, southwestern Yukon. *Canadian Journal of Forest Research* 18, 1270-1279.
- Cwynar, L.C. and Spear, R.W. 1991. Reversion of forest to tundra in the central Yukon. *Ecology* 72, 202-212.
- Cwynar, L.C., and Spear, R.W. 1995. Paleovegetation and paleoclimatic changes in the Yukon at 6 ka BP. *Geographie Physique et Quaternaire* 49, 29-35.

- D'Arrigo, R., Wiles, G., Jacoby, G., and Villaba, R. 1999. North Pacific sea surface temperatures: past variations inferred from tree rings. *Geophysical Research Letters* 26, 2757-2760.
- Dansgaard, W. 1964. Stable isotopes in precipitation. *Tellus* 16, 436-468.
- Davi, N.K., Jacoby, G.C., and Wiles, G.C. 2003. Boreal temperature variability inferred from maximum latewood density and tree-ring width data, Wrangell Mountain region, Alaska. *Quaternary Research* 60, 252-262.
- Dean, W.E. and Megard, R.O. 1993. Environment of Deposition of CaCO₃ in Elk Lake, Minnesota. In: Bradbury, J.P. and Dean, W.E. (Eds.), *Elk Lake, Minnesota: Evidence for Rapid Climate Change in the North-Central United States*. Geological Society of America Special Paper 276, Boulder. pp. 97-113.
- Dean, W.E., and Stuiver, M. 1993. Stable carbon and oxygen isotope studies of the sediments of Elk Lake, Minnesota. In: Bradbury, J.P. and Dean, W.E. (Eds.), *Elk Lake, Minnesota: Evidence for Rapid Climate Change in the North-Central United States*. Geological Society of America Special Paper 276, Boulder. pp. 163-180.
- Dean, W.E. 1999. The carbon cycle and biogeochemical dynamics in lake sediments. *Journal of Paleolimnology* 21, 375-393.
- Denton, G.H. 1974. Quaternary glaciations of the White River Valley, Alaska, with a regional synthesis for the northern St. Elias Mountains, Alaska and Yukon Territory. *Geological Society of America Bulletin* 85, 871-892.
- Denton, G.H., and Karlen, W. 1977. Holocene glacial and tree-line variations in the White River Valley and Skolai Pass, Alaska and Yukon Territory. *Quaternary Research* 7, 63-111.
- Digerfeldt, G. 1986. Studies on past lake level fluctuations. In: Berglund, B.E. (Ed.), *Handbook of Holocene Paleoecology and Paleohydrology*. J. Wiley, Chichester. pp. 127-143.
- Dyke, A.S., and Savelle, J.M. 2000. Holocene driftwood incursion to Southwestern Victoria Island, Canadian Arctic Archipelago, and its significance to Paleoceanography and Archeology. *Quaternary Research* 54, 113-120.
- Dyke, A.S., and Savelle, J.M. 2001. Holocene history of the Bering Sea Bowhead whale (*Balaena mysticetus*) in its Beaufort Sea summer grounds off southwestern Victoria Island, western Canadian Arctic. *Quaternary Research* 55, 371-379.

- Dyke, A.S., Andrews, J.T., Clark, P.U., England, J.H., Miller, G.H., Shaw, J., and Veillette, J.J. 2002. The Laurentide and Innuitian ice sheets during the Last Glacial Maximum. *Quaternary Science Reviews* 21, 9-31.
- Edwards, M.E. and Barker, E.D. 1994. Climate and vegetation in northeastern Alaska 18,000 yr B.P.-Present. *Palaeogeography, Palaeoclimatology, Palaeoecology* 109, 127-135.
- Edwards, M.E., Mock, C.J., Finney, B.P., Barber, V.A., and Bartlein, P.J. 2001. Potential analogues for paleoclimatic variations in eastern interior Alaska during the past 14,000 yr: atmospheric-circulation controls of regional temperature and moisture responses. *Quaternary Science Reviews* 20, 189-202.
- Edwards, T.W.D., Wolfe, B.B., and MacDonald, G.M. 1996. Influence of changing atmospheric circulation on precipitation $\delta^{18}\text{O}$ -temperature relations in Canada during the Holocene. *Quaternary Research* 46, 211-218.
- Environment Canada 2003. Canadian Climate Normals website. http://www.msc-smc.ec.gc.ca/climate/climate_normals/index_e.cfm.
- Epstein, S., Buchsbaum, R., Lowenstam, H.A., and Urey, H.C. 1953. Revised carbonate-water temperature scale. *Geological Society of America Bulletin* 62, 417-426.
- Farnell, R. Hare, G.P., Blake, E., Bowyer, V., Schweger, C., Greer, s., and Gotthardt, R. 2004. Multidisciplinary investigations of alpine ice patches in southwest Yukon, Canada: paleoenvironmental and paleobiological investigations. *Arctic* 57, 247-259.
- Fee, E.J., Hecky, R.E., Kasian, S.E.M. and Cruikshank, D.R. 1996. Effects of lake size, water clarity, and climatic variability on mixing depths in Canadian Shield lakes. *Limnology and Oceanography* 41, 912-920.
- Finney, B.P., Edwards, M.E., Abbott, M.B., Barber, V., Anderson, L. and Rohr, M. 2000. Holocene Precipitation Variability in Interior Alaska. 30th Arctic Workshop Program and Abstracts, Institute for Arctic and Alpine Research, Boulder, 60.
- Finney, B.P., Gregory-Eaves, I., Sweetman, J., Douglas, M.S.V., and Smol, J.P. 2000. Impacts of climatic change and fishing on Pacific salmon abundance over the past 300 years. *Science* 290, 795-799.
- Finney, B.P., Gregory-Eaves, I., Douglas, M.S.V., and Smol, J.P. 2002. Fisheries productivity in the northeastern Pacific ocean over the past 2,200 years. *Nature* 416, 729-733.

- Fisher, D.A., Bourgeois, J., Demuth, M., Koerner, R.M., Parnandi, M., Sekerka, J., Zdanowicz, C., Zheng, J., Wake, C., Yalcin, K., Mayewski, P., Kreutz, C., Osterberg, E., Dahl-Jensen, D., Goto-Azuma, K., Holdworth, G., Steig, E., Rupper, S., Waskiewicz, M., 2004. Mount Logan ice cores: the water cycle in the North Pacific in the Holocene. AGU Fall Abstracts, Reference number 1205. <http://www.agu.org/meetings/fm04alf6.html>.
- Friedman, I., and O'Neil, J.R. 1977. Compilation of stable isotope fractionation factors of geochemical interest. In: Fleischer, M (Ed.), Data of Geochemistry, Sixth Edition, Chapter KK. United States Geological Survey Professional Paper 440-KK, Boulder. pp. 12.
- Gat, J.R., 1995. Stable Isotopes of fresh and saline lakes. In: Lerman, A, Imboden, D.M., Gat, J.R. (Eds.), Physics and Chemistry of Lakes 2nd edition. Springer-Verlag, New York and Amsterdam, pp. 139-165.
- Gonfiantini, R., Frohlich, K., Araguas-Araguas, L., and Rozanski, K., 1998: Isotopes in groundwater hydrology. In: Kendall, C. and McDonnell, J.J (Eds), Isotope Tracers in Catchment Hydrology. Elsevier, Amsterdam. pp. 203-246.
- Hammerlund, D., Barnekow, L., Birks, H.J.B., Buchardt, B., and Edwards, T.W.D. 2002. Holocene changes in atmospheric circulation recorded in the oxygen-isotope stratigraphy of lacustrine carbonates from northern Sweden. *The Holocene* 12, 339-351.
- Hammerlund, D., Björck, S., Buchardt, B., Israelson, C., and Thomsen, C.T. 2003. Rapid hydrological changes during the Holocene revealed by stable isotope records of lacustrine carbonates from Lake Igelsjön, southern Sweden. *Quaternary Science Reviews* 22, 353-370.
- Hare, S.R., and Francis, R.C. 1994. Climate change and salmon production in the Northeast Pacific Ocean. In: Beamish, R.J. (Ed.), *Climate Change and Northern Fish Populations*. Canadian Special Publication in Fish and Aquatic Science v. 121. pp. 1-33.
- Harrison, S.P. and Digerfeldt, G. 1993: European lakes as palaeohydrological and palaeoclimatic indicators. *Quaternary Science Reviews* 12, 223-248.
- Heiri, O., Lotter, A.F., and Lemcke, G. 2001. Loss on ignition as a method for estimating organic and carbonate content in sediments: reproducibility and comparability of results. *Journal of paleolimnology* 25, 101-110.
- Herczeg, A.L., and Fairbanks, R.G. 1987. Anomalous carbon isotope fractionation between atmospheric CO₂ and dissolved inorganic carbon induced by intense photosynthesis. *Geochimica Cosmochimica Acta* 51, 895-899.

- Heusser, C.J., Heusser, L.E., and Peteet, D.M. 1985. Late-Quaternary climatic change on the American North Pacific Coast. *Nature* 316, 485-487.
- Hodell, D.A., Schelske, C.L., Fahnenstiel, G.L. and Robbins, L.L. 1998. Biologically induced calcite and its isotopic composition in Lake Ontario. *Limnology and Oceanography* 43, 187-199.
- Holdsworth, G., Krouse, H.R., and Nosal, M. 1992. Ice core climate signals from Mount Logan, Yukon A.D. 1700-1897. In: Bradley, R.S. and Jones, P.D. (Eds.), *Climate Since A.D. 500*. Routledge, London. pp. 483-516.
- Hu, F.S., Ito, E., Brubaker, L.B. and Anderson, P.M. 1998. Ostracode geochemical record of Holocene climatic change and implications for vegetational response in the northwestern Alaska Range. *Quaternary Research* 49, 86-95.
- Hu, F.S. and Shemesh, A. 2003. A biogenic-silica $\delta^{18}\text{O}$ record of climatic change during the last glacial-interglacial transition in southwestern Alaska. *Quaternary Research* 59, 379-385.
- Hu, F.S., Kaufman, D., Yoneji, S., Nelson, D., Shemesh, A., Huang, Y., Tian, J., Bond, G., Clegg, B., and Brown, T. 2003. Cyclic variation and solar forcing of Holocene climate in the Alaskan subarctic. *Science* 301, 1890-1893
- IAEA/WMO 2001. Global Network of Isotopes in Precipitation (GNIP) and Isotope Hydrology Information System (ISOHIS). International Atomic Energy Agency and World Meteorological Organization. <http://isohis.iaea.org/>.
- Ingraham, N.L. 1998. Isotopic variations in precipitation. In: Kendall, C. and McDonnell, J.J (Eds.), *Isotope Tracers in Catchment Hydrology*. Elsevier, Amsterdam. pp. 87-118.
- Jones, V.J., Leng, M.J., Solovieva, N., Sloane, H.J., and Tarasov, P. 2004. Holocene climate of the Kola Peninsula; evidence from the oxygen isotope record of diatom silica. *Quaternary Science Reviews* 23, 833-839.
- Keenan, T.J., and Cwynar, L.C. 1992. Late Quaternary history of black spruce and grasslands in southwest Yukon Territory. *Canadian Journal of Botany* 70, 1336-1345.
- Kendal, C. 1998: Tracing nitrogen sources and cycling in catchments. In: Kendall, C. and McDonnell, J.J (Eds.), *Isotope Tracers in Catchment Hydrology*. Elsevier, Amsterdam. pp. 519-576.

- Lacourse, T. and Gajewski, K. 2000. Late Quaternary vegetation history of Sulfur Lake, southwest Yukon Territory, Canada. *Arctic* 53, 27-35.
- Lamorueax, S. and Cockburn, J.M.H. in Press: Timing and controls over neoglacial expansion in the northern coast mountains, British Columbia. *The Holocene*.
- Latif, M. and Barnett, T.P. 1994. Causes of decadal climate variability over the North Pacific and North America. *Science* 266, 634-637.
- Lauriol, B., Grimm W., Cabana, Y., Cinq-Mars, J. and Geurtz, M.A. 2001. Cliff-top eolian deposits as indicators of Late Pleistocene and Holocene Beringia. *Quaternary International* 87, 59-79.
- Lauriol, B., Duguay, C.R. and Riel, A. 2002. Response of the Porcupine and Old Crow rivers in northern Yukon, Canada, to Holocene climatic change. *The Holocene* 12, 27-34.
- Leng, M.J. and Anderson, N.J. 2003. Isotopic variation in modern lake waters from western Greenland. *The Holocene* 13, 605-611.
- Lerbekmo, J.F. and Campbell, F.A. 1969. Distribution, composition and source of the White River ash, Yukon Territory. *Canadian Journal of Earth Sciences* 6, 109-116.
- Mackay, J.R. 1992. Lake stability in an ice-rich permafrost environment: examples from the western arctic coast. In: Robarts, R.D. and Bothwell, M.L. (Eds.), *Aquatic Ecosystems in Semi-arid Regions: implications for Resource Management*. Symposium Series 7, Environment Canada, Saskatoon. pp. 1-25.
- Mann, D.H. and Hamilton, T.D. 1995. Late Pleistocene and Holocene paleoenvironments of the North Pacific coast. *Quaternary Science Reviews* 14, 449-471.
- Mann, D.H., Crowell, A.L., Hamilton, T.D. and Finney, B.P. 1998. Holocene geologic and climatic history around the Gulf of Alaska. *Arctic Anthropology* 35, 112-131.
- Mantua, N.J., Hare, S.R., Zhang, Y., Wallace, J.M. and Francis, R.C. 1997. A Pacific interdecadal climate oscillation with impacts on salmon production. *Bulletin of the American Meteorological Society* 78, 1069-1079.
- McConnaughey, T. 1991. Calcification in *Chara corallina*: CO₂ hydroxylation generates protons for bicarbonate assimilation. *Limnology and Oceanography* 36, 619-628.

- McConnaughey, T.A., LaBaugh, J.W., Rosenberry, D.O. and Striegel, R.G. 1994. Carbon budget for a groundwater-fed lake: calcification supports summer photosynthesis. *Limnology and Oceanography* 39, 1319-1332.
- McKenzie, J.A. 1985: Carbon isotopes and productivity in the lacustrine and marine environment. In: Stumm, W (Ed.), *Chemical Processes in Lakes*. J. Wiley, Toronto. pp. 99-118.
- Mock, C.J., Bartlein, P.J., and Anderson, P.M. 1998. Atmospheric circulation patterns and spatial climatic variations in Beringia. *International Journal of Climatology* 18, 1085-1104.
- Moore, G.W.K., Alverson, K., and Holdsworth, G. 2002a. Variability in the climate of the Pacific Ocean and North America as expressed in the Mount Logan ice core. *Annals of Glaciology* 35, 423-429.
- Moore, G.W.K., Holdsworth, G., and Alverson, K. 2002b. Climate change in the North Pacific region over the past three centuries. *Nature* 420, 401-403.
- Morlan, R.E., and Cinq-Mars, J. 1982. Ancient Beringians: human occupation in the late Pleistocene of Alaska and the Yukon Territory. In: Hopkins, D.H., Matthews, J.V. Schweger, C.E. and Young, S.B. (Eds.), *Paleoecology of Beringia*. Academic Press, New York. pp. 353-381.
- Morlan, R.E. and Workman, W.B. 1980. Prehistoric man in the southwest Yukon. In: Theberge, J.B. (Ed.) *Kluane: Pinnacle of the Yukon*. Doubleday Canada Ltd., Toronto. pp. 97-107.
- Oana, S., and Deevey, E.S. 1960. Carbon-13 in lake waters, and its possible bearing on paleolimnology. *American Journal of Science* 258-A, 253-272.
- Pienitz, R., Smol, J.P. and Lean, D.R.S. 1997. Physical and chemical limnology of 59 lakes located between the southern Yukon and the Tuktoyaktuk Peninsula, Northwest Territories (Canada). *Canadian Journal of Fisheries and Aquatic Sciences* 54, 330-346.
- Pienitz, R., Smol, J.P., Last, W.M., Leavitt, P.R. and Cumming, B.F. 2000. Multi-proxy Holocene paleoclimatic record from a saline lake in the Canadian subarctic. *The Holocene* 10, 673-686.
- Plummer, L.N. and Busenberg, E. 1982. The solubility of calcite, aragonite, and vaterite in CO₂-H₂O solutions between 0 and 90°C, and an evaluation of the aqueous model for CaCO₃-CO₂-H₂O equilibria. *Geochimica Cosmochimica Acta* 44, 1011-1040.

- Ramisch, F., Ditrich, M., Mattenberger, C., Wehrli, B. and Wüest, A. 1999. Calcite dissolution in two deep eutrophic lakes. *Geochimica et Cosmochimica Acta* 63, 3349-3356.
- Richter, D.H., Preece, S.J., McGimsey, R.G. and Westgate, J.A. 1995. Mount Churchill, Alaska: source of the late Holocene White River Ash. *Canadian Journal of Earth Science* 32, 741-748.
- Ritchie, J.C., Cwynar, L.C. and Spear, R.W. 1983. Evidence from north-west Canada for an early Holocene Milankovitch thermal maximum. *Nature* 305, 126-128.
- Ritchie, J.C. and Harrison, S.P. 1993. Vegetation, lake levels, and climate in western Canada during the Holocene. In Wright, H.E., Kutzbach, J.E., Webb, T. III., Ruddiman, W.F., Street-Perrott, F.A., and Bartlein, P.J. (Eds.), *Global Climate since the Last Glacial Maximum*. University of Minnesota Press, Minneapolis. pp 401-414.
- Robinson, S.D. 2001. Extending the Late Holocene White River Ash distribution, Northwestern Canada. *Arctic* 54, 157-161.
- Rosqvist, G., Jonsson, C., Yam, R., Karlén, W., and Shemesh, A. 2004. Diatom oxygen isotopes in pro-glacial lake sediments from northern Sweden: a 5000 year record of atmospheric circulation. *Quaternary Science Reviews* 23, 851-859.
- Rozanski, K., Araguas-Araguas, L., and Gonfiantini, R. 1992. Relation between long-term trends of oxygen-18 isotope composition of precipitation and climate. *Science* 258, 981-985.
- Rozanski, K., Araguás-Araguás, L., and Gonfiantini, R. 1993. Isotopic patterns in modern global precipitation. In: Swart, P.K. Lohman, K.C., McKenzie, J., and Savin S. (Eds.), *Climate Change in Continental Isotopic Records*. American Geophysical Union, Geophysical Monograph 78, Washington D.C. pp. 1-36.
- Rupper, S., Steig, E.J., and Roe, G. 2004. The relationship between snow accumulation and Mt. Logan, Yukon, Canada and climate variability in the North Pacific. *Journal of Climate* 17, 4724-4739.
- Shemesh, A., Rosqvist, G., Rietti-Shati, M., Rubensdotter, L., Bigler, C., Yam, R., and Karlén, W. 2001. Holocene climatic change in Swedish Lapland inferred from an oxygen-isotope record of lacustrine biogenic silica. *The Holocene* 11, 447-454.
- Siegenthaler, U., and Eicher, U. 1986. Stable oxygen and carbon isotope analyses. In: Berglund, B.E. (Ed.), *Handbook of Holocene Paleoecology and Paleohydrology*. J. Wiley, Chichester. pp. 407-422.

- Spear, R.W. and Cwynar, L.C. 1997. Late Quaternary vegetation history of White Pass, Northern British Columbia, Canada. *Arctic and Alpine Research* 29, 45-52.
- Spooner, I.S., Barnes, S., Baltzer, K.B., Raeside, R., Osborn, G.D., and Mazzucchi, D. 2003. The impact of air mass circulation dynamics on late Holocene paleoclimate in northwestern North America. *Quaternary International* 108, 77-83.
- Stabel, H-H. 1986. Calcite precipitation in Lake Constance: chemical equilibrium, sedimentation, and nucleation by algae. *Limnology and Oceanography* 31, 1081-1093.
- Street-Perrott, F.A., and Harrierson, S.P. 1985. Lake level fluctuations. In: Hecht, A.D. (Ed), *Paleoclimate Data and Modeling*. Wiley, New York, pp. 291-340.
- Streten, N.A. 1974. Some features of the summer climate of interior Alaska. *Arctic* 27, 272-286.
- Stuart, S.L., Helmer, J.W. and Hills, L.V. 1989. The Holocene paleoecology of Jenny Lake area, southwest Yukon, and its implications for prehistory. *Arctic* 42, 347-353.
- Stuiver, M., Reimer, P.J., Bard, E., Beck, J.W., Burr, G.S., Hughen, K.A., Kromer, B., McCormac, F.G., v.d. Plicht, J., and Spurk, M. 1998. Radiocarbon age calibration 24,000 - 0 cal BP. *Radiocarbon* 40, 1041-1083.
- Szeicz, J.M., and MacDonald, G.M. 1995. Dendroclimatic reconstruction of summer temperature in Northwestern Canada since A.D. 1638 based on age-dependent modeling. *Quaternary Research* 44, 257-266.
- Szeicz, J.M., and MacDonald, G.M. 1996. A 930-year ring-width chronology from moisture sensitive white spruce (*Picea glauca* Moench) in Northwestern Canada. *The Holocene* 6, 345-351.
- Talbot, M.R. 1990. A review of the palaeohydrological interpretation of carbon and oxygen isotopic ratios in primary lacustrine carbonates. *Chemical Geology (Isotope Geosciences Section)* 80, 261-279.
- Thompson, R. 1986. Paleomagnetic Dating. In: Berglund, B.E. (Ed.) *Handbook of Holocene Paleoecology and Paleohydrology*. J. Wiley, Chichester. pp. 313-328.
- Trenberth, K.E., and Hurrell, J.W. 1994. Decadal atmosphere-ocean variations in the Pacific. *Climate Dynamics* 9, 303-319.

- Vardy, S.R., Warner, B.G. and Aravena, R. 1997. Holocene climate effects on the development of a peatland on the Tuktoyaktuk Peninsula, Northwest Territories. *Quaternary Research* 47, 90-104.
- von Grafenstein, U., Erlenkeuser, H., Muller, J., Trimborn, P., and Alefs, J. 1996. A 200-year mid-European air temperature record preserved in lake sediments: an extension of the $\delta^{18}\text{O}_p$ -air temperature relation into the past. *Geochimica Cosmochimica Acta* 60, 4025-4036.
- Wahl, H.E., Fraser, D.B., Harvey, R.C., and Maxwell, J.B. 1987. Climate of the Yukon. *Climatological Studies Number 40*, Environment Canada. pp. 323.
- Wake, C.P., Yalcin, K., and Gundestrup, N.S. 2002. The climate signal recorded in the oxygen-isotope, accumulation and major-ion time series from the Eclipse ice core, Yukon Territory, Canada. *Annals of Glaciology* 35, 416-422.
- Wang, X.-C. and Geurts, M. 1991. Late Quaternary pollen records and vegetation history of the southwest Yukon Territory: a review. *Géographie Physique et Quaternaire* 45, 175-193.
- West, K.D. and Donaldson, J.A., 2000. Evidence for winter eruption of the White River Ash (eastern lobe), Yukon Territory, Canada. Canadian Society of Exploration Geophysicists Conference Abstract. www.cseg.ca/conferences/2000/874.pdf.
- Workman, W.B. 1978. Prehistory of the Aishih-Kluane area, southwest Yukon Territory. *Archaeological survey of Canada Paper no. 74*. National Museum of Man Mercury Series, National Museums of Canada, Ottawa. pp. 592.
- Wiles, G.C., D'Arrigo, R.D., and Jacoby, G.C. 1998. Gulf of Alaska atmosphere-ocean variability over recent centuries inferred from coastal tree-ring records. *Climatic Change* 38, 289-306.
- Wiles, G.C., Barclay, D.J., and Calkin, P.E. 1999. Tree-ring-dated 'Little Ice Age' histories of maritime glaciers from western Prince William Sound, Alaska. *The Holocene* 9, 163-173.
- Wiles, G.C., D'Arrigo, R.D., Villalba, R., Calkin, P.E. and Barclay, D.J. 2004. Century-scale solar variability and Alaskan temperature change over the past millennium. *Geophysical Research Letters* 31, L15203, doi:10.1029/2004GL020050.
- Wolfe, B.B., Edwards, T.W.D., Jiang, H., MacDonald, G.M., Gervais, B.R., and Snyder, J.A. 2003. Effect of varying oceanicity on early- to mid-Holocene palaeohydrology, Kola Peninsula, Russia: isotopic evidence from treeline lakes. *The Holocene* 13, 153-160.

Wright, J.V. 2001. A History of the Native People of Canada. Canadian Museum of Civilization web site.<http://www.civilization.ca/archo/hnpc/npprefae.html>

Yu, Z., McAndrews, J.H., and Eicher, U. 1997. Middle Holocene dry climate caused by change in atmospheric circulation patterns: evidence from lake levels and stable isotopes. *Geology* 25, 251-254.